UNIVERSITA' DEGLI STUDI DI PADOVA

DIPARTIMENTO DI SCIENZE ECONOMICHE ED AZIENDALI "M.FANNO"

DIPARTIMENTO DI MATEMATICA "TULLIO LEVI CIVITA"

CORSO DI LAUREA MAGISTRALE IN ECONOMICS AND FINANCE

TESI DI LAUREA

"A SHADOW RATE MODEL APPLIED TO THE EUROZONE: REAL TIME ESTIMATION AND MODEL IMPLIED LIFTOFF FORECASTS"

RELATORE:

CH.MO PROF. CLAUDIO FONTANA

LAUREANDO/A: CRISTIANO RONCHI

MATRICOLA N. 1219559

ANNO ACCADEMICO 2021 – 2022

Dichiaro di aver preso visione del "Regolamento antiplagio" approvato dal Consiglio del Dipartimento di Scienze Economiche e Aziendali e, consapevole delle conseguenze derivanti da dichiarazioni mendaci, dichiaro che il presente lavoro non è già stato sottoposto, in tutto o in parte, per il conseguimento di un titolo accademico in altre Università italiane o straniere. Dichiaro inoltre che tutte le fonti utilizzate per la realizzazione del presente lavoro, inclusi i materiali digitali, sono state correttamente citate nel corpo del testo e nella sezione 'Riferimenti bibliografici'.

I hereby declare that I have read and understood the "Anti-plagiarism rules and regulations" approved by the Council of the Department of Economics and Management and I am aware of the consequences of making false statements. I declare that this piece of work has not been previously submitted – either fully or partially – for fulfilling the requirements of an academic degree, whether in Italy or abroad. Furthermore, I declare that the references used for this work – including the digital materials – have been appropriately cited and acknowledged in the text and in the section 'References'.

Firma (signature) 

Acknowledgments

Alla mia famiglia, ai miei amici e ad Iliana.

Contents

Introduction

Over the last fifteen years, following the global financial crisis and the European sovereign debt crisis, the introduction of negative interest rates policies has been a quite particular event for our economies. Nowadays it is somehow surprising to find articles and books published prior the financial crisis in which authors rule out any possibility for interest rates to cross the zero lower bound. However, the most recent events showed the world how unpredictable the economic scenario can be.

The context considered for this dissertation is the European one, with the focus being on the European Central Bank, one of the major central banks that resorted to the negative interest rate policy (NIRP) significantly. This is the reason why in chapter 1 we introduce the concepts and the intuition behind the NIRP, as well as its effects on economic agents. After providing an overview on which are the central banks that implemented such policy, we present the main monetary policy tools at disposal of the European Central Bank. In chapter 2 we recall the main theoretical concepts of interest rate theory as well as continuous time short rate models, with a particular focus on the Vasicek and the Hull-White model.

Given the particular macroeconomic framework we find ourselves in, interest rate modelling had to adopt new solutions in dealing with negative deposit rates and yield curves. The analysis carried out in this thesis implements one of these solutions, namely the "shadow rate model", which is based on a simple and intuitive mechanism introduced by Black (1995). In particular, under some assumptions, the mechanism prevents the short rate to take values below a given lower bound. By relying on the mechanism, in this dissertation we explore how different specifications of such lower bound affect a shadow rate model's performance in terms of parameters estimates, goodness of fit and forecasting liftoff horizons, namely the length of time after which we can expect the short rate to cross the lower bound from below. Therefore, in chapter 3, we start describing the most common problems in modelling interest rates in a NIRP environment, and we present the "zero lower bound mechanism" by explaining how it helps in solving such problems.

The last chapter is dedicated to the empirical analysis. Given two different lower bound specifications, namely a single lower bound and a regime switching lower bound, we estimate their corresponding shadow rate models over the entire sample period (i.e. from August 2005 to September 2021) by employing end-of-month observations of the Euro OIS yield curve. Given the decisions of the ECB to cut the deposit rate several times below zero, the aim of the estimation is to test the ability of the different lower bound specifications to capture the shifts in interest rates in negative territory that were driven by such cuts. Thus, we compare the

different models' performance after estimating their parameters as if we were doing it "real time", meaning that we first set ourselves at the beginning of 2014 and we re-estimate the two models at the beginning of each year up to 2021 by adding, at each re-estimation date, the last twelve end-of-month observations. Subsequently, by means of a Monte Carlo simulation we derive the models-implied liftoff horizons to explore how the two lower bound specification affects such measure. Additionally, we provide a comparison with respect to the real market expectations provided by the ECB Survey of Monetary Analysts (SMA) for the periods of May and August 2021.

CHAPTER 1

1. The negative interest rate policy (NIRP)

In this chapter we provide a brief overview of the negative interest rate policy (NIRP) and its worldwide implementation. We then focus on the European macroeconomic framework, and we close the chapter with a discussion about the economic agents that may benefit and those that may lose in a negative interest rate environment.

1.1. What is the NIRP

The NIRP is an unconventional monetary policy tool which consists in the central bank to set some key policy rates in negative territory, that is below what was commonly perceived to be a "zero-lower bound". Considering the rationale and the objectives behind this policy, one can think of the NIRP to be the natural continuation of the classic expansionary monetary policy below the "zero-lower bound". This poses questions regarding where the effective lower bound actually is, as long as the cash option remains available to economic agents.

IMF (2017) provides some case studies, from which it is quite easy to understand the main objectives of the NIRP, that is generally applied within a more complex picture of conventional and unconventional monetary policies. We find the pursue of inflation targets, the support of the credit market in a perspective of growth stimulation, but also fixed exchange rate defence as main objectives.

Generally speaking, a positive interest rate implies a lender to earn interests on a given amount lent to a counterparty. Contrarily, a negative interest rate implies a cost for the lender, who may decide to manage liquidity in a different way. This is exactly the case of financial institutions: if on the one hand, in a context of low interest rates, they may raise cheaper funding liquidity, on the other they typically earn a negative return from holding excess reserves with the central bank implementing the NIRP. Effects on both the credit activity and the money markets are natural consequences, as banks have the incentive to lend any excess of liquidity to businesses and households, therefore stimulating investments and consumption.

The feasibility of a long run implementation of such policies is object of discussion. The main issues concern financial intermediaries profitability and households' willingness to earn a negative rate on deposits rather than holding cash (see Bech and Malkhozov 2016 and Blanke and Krogstrup 2016 for a general overview about these issues). However, we will come back to these aspects in section 1.4.

1.2. The NIRP implementation around the world

Although the focus of this dissertation is on the euro area, the European Central Bank (ECB) was not the only monetary authority to adopt negative interest rates. Among the others, policy rates have been set negative also in Denmark, Sweden, Japan and in Switzerland, even though the motives behind their introduction were quite different. Let us discuss all these cases respectively.

In order to pursue its price stability mandate in a situation of persistent low inflation expectations and to stimulate lending into the economy, Draghi (2014) announced on the 5th of June 2014 the ECB's decision to set the deposit facility rate at negative 0.1 percent starting from the 11th of the same month. After June 2014, further adjustments took place, with the deposit facility rate to finally reach a negative 0.5 percent in September 2019.[1] Notice that the ECB's NIRP, which had no precedent in the euro area, was actually an integral part of a more general set of monetary policies. In particular, the package introduced in June 2014 came along with reductions in other key interest rates, such as the one on the main refinancing operations and the rate on the marginal lending facility, but also with the introduction of the "Targeted longer-term refinancing operations (TLTRO),[2] and preparatory work related to outright purchases of asset-backed securities" (ECB 2014a).

Going back in history, one of the first countries that adopted the NIRP was Denmark, but its purposes were different from the ones of the ECB. As the mandate of the Danmarks Nationalbank (DN) is to ensure low inflation by relying on both monetary and foreign-exchange policies, including intervention in the foreign-exchange market,[3] the defence of the exchange rate was the cause of the NIRP. As indicated in IMF (2017), following a solid growth in 2010, a significant output gap in 2011 and the euro area struggling with the sovereign debt crisis, the Danish Krone was perceived to be a safe currency, with a consequent appreciation against the euro from the middle of 2011. The DN intervened by charging banks a certificate of deposits rate of negative 0.2 percent from July 2012, and by taking corrective interventions in the foreign exchange market aimed at supplying krone and increasing foreign currency reserves. IMF (2017) underlines how Denmark had to deal with huge capital inflows in the early 2015 as well, as a consequence of the ECB Asset Purchase Programme and the Swiss National Bank's decision to abandon the exchange rate floor against the euro. The DN response was aligned

[1] See ECB's website: https://www.ecb.europa.eu/stats/policy_and_exchange_rates/key_ecb_interest_rates/html/index.en.html

[2] The complementary policies are usually as much as important as the NIRP. For example, for what concerns the ECB, the introduction of the TLTRO, an unconventional tool with the aim of providing banks with additional term funding, is considered to be the starting point of the Asset Purchase Programme (APP). See: https://www.ecb.europa.eu/mopo/implement/app/html/index.en.html

[3] See Danmarks Nationalbank's website: https://www.nationalbanken.dk/en/marketinfo/Pages/default.aspx

with the corrective actions taken in 2011, with the Certificate of deposit rate set at negative 0.75 percent in February 2015 along with foreign exchange market interventions. Eventually, the DN reached its objective, and the Certificate of deposit rate was raised to negative 0.65 in January 2016.[4]

The case of Sweden seems to go hand in hand with the ECB one, as it must be contextualized in an environment of low inflation expectations. The Sveriges Riksbank (SR) set a zero-repo rate in October 2014, with a further reduction to negative 0.10 percent in February 2015 and, to sustain the increase in monetary base, the SR committed itself in purchasing public debt as well. To give the idea of the magnitude of the intervention, notice that in February 2016 the RN charged an historical minimum repo rate of negative 0.5 percent (see Sveriges Riksbank 2019) and, by the middle of the same year, public debt holdings reached 30% of the outstanding nominal government bonds (see Bech and Malkhozov 2016). As IMF (2019) suggests, the effects on inflation were positive, as we witness a HICP inflation and a Core HICP inflation of 1.4 and 0.9 respectively at the end of 2016, and 1.8 and 1.6 at the end of in 2017. On top of that, even though the RN has no exchange rate target,[5] Sveriges Riksbank (2019) shows the intervention had positive side effects for the exchange rate as well: the lowering of the government yield helped stabilizing the Swedish Krona, that was previously experiencing an appreciation.

The Bank of Japan (BoJ) followed the example of the ECB and the other European central banks by announcing, at the end of January 2016, the introduction of the "Quantitative and Qualitative Monetary Easing (QQE) with a Negative Interest Rate" programme “in order to achieve the price stability target of 2 percent at the earliest possible time” (Bank of Japan 2016). The peculiar feature of the japanese NIRP was the Three-Tier System: each financial institution’s current account outstanding balance was divided in three tiers, to which it was assign respectively a positive interest rate of 0.1 percent, a zero-interest rate and a negative interest rate of 0.1 percent according to some criteria that penalized reserves exceeding the required amount. Also in this case, as pointed out by IMF (2017) the NIRP must be considered within the broader picture of the QQE asset purchase program, that was initiated as a remedial measure to a weak production growth and a sharp decline in inflation at the end of 2015.

For what concerns Switzerland, the motives that led to the adoption of the NIRP date back to the global financial crisis in 2008 and the sovereign debt crisis in 2010. The Swiss case study in IMF (2017) explains that in such uncertain financial conditions, the perception of the Swiss

[4] See Danmarks Nationalbank’s website: https://www.nationalbanken.dk/en/marketinfo/official_interestrates/Pages/Default.aspx

[5] See Sveriges Riksbank’s website: https://www.riksbank.se/en-gb/about-the-riksbank/the-tasks-of-the-riksbank/

Franc to be a safe currency created a significant appreciation pressure. As a response, the Swiss National Bank (SNB) decided to set a floor on the exchange rate against the euro in September 2011, that is "with immediate effect, it will no longer tolerate a EUR/CHF exchange rate below the minimum rate of CHF 1.20" (Swiss National Bank 2011). Bech and Malkhozov (2016) reports that three years later, in order to defend the CHF minimum rate, the SNB set an interest rate of negative 0.25 percent on sight deposit account balances, but in January 2015 the appreciation pressure forced the SNB to discontinue the CHF minimum rate and, in the hope of discouraging investments in the country, the SNB lowered interest rate on sight deposit to negative 0.75 percent. As in the japanese case, this NIRP was based on a tiering system which provides for an exemption threshold of sight deposits at the SNB below which negative interest rates were not charged. Similarly to the Danmarks Nationalbank, also in Swiss National Bank (2014) it is remarked the purchase of foreign currency by the SNB was an important tool at the central bank disposal to keep appreciation pressures at bay.

1.3. The European framework

The primary goal of the European Central Bank is to ensure that price stability is maintained over the medium term by evaluating economic developments and by assessing how its policy decisions are transmitted to the economy.[6] In 2003, the ECB specified its aim to stabilize inflation rates "below, but close to, 2% over the medium term" ECB (2011). Having in mind the primary objective of the ECB, in this section we provide a broad description of the main instruments of monetary policy at its disposal. In this subsection, we mainly refer to ECB (2011).

1.3.1. The main instruments of monetary policy

The ECB toolbox of conventional monetary policies can be divided into three main categories: *open market operations*, *standing facilities* and *minimum reserve requirements*. As described in ECB (2011) the open market operations can be further classified in:

- *Main refinancing operations (MRO's)*: liquidity-providing operations which are carried out on a weekly basis, whose total available liquidity is previously decided by the ECB. They are short-term oriented operations, as their maturity is typically one week. Their procedure is based on a standard tender, that is in accordance with a pre-announced schedule which is supposed to help liquidity managers in planning funding. The ECB also decides whether to set up fixed-rate tenders or variable rate tenders, even though, from October 2008, MRO's are based on fixed-rate tenders with the full allotment of liquidity the commercial bank wish to transact. To participate, counterparties must fulfil

[6] See ECB's website: https://www.ecb.europa.eu/mopo/strategy/princ/html/index.en.html

general eligibility criteria, but substantially all the euro area credit institutions are potentially eligible.

- *Longer-term refinancing operations (LTRO's)*: liquidity-providing operations aimed at solving structural problems of liquidity.[7] They are conducted on a monthly basis. Typically they are characterized by a three-months maturity, whose rationale is to prevent financial institutions to rollover MRO's. If deemed necessary, the governing council may implement additional LTRO's with longer maturities (even up to a year). However, irrespectively of the maturity, LTRO's are based on a standard tender in a decentralized manner, with the ECB to act as a "rate taker" to not influence money market rates over such long terms. In normal circumstances they are pure variable rate tenders with the ECB announcing in advance the total liquidity to be allotted, while under exceptional circumstances they may be based on fixed-rate tenders with full allotment of liquidity needed (and requested) by each counterparty. As for MRO's all counterparties fulfilling the general eligibility criteria can participate.
- *Fine-tuning operations*: they are both liquidity-providing and liquidity-absorbing operations aimed at steering interest rates and smoothing their fluctuations due to unexpected liquidity events. Coherently with their objective, their frequency and maturity are not regular, and their procedure is generally a "quick" tender (it takes one hour from their announcement to the communication of the results).[8] To take part of these operations, given their characteristics, there is a list of around 2000 eligible counterparties.
- *Structural operations*: they aim at adjusting the liquidity amount in the market over longer horizons by means of liquidity-providing and liquidity-absorbing operations. By being conducted at the initiative of the governing council, their frequency can be regular or non-regular, and they can be based on either standard tenders or bilateral procedures.

The second main category of the monetary policy's toolbox concerns the standing facilities, which allow the central bank to manage liquidity positions vis-à-vis single counterparties, but only at their initiative. Indeed, they are implemented upon request of commercial banks, either because in need of additional liquidity or in need of liquidity absorption. ECB (2011) explains that the ad-hoc request of liquidity provisions (or liquidity absorption) implies a cost (or a profit) for commercial banks that is unfavourable with respect to the one they would incur in the money market. ECB (2011) distinguish the standing facilities into:

[7] The Targeted longer-term refinancing operations (TLTRO's) mentioned in the previous section are particular types of LTRO's, whose main features are the advantageous conditions in terms of interests, and the focus on the private sector.
[8] Under exceptional circumstances, they may even be bilateral procedures.

- *Marginal lending facility (MLF)*: it allows a counterparty that fulfils the general eligibility criteria, to obtain liquidity with an overnight maturity from its national central bank. The interest rate under the facility is instead defined at the discretion of the ECB's governing council. Liquidity amounts can be provided with no limits, but only against eligible assets, either through overnight repurchase agreements or as overnight collateralised loans. Notice that the pre-specified rate on this type of facility implicitly determine the "cap" of the corridor of interest rates in the interbank market, in particular in the overnight money market.
- *Deposit facility (DF)*: it allows a counterparty that fulfils the general eligibility criteria, to deposit any excess amounts of liquidity with its national central bank. Also for this facility, the maturity can only be overnight, with interests payment calculated on a pre-specified fixed rate.[9] The deposit facility rate outlines the "floor" of the corridor which characterizes the overnight money market.

As we mention before, the third element described in ECB (2011) which composes the toolkit of the monetary policy is the minimum reserve requirements. Generally speaking, commercial banks must hold balances on their current accounts (i.e. "required" reserves) with the corresponding national central bank (NCB) for a given amount calculated on the basis of their reserve base. There are three fundamental elements of the minimum reserves system which worth attention. Let us quickly explain them:

-The *reserve base*: it refers to the bank's financial liabilities considered for the minimum reserve requirements' calculation, to which reserve ratios are applied. The bank's liabilities subject to reserve requirements are distinguished in terms of maturity. Specifically, short-term liabilities are applied a positive reserve ratio (that to date is one percent) while longer maturity liabilities are applied another reserve ratio (which currently is a zero-reserve ratio). At the same time, the minimum reserves regulations specify some criteria according to which some financial liabilities may be excluded from the reserve base.

-The *averaging provision*: it indicates the reserve requirement (i.e. the average balance) that a commercial bank must hold with the NCB over the maintenance period. In other words, banks are given the possibility to hold a balance deficit (or a surplus) over their reserve requirement, provided that they counter the imbalance before the end of the maintenance period (i.e. when the reserve requirement becomes binding). As stated in ECB (2011), one of the objectives of

[9] Given the importance of the facility, the governing council can change or adapt the features of the facility and, if deemed necessary, even suspend it.

the averaging provision is to favour conditions for the stabilization of money market interest rates.[10]

-The *maintenance period* is the time window underlying the averaging provision compliance. More precisely, the average of the daily balances on the institution's current account must comply with the averaging provision. ECB (2011) indicates the maintenance period lasts around a month and an indicative maintenance period schedule is published by the ECB three months before the start of each calendar year.[11]

Besides the commonly known prudential liquidity purposes, ECB (2011) specifies a second key objective of the minimum reserve requirement, meaning the creation of a structural liquidity shortage in the system, that leads the increase of commercial banks' demand of credit in order to comply with the averaging provision. The credit demand may be addressed to both the interbank market and the central bank, making it easier for the latter to influence interest rates levels.

1.3.2. The transmission of the NIRP to the money market rates: evolution and features

Recent assessments, such as ECB (2020a), state that so far the NIRP has reached its objectives. As a matter of fact, we witness a boost of the economic activity through an increase in lending volumes (which offsets lower interest income) and an improvement of creditworthiness. Finally, it is contributing to price stability. However, the aim of this section is to provide some intuitions about how negative policy rates are supposed to be transmitted to the economic system. This is not an easy task,[12] but we provide general intuitions. For further theoretical details we address the reader to Beyer at all. (2017), sections 2 and 3. For an assessment about the NIRP results, we refer to ECB (2020a), sections 3 and 4, along with Arteta et al (2016) which analyse implications on some key financial variables (such as lending rates, sovereign bond yields and inflation) both in the eurozone and outside.[13]

The interest rate channel

The fundamental element to consider for what concerns the interest rate channel is the interbank market. ECB (2011) and Beyer at all. (2017) suggest the implementation of liquidity-providing or liquidity-absorbing operations in order to steer money market rates, depend on the

[10] Consider, for example, the case in which a bank believes that short-term rates are likely to decline at the end of the maintenance period. The compliance with the average provision at the end of the maintenance period allows the bank to destinate reserves to lending at first and run surpluses only at the end of the period by borrowing at a possibly lower rate

[11] The rationale behind scheduling is to help banks managing their liquidity over the year.

[12] Beyer et al. (2017) indicate the influence on the economy occur through a myriad of transmission mechanisms of the monetary, macroprudential and microprudential policies, as well as the interactions between them.

[13] Notice this assessment dates year 2016, therefore it considers just the first two cuts of the ECB.

level of liquidity in the interbank market, and to the inflation target the ECB wants to achieve.[14] In order to understand how the ECB steered interest rates overtime, in figure 1 we plot the evolution from January 1999 to September 2021 of the key policy rates, and two of the most relevant money market rates: the EONIA and the one-month maturity EURIBOR. It is quite evident the interest rates charged by the ECB on standing facilities delineate the range (i.e. "corridor" of interest rates) within which money market rates fluctuate. More precisely, the rate under the deposit facility and that under the marginal lending facility respectively define the floor and the cap of the overnight interbank market. As a matter of facts, the "revolutionary" package announced by Mario Draghi to counter low inflation expectations in June 2014 was firstly transmitted in the interest rate channel. As announced in ECB (2014b) the package included a cut on the MRO's and the MLF interest rates, that were lowered to 0.15 and 0.40 percent, respectively. On top of that, the deposit facility rate was set at a negative 0.10 percent. During the press conference on the very same day, which sets the beginning of the NIRP in the euro area, Draghi (2014) stated that, according to him, the "lower bound was reached", but he did not rule out the possibility of potential future "technical adjustments".

As we can see in figure 1, to date we witness four downward adjustments in the deposit facility rate (currently at negative 0.5 percent) after the initial cut in June 2014, as well as two downward adjustments in the marginal lending facility rate (currently at positive 0.25 percent), and two downward adjustments in the marginal refinancing operation's rate (currently at a zero-rate). Regardless the cuts being in negative territory, Bech and Malkhozov (2016) argue negative interest rates have been transmitted to the money market exactly as normal (i.e. in positive territory) interest rate cuts do, with the EONIA moving as well in negative territory from August 2014. Figure 1 is also quite useful to spot differences between the dynamics of interbank rates before and after the breakthrough of June 2014. From January 1999 to 2014, we witness significant volatility in both the EONIA and the $EURIBOR_{1m}$, with the EONIA remaining attached to the MROs rate until the peak of October 2008, a signal of the notorious liquidity troubles in money markets during the global financial crisis. Due to the unconventional measures adopted by the ECB to keep at bay the effects of the financial crisis[15] and then the sovereign debt crisis we witness a consistent downshift of the corridor, with the EONIA floating at a level which is very close to the corridor's floor, reflecting the great amount of liquidity in the system. The introduction of the NIRP narrowed the corridor and accentuated the downward

[14] The uncertainty of the lag period between the central bank's action and the actual effect on interest rates is a big issue in monetary policy making, but it is outside the focus of this dissertation

[15] For example, along with low policy rates, the unlimited credit provided to financial institutions through "fixed rate full allotment" on all the refinancing operations (see ECB 2010) was one of the first measures that enhanced the liquidity provision to the interest rate channel.

pressure on the EONIA. Indeed, although the corridor is not violated when its floor is negative, the so-called "stickiness" of interbank rates to the corridor's floor is quite evident.

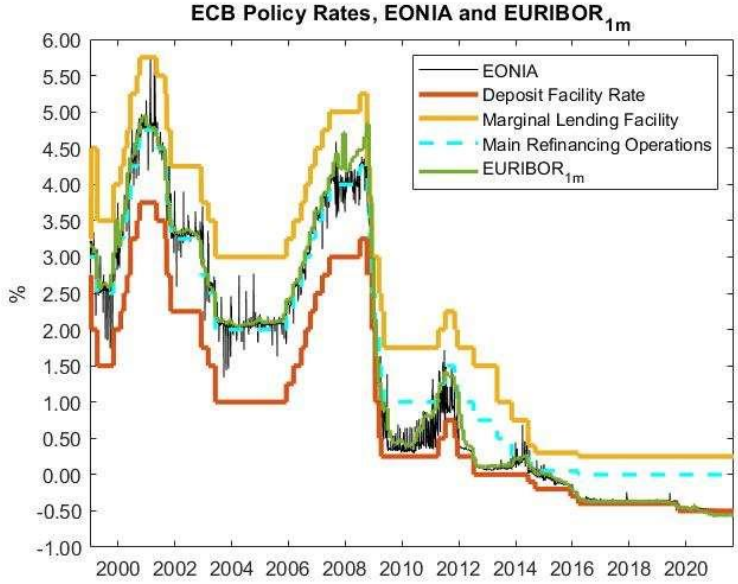

Figure 1. EONIA, $EURIBOR_{1m}$, and Policy Interest Rates: 04/01/1999 – 31/08/2021. Market holidays dates not considered.
Source: Statistical Data Warehouse, European Central Bank. Available at: **https://sdw.ecb.europa.eu/**

We will come back to these issues in interest rates' dynamics in chapter 3 to discuss how they affects the most common continuous-time short rate models, but figure 1 already provide us with some good intuitions that are worth of notice. In particular, we anticipate three elements which characterized interest rates' dynamics after the negative interest rate breakthrough:

-The traditional idea of a zero lower bound is nowadays outdated, as it is replaced by the idea of a negative, and possibly time-varying, lower bound. Thus, the real question concerns where the lower bound actually lies.

-Interest rates float in negative territory for very long periods of time;

-They tend to be quite stable and almost attached to the (negative) monetary policy lower bound. As we can see graphically, this is true not just for the EONIA, but for the $EURIBOR_{1m}$ as well, which "breaks" the floor of the deposit facility rate at the beginning of 2021.

The credit channel

Once the corridor has been set, the main objective of the ECB is to pass negative interest rates to the credit activity, in order to stimulate borrowing from corporations and households. Beyer at all. (2017) explain that as inflation do not react immediately to changes in interest rates, the real cost of borrowing charged on corporate loans and household mortgages will decrease, encouraging credit and purchase of goods and services. This will in turn boost production, demand for labour and finally the level of prices. However, as pointed out by Arteta

et al. (2016), the "pass through" may not be so straightforward, as financial institutions may be reluctant to lend, given the erosion of interest income and the credit risk being entirely on their shoulders. On the other hand, policy rates affect banks' interest expenses as well, by making it cheaper to gather funding liquidity both in terms of retail deposits and general wholesale funding. However, up to date, negative interest rates have not been charged to depositors in a relevant way,[16] as this may trigger substantial deposit withdrawing by those for which cash is a valid option.

Arteta et al (2016) continue that lower rates on loans and mortgages actually reflect banks' cheaper wholesale funding, while banks which have a predominant share of deposit funding struggle to reduce rates on interest earning assets, as it would further shrink their profitability. This is confirmed also in more recent studies, such as ECB (2020a), which include in the analysis interest rate cuts subsequent to 2016: banks with a more heterogeneous funding have been able to reduce interest expenses and preserve their intermediation margin, while banks whose funding structure is mainly deposits (retail and corporate) find it more difficult to (proportionally) reduce their interest expenses when facing cuts in interest income. ECB (2020a) denotes how the problem may become significant in case negative rates persist overtime, eventually leading those credit institutions to change their funding structure. Finally, the uncertainty regarding retail deposit's lower bound is amplified by deposits and cash not being perfect substitutes, given the fact that banks provide payment services that would not be accessible with cash-only, that is "this convenience has an intrinsic monetary value" ECB (2020a).

Other transmission channels

To underline how the different channels are connected with each other, we provide some hints about other transmission channels linked with the very first NIRP packages of June 2014. Arteta et al. (2016) argue that *asset prices and wealth channels* definitely play a role. More specifically, in response to lower interest rate levels, investors may increase purchases, and thus valuations of risky instruments (such as equities) which in turn could prompt investments by the issuing firms and by the holders of such instruments. On top of that, Beyer at all. (2017) add that valuation effects impact on collaterals' values, with consequences on credit activities, meaning the amounts that can be borrowed against the affected collateral. In such a context, we may witness the so-called "*wealth effect*": portfolio's value of risky instruments become more valuable, making owners wealthier and more prone to increase their consumption's level.

[16] As we discussed in section 1.4 negative rates were mostly applied on large-sized current accounts.

Additionally, the *risk-taking channel* induce risk seekers in a low-rates environment to look for higher-return opportunities. These types of investments may lead to a further ease of financing towards riskier activities as well, allowing the liquidity stimulus to expand in the economy not only via banking system. In this regard, notice how a cut in interest rates could create downward pressure on the longer-maturity rates of the yield curve, potentially leading to its inversion. This is due to market agents which anticipate (or react to) interest rates' cuts and try to "lock in" the long-term rates currently prevailing in the market. The same intuition applies for the return-seeking agents, thus creating an upward pressure on long term bond prices. As the ECB (2020a) suggests, this allows the monetary accommodation to spread over the whole terms structure, and not just to the short end of the yield curve.[17] Finally, among the transmission channels employed by the ECB's NIRP package of June 2014, we find the *money channel*, that is called upon by the preparatory work for the APP[18] and the TLTRO introduction,[19] but also the *expectation channel*, regarding which the forward guidance given by the ECB's president by not excluding further cuts, was a fundamental element.

1.4. The effects of negative interest rates on economic agents

The first market agents which are directly affected by the monetary policies are, of course, the commercial banks. We have already mentioned that the erosion of interest income cannot be fully compensated by the cheaper funding costs, especially for those intermediaries relying mostly on retail deposits. However, the European banking survey of the first quarter 2020 provides additional details. Specifically, in ECB (2020b)[20] we see the majority of the institutions claim the negative deposit facility rate (included the two-tier system[21]), has affected their profitability mostly because of the lower lending rates across all the different loan categories. On the other hand, lending volumes towards enterprises increased, as well as housing loans and consumer credit. The results of the survey are confirmed by empirical analysis as well. Klein (2020), by means of data of euro area banks, shows the positive association between net interest margin and lending that we normally observe does not hold (i.e. it becomes statistically insignificant) in periods of short-term negative rates. The intuition

[17] Theoretically speaking, the effects on the long end of the yield curve described above are also coherent with the expectation hypothesis: persistent negative/low short-term rates should lead to lower long-term rates as well. As a matter of fact, ECB (2020) argues that after June 2014 agents expectations about future short-term rates have a non-negligible probability of being negative, and the further cuts increased the likelihood that the June 2014 cuts were not temporary.

[18] The package has laid the foundations for the APP, which subsequently led to a consistent increase in the monetary base.

[19] Theoretically, more lending should imply, via monetary multiplier, an increase in money supply (see Beyer at al. 2017).

[20] The questions were made from the 19th of March 2020 to the 3rd of April 2020, and it explicitly asks ad-hoc questions regarding the impact of the negative DFR (along with the two-tier system) on profitability over the last and the next 6 months.

[21] The two-tier system was introduced by the ECB on the 30th of October 2019. For each institution is calculated an "allowance", that is an amount of reserves, in excess of the compulsory ones, to which it is applied a remuneration of zero percent. See: https://www.ecb.europa.eu/mopo/two-tier/html/index.en.html

is that increasing the credit activity with the aim of offsetting the margin's erosion helps banks to support profitability. Notice the profitability issue and the uncertainty regarding the duration of negative rates concerns insurance companies, investment funds and pension funds as well. By promising (or aiming) at providing consistent returns to investors, they may not be able to cover the interest liability with a sufficiently high interest income. Intuitively, the issue is more serious compared to banks: if the latter may implement internal reorganizations, cost-cutting, or cross subsidization,[22] pension funds or insurance companies cannot rely in the same way on these strategies. On top of that, pension funds are typically required to invest a given share of their liquidity in top-rated instruments, which are not quite profitable in a low-rate environment.[23]

Along with financial institutions, the NIRP have mixed effects on depositors and firms: the stimulation of the credit channels favour their access to credit, but, on the other hand, depositors and firms' will earn no interest on their deposits, especially on the demand ones. The problem is amplified for corporations, whose cost of cash storage is higher compared to depositors. So far, we do not witness negative rates applied to demand deposits of regular savers in the euro area, but there have been cases concerning the demand deposits of the wealthiest clients.[24]

Finally, governments, especially the ones with a high debt-to-GDP ratio, do benefit from the general low-interest context. However, the negative policy rates of the central bank are not the primary determinant of the government's ability to raise cheap funding. Among various reasons, we find the implementation of large-scale asset purchase programs (particularly relevant for the euro area governments), but also the great worldwide demand of safe assets and the attractiveness of medium-high yields of government bonds. For what concerns the latter, even if a government's security is not top rated, it may be seen as profitable, and relatively safe, compared to risky assets issued by other market agents. It is therefore difficult to quantify the effects of the NIRP per se' on government bond yields, but for sure governments are the true winners in such an environment. In front of a consistent drop of OIS rates and sovereign bond yields from the first cuts in June 2014 to the end of 2019, Giacomo Carboni, Wolfgang Lemke and Daniel Kapp estimated the isolated effect of the NIRP on sovereign bond yields by the end of 2019, reaching the conclusion that the two-year maturity and the ten-year maturity yields

[22] Since their business model also concerns the provision of payment services, banks can either charge higher fees and commissions or sell new types of product and services to customers which have been attracted by low-interest loans, high-interest certificates of deposit, and so on.

[23] For example, the German 30-year bund was sold at an average yield of negative 0.11% for the first time at an auction in August 2019. See: https://www.reuters.com/article/germany-auction-idUSL5N25H29G

[24] For example, UniCredit in Italy. See: https://www.reuters.com/article/us-unicredit-rates-idUSKBN1WT1L1

have been lowered by around 40 basis points and 35 basis points, respectively. For further details, see ECB (2020a), Article 2.

CHAPTER 2

2. Short rate models in continuous time

In the following we provide the theoretical framework of the continuous-time short rate models. We start from the most important concepts of interest rate theory, such as basic definitions and zero-coupon bonds' valuation, ending up discussing the Vasicek and the Hull-White models. Although the empirical analysis of this dissertation is not focused on pricing applications, we think it is important to present the fundamental ideas of arbitrage-free pricing theory, in particular with respect to zero-coupon bonds. The purpose is to highlight the importance of the (risk-free) short rate path and its evolution over time in bonds and interest rate derivatives' valuation. For the discussion of section 2.1. we mainly refer to the definitions of Björk (2009), Brigo and Mercurio (2006). We use Hull (2014) as a main reference for what concerns OIS rates.

2.1. Basic concepts and notation

The first element to consider in zero-coupon bond pricing theory is the concept of (risk-free) "short rate". In facts, as it will be clearer ahead in the chapter, bond prices entirely depend on the path of the short rate under the Q-measures.

Definition: The *short rate* at time t denoted by $r(t)$ is the instantaneous spot rate prevailing at time t for the interval $[t, t+dt]$ where dt is an infinitesimal period of time. The short rate $r(t)$, under the P-measures, is the solution of the following SDE:

$$dr(t) = \mu\big(t, r(t)\big)dt + \sigma\big(t, r(t)\big)dW^P(t) \tag{2.0}$$

where $dW^P(t)$ is the infinitesimal change of a Wiener process under the P-measures at time t.

Definition: The value at time $t \geq 0$ of a ***money market account*** B_t, also commonly referred to as *bank account*, can be defined as:

$$\mathrm{B_t} = \exp\left(\int_0^t r(s)ds\right), \tag{2.1}$$

where:

$$\begin{cases} dB(t) = r(t)B(t)dt \\ B(0) = 1 \end{cases}. \tag{2.2}$$

This means that investing 1€ at time zero in a bank account paying a stochastic interest rate $r(t)$ on a continuous basis, yields to a bank account value equal to (2.1) at time $t \geq 0$. The rate

$r(t)$ paid by the bank is considered "risk-free", and it is an instantaneous spot rate (i.e. short rate).

Definition: A ***zero-coupon bond*** with maturity time T, also known as *T-bond* or *ZCB bond*, is a contract which pays a *face value* of one unit of currency at time T, with no intermediate payments. Its price at a generic time t is indicated as $P(t,T)$, and $P(T,T) = 1$ for every T.

The value of $P(t,T)$ is fundamental for what concerns bond pricing theory, since every coupon-bond, under the assumption of the existence of a market for all possible T-bonds, can be evaluated as a composition of T-bonds. In facts, what we observe in the market are mainly *coupon bonds*, that guarantee the bondholder a stream of cash inflows which is typically predetermined. For further details see Björk (2009), section 22.3.

As we will see in the following section, the price of zero-coupon bonds and thus coupon bonds depends only on the underline path of the short rate, meaning their value *derives* from the short rate. However, in financial markets, bonds are not considered to be actual derivative contracts. Among the latter, a fundamental derivative contract in interest rate theory is the *interest rate swap.* We provide the definition of such instrument in its elementary and most common form.

Definition: An ***interest rate swap*** is a derivative contract entered at T_0 with ending date T that obliges its buyer to exchange fixed payments for floating payments at pre-determined points in time over the interval $[T_0, T]$. The fixed payments, commonly referred to as the *"fixed leg"* of the swap, are anchored to a fixed rate R, known as *swap rate*, while the floating ones are indexed to a reference rate, and they are referred to as the "*floating leg*" of the swap. Typically, the reference rate is an interbank rate, such as the Libor or the Euribor, and both the swap rate and the reference rate are applied to a pre-determined principal value K.

By assuming equally spaced payment dates T_i for $i = 1, \dots, n$, where $T_n = T$ and $T_i - T_{i-1} = \delta$, and assuming a Euribor spot rate, indicated as $E(T_{i-1}, T_i)$,[25] as a reference rate, the floating payment at a generic time T_i will be equal to

$$E(T_{i-1}, T_i)\delta K \ ,$$

where

$$E(T_{i-1}, T_i) = -\frac{P(T_{i-1},T_i)-1}{(T_i - T_{i-1})P(T_{i-1},T_i)} .$$

[25] Notice the Euribor spot rate $E(T_{i-1}, T_i)$ is quoted at time $i-1$ for the for the interval $[T_{i-1}, T_i]$, but the payment occurs only at time T_i.

The fixed payment will instead be

$$R\delta K \ ,$$

and the net cash flow at time T_i will finally be equal to

$$\delta K[E(T_{i-1}, T_i) - R] \ .$$

Björk (2009), section 22.3.3 indicates that, using a cash flow replication argument by means of a self-financing bond strategy, the value $\pi(t)$ at time $t < T_0$ of an interest rate swap can be expressed as

$$\pi(t) = K \sum_{i=1}^{n} [P(t, T_{i-1}) - (1 + \delta R)P(t, T_i)] \ .$$

Notice that the value of the swap rate R is determined at the time of creation of the contract t, which we assume to be equal to the starting date of the swap T_0. Thus, under the assumption $t = 0 = T_0$, the swap rate R is determined in such a way that $\pi(0) = 0$, that is

$$R = \frac{1 - P(0, T_n)}{\delta \sum_{i=1}^{n} P(0, T_i)} \ .$$

We conclude the discussion regarding swap rates and thus current section by recalling the concept of OIS rates. The reason is that they are commonly perceived to be good approximations of risk-free rates, especially after the global financial crisis proved that the creditworthiness of the interbank market, as well as the governments' one, are not indisputable.

Definition: The ***overnight index swap*** is a particular type of interest rate swap, in which the reference rate of the floating leg is an *overnight index rate*. The fixed rate underlying the fixed leg which makes the value of the swap equal to zero is referred to as "*OIS rate*".[26] The overnight index swap has a starting date T_0 and an ending date T, and both rates are applied to a *notional amount* K.

It has to be noticed that the OIS rate is define over a given period, which is generally the overall time period of the swap. Swaps lasting more than 1 year are typically divided into multiple subperiods, even though the most liquid OIS markets are those of 1-month or 3-month swaps.

A natural question is how the overnight index rate is treated. Normally, the overnight rate, such as the EONIA, against which the OIS rate is exchanged, is typically rolled over day by day (comprised of principal and interests) over the period of reference, thus obtaining the geometric average of the overnight rates. Typically, the payments are settled at the end of the contract

[26] For further details see Hull (2014), section 9.2.

period (or at the end of each subperiod for the swaps lasting more than a year), to avoid actual cash flow exchanges during the lifetime of the contract.

The OIS rate leads us to the *Euribor-OIS spread*, one of the most important indicators of the "health state" of the interbank market. A high spread level suggests the presence of financial stress in the banking sector, with banks struggling in finding counterparties with a good creditworthiness status.

To better understand this concept, consider for example the 3-month Euribor rate. A three-month loan at the spot Euribor rate is the equivalent of a rate paid on a *term deposit*, from which the lender (or depositor) is going to earn the Euribor rate at the end of the 3-month period. In the meantime, the lender has no right for an early redemption of the loan (or deposit). On the other hand, the OIS rate corresponding to the same time period can be thought as a rate paid on a *demand deposit*, the lender has the option to deny the rollover in any point in time (everyday). In this way, the lender is hedged against a potential deterioration of the borrower's creditworthiness.[27] Clearly, the spread between the two reflects the credit risk associated with lending without the option of early repayment, meaning it is the risk premium asked to the borrower. At this point it should be quite clear to the reader the reason why we can think of OIS rates to be risk-free: the implicit option they consider allows the lending party to run a very little default risk while lending money to another. In facts, the risk is now confined in an overnight period of time.

Similarly to yield curves and (other) risk-free curves, we can think of a graphical representation of OIS rates over different maturities T: the ***OIS zero curve***. For what concerns the short end of the curve, the construction is favoured by the liquidity of short-term OIS market. In practice, as explained by Hull (2014), the 1-month OIS rate is interpreted as the 1-month zero risk free rate, the 3-month OIS rate is interpreted as the 3-month zero risk free rate, and so on. If there are OIS contracts divided into multiple subperiods, with settlements at the end of each sub-period, Hull (2014) specifies a swap rate can be interpreted as a par yield bond,[28] so that we can reduce the derivation of the OIS zero curve on a classical bootstrap method in which the periodic settlements are set equal to the principal amount of a (hypothetical) par yield bond. However, the main problem concerns the derivation of the OIS rates for the longest maturities. The typical solution is to consider the spread between the longest maturity OIS rate available (either from market quotations or resulting from the

[27] The intuition is even clearer by noting that the OIS rate is set in such a way that the swap it fairly priced. In other words, it can be seen as the geometric average of the reference rate over the period in question.

[28] This is done by assuming the OIS is fairly priced and its underlying fixed and floating legs are the equivalent of a fixed coupon bond and a floating bond, respectively. A further assumption is the former pays the OIS rate and, at the same time, the OIS curve is used for discounting. This means its value is equal to its principal. See Hull (2014), sections 7.6 and 9.2.

bootstrap method) and the "LIBOR/EURIBOR zero curve"[29] at the same maturity. Thus, the spread is assumed to be the same for all longer maturities, meaning the long end of the OIS curve is derived from the LIBOR/EURIBOR zero curve adjusted for the calculated spread.[30]

2.2. Pricing zero-coupon bonds in an arbitrage-free market

For this section, our main reference is Björk (2009) and Brigo and Mercurio (2006). Occasionally, we will also refer to Hull (2014). In the following sub-sections we will provide some hints about zero-coupon bond pricing theory, as well as the difference between P-measures and Q-measure. A necessary premise to be made is that we assume the existence of a zero-coupon bond arbitrage-free market for every maturity T, its frictionless nature, and the differentiability of all $P(t,T)$ with respect to maturity T. A further assumption requires the presence of the money market account described in (2.1) and (2.2). It will work as a risk-free asset in the bond market we just described.

2.2.1. The term structure equation

Before providing the treatment that leads to the term structure equation, it is useful to clarify the notation and the exact meaning that is given in this dissertation to the words "term structure" and "term structure equation", as many times they are object of confusion in the literature. The "*term structure"* is the function which associates a given maturity T to $P(t,T)$. Consequently, it represents how the bond price varies across different maturities. Instead, with the term "*term structure equation*" we define the PDE satisfied by the pricing function of a ZCB, for an arbitrary maturity T.

In order to find a pricing formula which allows us to solve the term structure equation that we are going to derive, it is important to start with a *basic intuition*: in an arbitrage free zero-coupon bond market, bond prices at different maturities must be consistent with each other, i.e. they must prevent any market agent to exploit profitable opportunities. As a consequence, if we manage to price a "reference" bond, we should be able to price all the others as long as they have shorter maturities.

The full treatment provided by Björk (2009) in section 23.2 is generally composed by three steps. First of all, we assume that the price of a pure discount bond (a T-bond) with maturity T, is a smooth function of time t and the short rate $r(t)$, whose SDE is (2.0). Formally, we express

[29] Interbank market rates' maturities, such as the LIBOR and the EURIBOR are available up to 12 months. However, the LIBOR/EURIBOR zero curve is derived by means of quoted swap rates. See Hull (2014), section 7 for additional details about the derivation of the LIBOR/EURIBOR zero curve.

[30] The same technique is implemented when long time series of OIS rates are needed. Since OIS rates became widespread from 2005/2006, if one needs the OIS curve prior the year in which the first OIS curve is available, a "spread-based" construction can be implemented.

$$P(t,T) = F^T(t, r(t)) \,. \tag{2.3}$$

Secondarily, consistently with what we said in the previous section, and given (2.3) we can write

$$F(T, r) = 1. \tag{2.4}$$

where r indicates any of all the possible realizations of the process $r(t)$ at $t = T$.

The third step of Björk derivation makes use of the construction of a self-financing portfolio of two bonds with maturities S and T, whose weights u_S and u_T make it risk-free. The weights are to be determined and $S < T$. By applying Itō's formula to (2.3), we respectively get the following dynamics for the T-bond and for the S-bond

$$dF^T = F^T \alpha_T dt + F^T \sigma_T d\mathrm{W}^{\mathrm{P}}, \tag{2.5}$$

$$dF^S = F^S \alpha_S dt + F^s \sigma_S d\mathrm{W}^{\mathrm{P}} \,, \tag{2.6}$$

where,

$$\alpha_T = \frac{F_t^T + \mu F_r^T + \frac{1}{2}\sigma^2 F_{rr}^T}{F^T} \,, \tag{2.7}$$

$$\sigma_T = \frac{\sigma F_r^T}{F^T} \,, \tag{2.8}$$

with the subscripts r and t in (2.7) and (2.8) indicating partial derivatives. Clearly, (2.7) and (2.8) are in the same form for the S-bond.

We can then express the infinitesimal rate of return of the portfolio,

$$\frac{dV}{V} = \left\{ u_T \frac{dF^T}{F^T} + u_S \frac{dF^S}{F^S} \right\} . \tag{2.9}$$

By substituting (2.5) and (2.6) in (2.9), and by manipulating the equation to separate the drift term from the volatility term, we get

$$dV = V \cdot \{u_T \alpha_T + u_S \alpha_S\} dt + \mathrm{V} \cdot \{u_T \sigma_T + u_S \sigma_S\} dW^P \,. \tag{2.10}$$

At this stage, the weights u_S and u_T must be determined in such a way that the volatility coefficient $\{u_T \sigma_T + u_S \sigma_S\}$ in (2.10) equals zero. This condition, along with the obvious one which requires the weights' sum to equal one, allows us to find:

$$u_T = -\frac{\sigma_S}{\sigma_T - \sigma_S}$$

$$u_S = \frac{\sigma_T}{\sigma_T - \sigma_S}$$

In this way, we rule out the influence of the Wiener component on the portfolio dynamics in (2.10). In other words, by holding the amount u_T of T-bonds and the amount u_S of S-bonds, the portfolio value dynamics is given by

$$dV = V \cdot \left\{\frac{\alpha_S\sigma_T - \alpha_T\sigma_S}{\sigma_T - \sigma_S}\right\} dt \ . \tag{2.11}$$

Under the assumption of no-arbitrage, the infinitesimal return of the riskless portfolio must be equal to the infinitesimal short rate return over the same interval $[t, t + \partial t]$, otherwise arbitrage opportunities would be possible. By formalizing the intuition we obtain

$$\frac{dV}{V} = \frac{\alpha_S\sigma_T - \alpha_T\sigma_S}{\sigma_T - \sigma_S} = r(t), \ \text{for all } t, \tag{2.12}$$

which can be rewritten as

$$\frac{\alpha_S(t) - r(t)}{\sigma_S(t)} = \frac{\alpha_T(t) - r(t)}{\sigma_T(t)} \ . \tag{2.13}$$

Equation (2.13) allows to introduce the fundamental concept of the *market price of risk* in an arbitrage-free bond market. In facts, it has to be noticed the right-hand side of (2.13) is a stochastic process which does not depend on S, while the same stands for the left-hand side with respect to the maturity T. In addition, the equal sign suggests they actually are the *same* process, which is the reason why in the literature it is referred to as *universal*. Let us formalize the intuition.

Definition: In an arbitrage-free bond market, there exist a universal process called ***market price of risk***, that only depends on current time t and on the instantaneous spot rate $r(t)$. It is generally defined as

$$\lambda(t) = \frac{\alpha_T(t) - r(t)}{\sigma_T(t)} \ , \text{for every maturity time } T. \tag{2.14}$$

In plain words, at a given time t, for every possible maturity time T, $\lambda(t)$ assumes the same value.

At this point, the careful reader will notice the numerator is composed by $\alpha_T(t)$, which belongs to the drift term of the T-bond SDE in (2.5), and by the risk-free rate $r(t)$. The former represents the expected rate of return[31] of the T-bond, while $r(t)$ represents the instantaneous profit an individual can make from putting its money in the deterministic bank account. The numerator is therefore quantifying how well the T-bond is (infinitesimally) performing with

[31] We write "expected" rate of return because even though we ruled out stochastic movements in the infinitesimal portfolio return, the T-bond SDE preserves its own Wiener process. Hence, there is a source of randomness.

respect to the risk-free short rate $r(T)$. Additionally, at the denominator we have the volatility $\sigma_T(t)$, that is the risk the same individual takes by investing in the T-bond. As a consequence, the market price for risk may be referred to as "excess return of the T-bond over the risk-free asset per unit of volatility".

To sum up, there are three elements that stand out from the concept of market price for risk:

I. It is independent of the maturity of the T-bond;
II. It depends on current time t and on the short rate $r(t)$, i.e. it changes overtime;
III. It is the risk premium over the risk-free rate per unit of volatility required by the market to the T-bond (for all T) to prevent arbitrage opportunities.[32]

Finally, we can derive the term structure equation by replacing (2.7) and (2.8) in (2.14) and by recalling the boundary condition of (2.4). Let us formalize its definition.

Definition: The ***term structure equation*** of an arbitrage-free zero-coupon bond market, which we can refer to as the *family of bond price processes*, is the following PDE,

$$\begin{cases} F_t^T + \{\mu - \lambda\sigma\}F_r^T + \frac{1}{2}\sigma^2 F_{rr}^T - rF^T = 0\,, \\ F^T(T,r) = 1\,, \end{cases} \tag{2.15}$$

whose solution is the pricing function $F^T(t, r(t))$.

Notice, μ and σ refer to the drift term and the volatility term of the SDE of $r(T)$ in (2.0), while the function $F^T(t, r(t))$ and its partial derivatives have been written without arguments for convenience.

Equation (2.15) is a standard PDE. However, as we pointed out earlier in the section, the market price of risk λ is a function of both the current time t and the instantaneous spot rate $r(t)$. This does not allow to determine λ within the model, so that it is impossible to solve (2.15). To do it, we should exogenously determine the market price of risk λ, as well as μ and σ.

The *risk neutral valuation formula* is derived straight from the term structure equation by means of a Feynman-Kac representation of $F^T(t, r(t))$.[33] In order to do that, we have to fix a point in time t and a point in space, that is $r(t) = r$. By means of Itō's formula applied to the following process

[32] At a given time t, the risk premium per unit of volatility required by the market is the same for all the instruments. In facts, whatever T-bond we consider, it will have dynamics that affect the numerator and the denominator, respectively through α_T and σ_T, in such a way to keep $\lambda(t)$ constant.

[33] Given a PDE with a boundary condition, that in our case is equation (2.15), the Feynman-Kac formula allows to find its solution exploiting the link of the PDE with a naturally associated SDE. For more details we address the reader to the Björk (2009), section 5.5.

$$exp\{-\int_t^s r(u)du\}F^T(s,r(s))\,, \tag{2.16}$$

where the function $F^T(t,r(t))$ satisfies (2.15), we obtain the following:

Definition: The ***risk neutral valuation formula*** of zero-coupon bond prices at a given time t, with realization $r(t)=r$ can be expressed as the risk neutral expected value of the final payoff (i.e. the face value of one unit of currency) discounted at present date t.

$$F^T(t,r)=E_{t,r}^Q\left[e^{-\int_t^T r(s)ds}\cdot 1\right]\,, \tag{2.17}$$

where $F^T(t,r)=P(t,T)$, and the expected value operator is taken under the risk neutral measures Q with the following dynamics of the short rate:

$$\begin{aligned} dr(s) &= \{\mu-\lambda\sigma\}ds+\sigma dW^Q(s)\,, \\ r(t) &= r\,. \end{aligned} \tag{2.18}$$

where $W^Q(s)$ is a Wiener process under the Q-measures.

It will now be clear to the reader the reason why the main result of this section is that bond prices entirely depend on the path of the short rate under the Q-measures.[34] As Björk (2009) points out, bonds are *deterministic contingent claims,*[35] but the risk neutral valuation formula is actually valid for whatever contingent claim depending on the short rate $r(T)$ we consider.

2.2.2. The risk neutral valuation of bond prices

The main result of the previous sub-section is the T-bond pricing function expressed as in (2.17), namely

$$F^T(t,r)=E_{t,r}^Q\left[e^{-\int_t^T r(s)ds}\right].$$

In order to better understand what we mean by taking the expectation $E_{t,r}^Q$, let us focus on the market price of risk in (2.14):

$$\lambda(t)=\frac{\alpha_T(t)-r(t)}{\sigma_T(t)}.$$

[34] The result is the risk neutral valuation principle of derivatives applied to T-bonds. For what concerns derivative contracts, the principle implies that, under the assumption of equality between the expected rate of return of the underlying asset and the risk-free rate, the derivative price is obtained by discounting its expected payoff at the risk-free rate.

[35] Differently from derivative contracts they pay a final payoff that is stochastic, a bond's face value is typically determined at the time of writing the contract.

By simply assuming the market price of risk $\lambda(t)$ equals zero, we obtain $\alpha_T(t) = r(t)$, where $\alpha_T(t)$ is the expected rate of return of the T-bond. This the classical underline assumption of a traditional risk neutral expectation.[36]

However, the derivation of the risk neutral valuation formula in (2.17) by means of a Feynman Kac representation of the pricing function $F^T(t, r(t))$ has shown the existence of alternative risk neutral worlds. In our particular case, the risk neutral measure Q depends not only on time t, but also on the short rate $r(t)$. It is important to point out that the reason for this result relies on the lack of completeness of the bond market we assumed in the first place.[37]

To understand the meaning of the martingale measure Q employed by the ZCB's valuation formula, we should focus on the SDE of the short rate $r(t)$ under the Q-measures. Its dynamics, expressed without arguments for sake of simplicity, are specified as in (2.18):

$$dr(t) = \{\mu - \lambda\sigma\}dt + \sigma dW^Q(t),$$
$$r(t) = r\ .$$

By discounting the final bond payoff at the risk neutral measures $E^Q_{t,r}$, the expectation will be affected not only by time, but also by the dynamics of $r(t)$ under Q. Thus, the market price of risk λ affects the bond's evaluation since it appears in (2.18).

The result is that the way the bond market prices risk is going to affect the bond's valuation. In other words, we have different martingale measures Q for different choices of market price for risk λ, with the latter being in turn affected by plenty of market factors (among which market participants' risk aversion and market forces, such as supply and demand, stand out as main determinants).

Moreover, it can be quickly shown that λ is going to affect the expected return of a T-bond as well. From equation (2.5) we have

$$dF^T = F^T\alpha_T dt + F^T\sigma_T d\mathrm{W}^{\mathrm{P}}\ ,$$

where, α_T and σ_T are given by (2.7) and (2.8).

By expressing (2.14) (and omitting the arguments for convenience) as $\alpha_T = r + \sigma_T\lambda$, and substituting it in the previous equation we get

$$dF^T = (r + \sigma_T\lambda)F^T dt + F^T\sigma_T d\mathrm{W}^{\mathrm{P}}\ .$$

---

[36] If this was the case, we would have simply indicated the expected value operator as E^Q_t (without the "r" subscript).

[37] In our market, the number of exogenously given traded assets without considering the risk-free asset is zero, while the sources of randomness equal one (i.e. the Wiener process). According to the meta-theorem (see Björk (2009), chapter 8), the market is arbitrage-free but not complete, meaning that it is not possible to replicate derivatives, such as a T-bond, with the assets we dispose of.

To some extent, the change in T-bond's price implied by how differently the market prices risk will be reflected by a different expected return of the bond itself. Notice that a change of λ affects the drift term of the T-bond, while the volatility term remains unchanged. This is one face of the Girsanov theorem which we will discuss in the following section.

Finally, it becomes clear that by determining the price dynamics of a T-bond, equation (2.14) allows to retrieve the market price for risk $\lambda(t)$, so that all the other S-bond prices, for $S < T$, can be determined by the term structure equation.

2.2.3. Objective measures and risk neutral measures

The previous section introduced a very clear distinction between the *physical* (or *objective*) measures P, and the *risk neutral* (*risk adjusted or martingale*) measures Q. The former relates to the real world, while the latter refers to a risk neutral world in which all market agents are, indeed, risk neutral. A generic stochastic process $X(t)$ under the objective measures is said to have *P-dynamics*, while under the risk neutral measures it has *Q-dynamics*.

Suppose that the stochastic process in question is the short rate $r(t)$. Once a model for the dynamics of $r(t)$ has been specified either under the Q-measures or the P-measures, its parameters are estimated by means of statistical techniques.[38]

For what concerns pricing applications, risk neutral measures are employed. Thus, the dynamics of the short rate process $r(t)$ must be modelled under the Q-measures. As suggested in Hull (2014), this is done by employing a cross-section of market data, such as bond prices, at a given time. In this way, we obtain the parameters estimates in the (artificial) risk neutral world according to the way the market "maps" prices in that point in time. One technique to calibrate models under the Q-measures is the minimization of the sum of squares of the difference between the data observed and the one predicted by a model.

Instead, for what concerns risk management applications, that is modelling the future, the dynamics of the short rate $r(t)$ must be modelled by means of time series of market data. The intuition is that by looking at the past history in the real (subjective) world we are able to predict its future, by incorporating in the model movements in interest rates that reflected "actual" expectations and distributions. This can be done either through regression methods of the change in rate on the rate level, or by means of maximum likelihood estimations.

2.2.4. The Girsanov theorem

A very important theorem to reconcile the real world with the risk neutral world is the *Girsanov theorem*, which concerns how to define the dynamics of a P-Wiener process under the Q-measures. In plain words, the theorem shows how the SDE of a process is affected by

[38] For example, what we employ in chapter 4 for our analysis is a Maximum Likelihood Estimation with Extended Kalman Filter.

changing its measure of reference. For a detailed derivation of the Girsanov theorem we address to Björk (2009) from section 11.2 to 11.5. Formalizations of the theorem can be find in Musiela and Rutkowski (1998), Appendix A and Brigo and Mercurio (2009), Appendix C.5. Here, we just enunciate the final result.

Björk (2009) derives the following result for the Girsanov theorem:

$$dW^P(t) = \varphi(t)dt + dW^Q(t), \tag{2.19}$$

with φ being a vector process and W^Q being a Wiener process under the Q-measures.[39] Therefore, for what concerns the Girsanov transformation towards the risk neutral measures of a generic process $X(t)$ with P-dynamics given by

$$dX(t) = \mu(t)dt + \sigma(t)dW^P(t), \tag{2.20}$$

the Girsanov theorem allow us to retrieve the corresponding Q-dynamics with a simple substitution of (2.19) in (2.20). The drift term will be affected, while the diffusion term will be invariant. By expressing the time-dependence with subscripts, we obtain

$$dX_t = (\mu_t + \sigma_t\varphi_t)dt + \sigma_t dW_t^Q.$$

As a matter of fact, we have already encountered this result in section 2.2.1. During the derivation of the term structure equation, the dynamics of the short rate $r(t)$ (both expressed without arguments for sake of simplicity) were specified as:

$$dr(t) = \mu dt + \sigma dW^P(t) \text{ , under the P-measures}$$

and

$$dr(t) = \{\mu - \lambda\sigma\}dt + \sigma dW^Q(t), \text{ under the Q-measures.}$$

The Q-dynamics differ from the P-dynamics just in the drift term because of the appearance of the market price of risk, with the volatility coefficient σ being equal. This result is indeed explained by the Girsanov Theorem.

We conclude the section by underlining the fact that the drift terms of the two SDE above, can be estimated *directly* by using the proper dataset, that is either a cross section for martingale modelling or a time series for what concerns the real world. To put it differently, μ, λ and σ are not estimated on a stand-alone basis, but they are implicit in the model's estimates. Brigo and Mercurio (2006) suggest a combination of statistical techniques can sometimes be useful: by

[39] For derivation purposes it is fundamental to define a likelihood process *L* under some particular assumptions, such as the one that L is a martingale. However, we do not enter in the details of the derivation, as what is important for our purposes is the Girsanov result.

exploiting the fact that σ is invariant, one can estimate its value under the P-measures and then estimate just μ and λ under Q. It is also common to use the historical σ as an initial estimate when a starting value is required by the statistical technique employed.

2.3. The Vasicek model and the Hull-White model

Given the importance of the short rate for pricing contingent claims as well as for risk management applications, there is a vast literature covering short rate models.[40] In this section we are going to discuss the Vasicek model and the Hull-White model, as they turned out to be suitable for the shadow rate model that we will present in the next chapter. We follow the notation of Brigo and Mercurio (2009) that is our main reference together with Björk (2009) and Musiela and Rutkowski (1998). In line with the literature, we discuss both models under the risk neutral measures Q.

2.3.1. The Vasicek model

In the ***Vasicek model***, that was introduced by Vasicek (1977), the short rate dynamics under the Q-measures[41] are defined as an *Ornstein-Uhlenbeck* process:

$$dr(t) = k[\theta - r(t)]dt + \sigma dW^Q(t), \qquad (2.21)$$
$$r(0) = r_0 \ ,$$

where the parameters k, θ , σ and r_0 are constant and positive.

Equation (2.21), is a *linear SDE*, thus it makes it is possible to easily derive its *unique solution*.[42] The process $r(t)$ described by the SDE in (2.21), obtained using Itō's lemma, is

$$r(t) = r(s)e^{-k(t-s)} + \theta\left(1 - e^{-k(t-s)}\right) + \sigma \int_s^t e^{-k(t-u)} dW^Q(u), \qquad (2.22)$$

for any $s \leq t$.

Given a set of information available at time s, denoted as the filtration $\mathcal{F}_S$, the conditional mean and variance of $r(t)$ under Q will be respectively[43]:

$$E[r(t)|\mathcal{F}_S] = r(s)e^{-k(t-s)} + \theta\left(1 - e^{-k(t-s)}\right) \qquad (2.23)$$

$$Var[r(t)|\mathcal{F}_S] = \frac{\sigma^2}{2k}\left[1 - e^{-2k(t-s)}\right]. \qquad (2.24)$$

Along with the linearity of the SDE, another important feature of an *Ornstein-Uhlenbeck* process is the *Gaussian property*, which favours the analytical tractability of the model. In

[40] We suggest Brigo and Mercurio (2009), chapter 3 for a detailed overview of short rate models. An alternative reference is Musiela and Rutkowski (1998), chapter 10.
[41] The model was originally introduced by Vasicek (1977) under the real-world measures.
[42] See Musiela and Rutkowski (1998), Lemma 10.1.2. The hint is to apply Itō's lemma to the process $Y_t = r_t e^{b(t-s)}$ with $t \geq s$.
[43] See Musiela-Rutkowski (1998), Lemma 10.1.2 for the derivation. The conditional mean and the conditional variance are derived by exploiting respectively the zero mean property and the Itō's isometry of the Itō's integral in (2.22).

particular, $r(t)|\mathcal{F}_S$ is normally distributed with *mean* and *variance* respectively given by (2.23) and (2.24).

Additionally, Musiela and Rutkowski (1998), point out that the limits which tend to infinity of (2.23) and (2.24), whose derivation is quite straightforward, are the following:

$$\lim_{t\to\infty} E[r(t)|\mathcal{F}_S] = \theta\ ,$$

$$\lim_{t\to\infty} Var[r(t)|\mathcal{F}_S] = \frac{\sigma^2}{2k},$$

concluding the short rate $r(t)$ has a *stationary distribution,* that is the Gaussian $N\left[\theta, \frac{\sigma^2}{2k}\right]$. On the other hand, as a direct consequence of the Gaussian distribution there are probabilities greater than zero for the short rate $r(t)$ to take negative values at any time t.[44]

Notice the parameter θ is sometimes referred to as the "*long run mean*" of the process. Indeed, it is clear the *mean reversion* of $r(t)$: when at a given time t the process $r(t)$ assumes a value lower than θ, the drift term of (2.21) will be positive, and it will be negative when $r(t)$ is greater than θ. The magnitude of the drift term, and thus the push given to the process towards the long run mean, is amplified or reduced by the parameter k, which is also called "*speed of reversion*".

The Gaussian property make the model very tractable from an analytical point of view. In particular, it is quite easy to calculate bond prices, and consequently spot rates and forward rates. From the previous section we know that a ZCB price is given by

$$F^T(t,r) = E^Q_{t,r}\left[e^{-\int_t^T r(s)ds}\cdot 1\right].$$

Björk (2009), in the context of a Gaussian short rate process, suggests a first ZCB pricing method: since the integral of the discount factor (i.e. $e^{-\int_t^T r(s)ds}$) is obviously a sum, the Gaussian property of $r(t)$ is transmitted to the integral. Thus, bond prices can be computed as the expectation of a log-normal stochastic variable.

Alternatively (and principally), Björk (2009) also provides the following result[45]:

Definition: The ***term structure***, meaning the graphical representation of $P(t,T)$ at any given point in time t, over all the possible maturities T can be expressed as:

$$P(t,T) = e^{A(t,T)-B(t,T)r(t)}, \qquad (2.25)$$

[44] In Vasicek (1977) and, more generally, up to a decade ago this possibility was seen as a great limitation of the model. In the next chapter we will discuss how and to what extent this limitation can actually be an advantage.

[45] The formula (2.25) is provided by Björk (2009), sections 24.3, 24.4. Additional derivations are provided by Musiela and Rutkowski (1998), chapter 10.
Note that Björk (2009) exploits the "affine term structure" form of the Vasicek model, as well as Musiela and Rutkowski (1998), Proposition 10.1.3.

where

$$B(t,T) = \frac{1}{k}\{1 - e^{-k(T-t)}\},$$

$$A(t,T) = \frac{\{B(t,T) - T + t\}\left(k^2\theta - \frac{1}{2}\sigma^2\right)}{k^2} - \frac{\sigma^2 B^2(t,T)}{4k}$$

Short rate models whose ZCB prices are expressed as in (2.25) are said to have an "*affine term structure*".[46] In Appendix A we (partially) derive this form in order to provide the logic behind the ZCB price formulas under the Vasicek and the Hull-White model.

Although the Vasicek model is quite tractable, there is a major issue in its practical feasibility concerning the *inversion of the yield curve,* meaning the estimation under the Q-measures of the set of parameters of a chosen short rate model, like the Vasicek one. By denoting the parameter vector $\alpha = [k, \theta, \sigma]$, we can express (2.21) in general terms as

$$dr(t) = \mu(t, r(t); \alpha)dt + \sigma(t, r(t); \alpha)dW^Q(t),$$

and, by solving the term structure equation (2.15), we can derive the *theoretical term structure*, namely $T \to P(t,T;\alpha)$, for all the possible values of T. If at $t = 0$ (i.e. today) we retrieve from market data the *empirical term structure*, that we denote as $T \to P^*(0,T)$, we can estimate, by means of an optimization algorithm, the parameter set α^*in such a way $T \to P(0,T;\alpha^*)$ best fits $T \to P^*(0,T)$.

Leaving aside the potential computational burden of this approach, the finite number of parameters to be estimated does not allow the theoretical term structure $T \to P(0,T;\alpha)$ to perfectly fit the observed term structure $T \to P^*(0,T)$, especially when the latter assumes "particular" shapes relative to the classical one. As the literature indicate, in facts we are dealing with a system composed by one equation for each possible maturity, meaning a system with an infinite number of equations and a finite number of parameters to be determined. Since the problem lies in the finite number of parameters, the issue will be there regardless of the calibration method employed, the number of maturities T considered, and the parameters' values obtained.

Intuitively, the solution is to introduce in the model an infinite number of parameters, that is equivalent to include a deterministic function of time, so that we improve the fit between the theoretical (and time-dependent) term structure $T \to P(0,T;\alpha(t))$ and the empirical term

[46] Terminology could be misleading. The term "affine term structure" used in the literature refers to the expression of the continously compounded spot rates implied by the short rate model and, indeed, affine in the short rate. However, in our dissertation, with the word "term structure" we refer to the family of prices of a ZCB over all the possible maturities. For further details regarding the affine term structure models (as affine in the short rate) we address to Brigo and Mercurio (2009), section 3.2.4.

structure $T \to P^*(0,T)$. This is the reason that led practitioners to prefer time-dependent parameters models over time-homogenous models (that is, with constant parameters)[47], as they allow to perfectly reproduce the initial market term structure $T \to P^*(0,T)$.[48]

2.3.2. The Hull-White (extended Vasicek) model

The Hull-White model is the time-varying version of the Vasicek model. We present one of its most popular version, by allowing the parameter θ of (2.21) to be deterministic and dependent on time.[49]

The short rate dynamics under the Q-measures are defined as

$$dr(t) = [\theta(t) - ar(t)]dt + \sigma dW^Q(t), \tag{2.26}$$

where θ is determined to perfectly fit the current observed term structure, while the parameters a and σ are constant and positive.

In order to fit the empirical term structure, it is more convenient to make a comparison between *forward rates* term structures[50]. More precisely, we want to fit the theoretical forward rate term structure denoted as $T \to f(0,T)$, with the empirical one $T \to f^*(0,T)$, where $f^*(0,T)$ denotes the market instantaneous forward rate at $t = 0$ for a maturity T, associated to the observed bond price $P^*(0,T)$. We express it as

$$f^*(0,T) = -\frac{\partial \ln P^*(0,T)}{\partial t},$$

It is shown[51] that θ must be determined as:

$$\theta(t) = \frac{\partial f^*(0,t)}{\partial t} + af^*(0,t) + \frac{\sigma^2}{2a}(1 - e^{-2at}), \tag{2.27}$$

where $\frac{\partial f^*(0,t)}{\partial t}$ is the partial derivative of the market instantaneous forward rate $f^*(0,t)$ with respect to time. Equation (2.27) allows the theoretical term structure to perfectly fit the one observed in the market, meaning $T \to P(0,T)$ will equal $T \to P^*(0,T)$, for all the possible T.

---

[47] Brigo and Mercurio (2009) define time-homogeneous models as "endogenous" because of the (endogenous) predicted term structure they produce which does not perfectly fit the observed one. At the same time, short rate models with time-varying parameters are defined as "exogenous", because of the exogenous nature of their predicted term structure.

[48] As pointed out by Hull (2014), time-homogeneous models can still be valid for simulations over long horizon, in particular for those applications in which the current term structure is not particularly important.

[49] This is the simplest version of the Hull-White model, with the only parameter θ to be time-dependent. However, the model was originally presented in the version which allows all parameters to depend on time. See Hull and White (1990).

[50] To understand how to reconcile a forward term structure with a price term structure see Björk (2009) Lemma 22.4. In short, the relationship between forward rates and bond prices is specified as $P(t,T) = exp\left\{-\int_t^T f(t,s)ds\right\}$.

[51] For the derivation of the equation (3.11) we suggest to Björk (2009), section 24.4.4, where the derivation is based on the affine term structure form of the Hull-White model. Alternatively, a derivation of the Hull-White model and thus of equation (3.11) is provided by Hull (2004), Technical Note No. 31 that can be find at the following link: http://www-2.rotman.utoronto.ca/~hull/technicalnotes/TechnicalNote31.pdf

Similarly to the Vasicek case, from the linear SDE in (2.26) we can derive a *unique solution.*[52] The process $r(t)$ described by the dynamics in (2.26), for any $s \leq t$, is

$$\begin{aligned} r(t) &= r(s)e^{-a(t-s)} + \int_s^t e^{-a(t-u)}\theta(u)du + \sigma\int_s^t e^{-a(t-u)}dW^Q(u) \\ &= r(s)e^{-a(t-s)} + \alpha(t) - \alpha(s)e^{-a(t-s)} + \sigma\int_s^t e^{-a(t-u)}dW^Q(u) \end{aligned} \tag{2.28}$$

where

$$\alpha(t) = f^*(0,t) + \frac{\sigma^2}{2a^2}(1-e^{-at})^2.$$

Given a set of information available at time s, denoted as $\mathcal{F}_S$, the conditional mean and variance of $r(t)$ under Q will be respectively[53]:

$$E[r(t)|\mathcal{F}_S] = r(s)e^{-a(t-s)} + \alpha(t) - \alpha(s)e^{-a(t-s)} \tag{2.29}$$

$$Var[r(t)|\mathcal{F}_S] = \frac{\sigma^2}{2a}\left[1-e^{-2a(t-s)}\right]. \tag{2.30}$$

We recall an *Ornstein-Uhlenbeck* process like the one in (2.26) has the *Gaussian property*, that is $r(t)|\mathcal{F}_S$ is normally distributed with *mean* and *variance* respectively given by (2.29) and (2.30). As a consequence, normality allows $r(t)$ to take negative values for every time t with positive probability.

Finally, we are now going to define the term structure of bond prices in the Hull-White model. By referring to Björk (2009) we provide the following definition:

Definition: The ***term structure*** $P(t,T)$ at any given point in time t, over all the possible maturities T can be expressed as:

$$P(t,T) = e^{A(t,T)-B(t,T)r(t)},$$

where $A(t,T)$ and $B(t,T)$ are the solutions of

$$\begin{cases} B_t(t,T) = aB(t,T) - 1\,, \\ B(T,T) = 0. \end{cases}$$

$$\begin{cases} A_t(t,T) = \theta(t)B(t,T) - \frac{1}{2}\sigma^2B^2(t,T), \\ A(T,T) = 0. \end{cases}$$

that are

[52] The first expression of (12) is obtain by Itō's lemma applied to the process $Y(t) = r(t)e^{a(t-s)}$, while the second expression is obtained by substituting (3.11) in the first expression.

[53] As before, the conditional mean and the conditional variance, exploit respectively the zero mean property and the Itō's isometry of the Itō's integral in (3.12).

$$B(t,T) = \frac{1}{a}\{1 - e^{-a(T-t)}\},$$

$$A(t,T) = \int_t^T \left\{\frac{1}{2}\sigma^2 B^2(s,T) - \theta(s)B(s,T)\right\} ds.$$

where θ is expressed in (2.27) and $B_t(t,T)$ is the partial derivative of $B(t,T)$ with respect to time.

CHAPTER 3

3. Shadow rate models in continuous time

3.1. Problems in a negative interest rate environment

Negative interest rate policies are probably the most "revolutionary" unconventional tool implemented by many central banks over the last decade, as it led economists, analysts, and mathematicians to face challenges in terms of interpretation and analytical computation. In particular, there are several drawbacks in applying the classic interest rate models in contexts in which interest rates fluctuate in negative territory. On the other hand, the Gaussian property of the Gaussian models is a necessary pre-requisite to address the problem, but also such models are not immune from shortcomings. In the literature, a common solution is the implementation of the "shadow rate" approach, whose idea was firstly introduced by Black (1995).

3.1.1. The natural zero-lower bound

We now discuss why the classical short rate models are not optimal in modelling the dynamics of the negative rates we observe in the market. Let us list some most common short rate models in the literature[54]:

- Vasicek $dr_t = k[\theta - r_t]dt + \sigma dW_t,$
- Cox-Ingersoll-Ross (CIR) $dr_t = k[\theta - r_t]dt + \sigma\sqrt{r_t}dW_t,$
- Dothan $dr_t = ar_t dt + \sigma r_t dW_t,$
- Hull-White (extended CIR) $dr_t = [\Theta - k_t r_t]dt + \sigma_t\sqrt{r_t}dW_t,$

Models that are log-normally distributed (for example, the Dothan model) or which entail square root processes (for example, the CIR and its Hull-White extension) are not able, by construction, to predict interest rates evolutions in negative regions, as they embody a "natural" zero-lower bound. In practice, there exist methods that permit to these models to describe negative rates, such as shifting methods to allow $r(t)$ to take negative values. This implies

[54] The subscript t denotes time-dependence.

valuation challenges with respect to the shift parameter. However, these techniques are outside the scope of this dissertation.

There are some points to mention regarding the unsuitability of the above-mentioned models. A lognormal process and a square root process, not only rule out negative values for $r(t)$, but do not even allow $r(t)$ to take value of zero. To be more precise, we can underline as in Lemke and Vladu (2016) the difference between the *floor* and the *effective lower bound* (interpreted as the level around which interest rates fluctuate with low volatility during the NIRP): if in the euro area the standing facilities of the ECB denote the cap and the floor of the interest rate's corridor, it is clear that the deposit facility rate (from here on denoted as "DFR") cannot be consider as the effective lower bound, but rather a floor that, as explained in section 1.3.1, is not (typically) reached by the interest rates we observe in the interbank market. Of course, the lower the DFR (i.e. the floor) and the lower the effective lower bound *should* be, at least for "reasonable" negative values of the DFR. However, the *spread* between the two might increase the lower the DFR is.[55]All of this to say that as long as the floor set by the ECB is zero (as it was from July 2012 to June 2014), both types of processes might be still applicable.

As a matter of fact, the true problem of lognormal processes, on top of ruling out negative values for $r(t)$, concerns the volatility implied by the short rate dynamics. Black (1995) specifies that a major issue is the volatility decreasing substantially as the rate approaches zero, that is too rapid compared to what we see in reality.[56] For what concerns the square root processes, such as the CIR, the square root diffusion term prevents $r(t)$ to take negative values, as it was originally introduced to ensure the positive sign of $r(t)$.

Eventually, the main drawback (i.e. the Gaussian property) of the linear SDE models turned out to be suitable with the application of the shadow mechanism, which will be discussed in the section 3.2. Nonetheless, the allowance of negative rates is not sufficient: as we saw in figure 1, interest rates floating in negative territory show some peculiar features that a short rate model must reproduce.

Let us discuss two crucial application problems of the Gaussian models in describing interest rates at the zero lower bound (from now on denoted as *ZLB*). For further details regarding these issues we address the reader to Krippner (2015), chapter 2.[57]

---

[55] The intuition might sound quite rudimentary but in facts there are no evidence of where the effective lower bound actually is. In other words, how deep interest rates' can go remains a big question mark of the NIRP.

[56] It must be also said that, if a lognormal process is implemented to model negative rates' dynamics by means of a shifting technique, this property turns out to be quite valuable. In facts, as we describe in the next subsection, negative rates are characterized by a "stickiness property" when they approach the zero lower bound.

[57] The discussion provided refers to US data, but the problems are of course the same whatever dataset we consider.

3.1.2. The Gaussian property

The *Gaussian property* of the short rate $r(t)$ allows $r(t)$ to freely move in negative territory once it approaches the *ZLB*. Let us denote the probability of $r(t)$ to assume a negative value at time t as $P(r(t) < 0)$. Before the NIRP breakthrough, Gaussian short rate models were implemented with the idea of bearing a little probability $P(r(t) < 0)$. However, when the model is calibrated, either under the P-measures or under the Q-measures, on the basis of interest rates' data observed in a negative environment, $P(r(t) < 0)$ becomes substantial, meaning $r(t)$ is allowed to move in negative regions with *non-negligible probabilities* when it fluctuates close to the *ZLB*.

In practice, this creates problems for term-structure modelling as well. On the basis of the terminology and notation of Krippner (2015), we denote $R(t,\tau)$ as the *Gaussian spot rate* determined at t for the *time to maturity* τ, that is over the interval of time $[t, t+\tau]$. $R(t,\tau)$ can be expressed as the mean of the expected short rates (i.e. forward rates).[58] Let us formalize the concept.

Definition: The *standard continuous-time term structure relationship*, is defined as

$$R(t,\tau) = \frac{1}{\tau}\int_0^\tau f(t,u)du, \tag{3.1}$$

with $f(t,\tau)$ being the *Gaussian forward rate* prevailing at time t.

Given the integral properties, we conclude Gaussian forward rates $f(t,\tau)$ and Gaussian spot rates $R(t,\tau)$ also have non-negligible probabilities of assuming negative values. However, this is at odds with reality: if, on the one hand, interest rates take negative values, on the other they are bounded by a lower bound, denoted as *LB*, that we can assume to be equivalent to the monetary policies' rates imposed by the central bank (in our case the DFR).[59] Hence, this is the first issue that must be addressed in modelling the dynamics of negative interest rates.

3.1.3. The stickiness of interest rates and the volatility issue

In chapter 1, while discussing figure 1, we have pointed out how different the volatility in the EONIA and the EURIBOR_{1m} is after the DFR is set below zero. In facts, the low volatility of the DFR and of the overnight rates are transmitted into the short-term interest rates, which tend to be attached to the lower bound for long periods of time. We refer to this feature as the "*stickiness of interest rates*".

---

[58] Note that the relationship between short rates and forward rates involves an additional term, that is the volatility effect.

[59] As previously discussed, we might think the effective LB to be slightly above the floor set by the DFR. However, for simplicity, we do not consider any spread between the two and we assume the LB at any time t to be equal to the DFR at the same t.

In figure 2 we plot four maturities of the EURIBOR, namely 1-month, 3-month, 6-month and 1-year maturities, together with the DFR. The series go from the 1st of January 1999 to the 31st of December 2020.

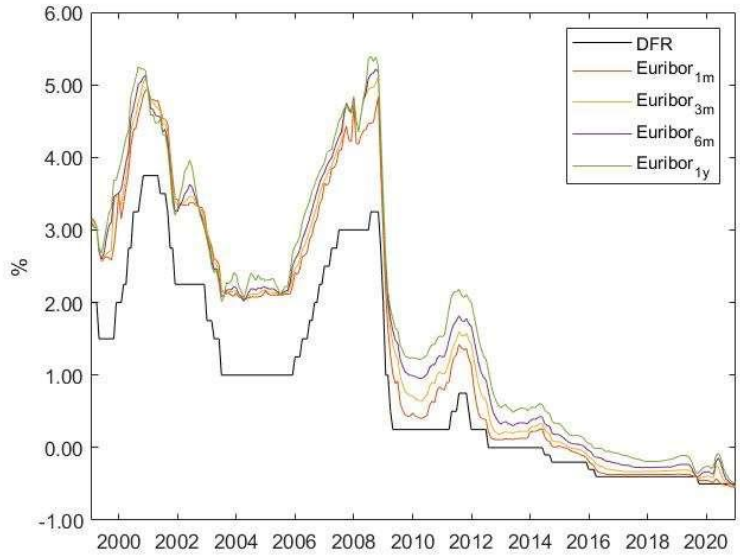

Figure 2. $Euribor_{1m}$, $Euribor_{3m}$, $Euribor_{6m}$, $Euribor_{1y}$ and DFR: 31/01/1999 – 31/12/2020. End of month observations.
Source: Statistical Data Warehouse, European Central Bank. Available at: **https://sdw.ecb.europa.eu/**

Let us consider, for example, the 1-month Euribor and the 1-year Euribor. After the introduction of the NIRP, the flatness of all rates is evident. If we split the time window in two period, before June 2014 and after June 2014, we find the average historical monthly volatility[60] before June 2014 is approximately 0,28% and 0,30%, respectively, while the average historical monthly volatility after June 2014 is 0,04% and 0,07%.

To strengthen the idea of the stickiness feature, in figure 3 we plot daily observations of the EONIA rate over the interval which goes from March 2016 to September 2019, that is the period over which the DFR is set to a negative 0.40. The EONIA fluctuates in a very restricted range with occasional daily spikes, up to a maximum value of -0,241, and down to a minimum of -0,379. The average value over the period is -0,356. Subsequently, from the cut in September 2019 up to date,[61] meaning the period over which the DFR is set to a negative 0.5, the EONIA reaches a maximum of -0,426 and a minimum of -0,498, with an average value of -0,46742. The shift in lower bound occurring in September 2019 is quite evident.

[60] We calculated the square root of the sum of the squared differences between each end of month observation and the average of the end of month observations over the year, divided by the number of end of month observations in a year.
[61] The EONIA daily observations we have at our disposal are up to the 6th of September 2021.

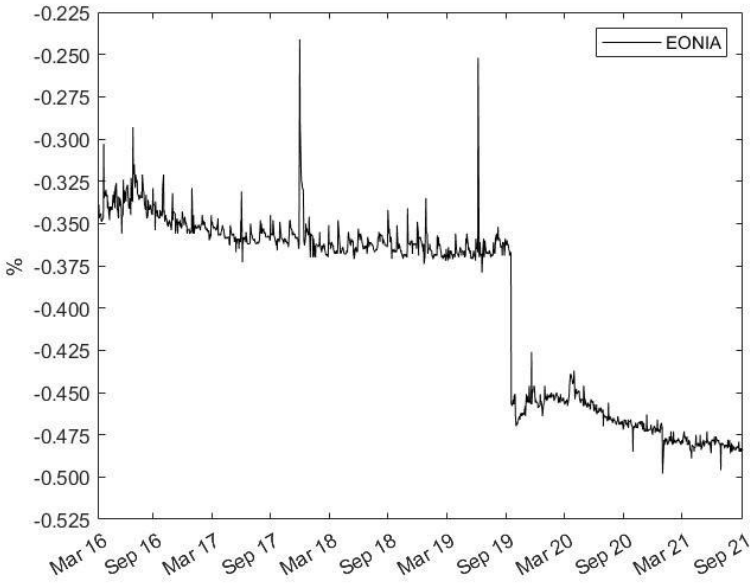

Figure 3. EONIA rate: 16/03/2016 – 06/09/2021. Daily observations. Market holidays dates not considered.
Source: Statistical Data Warehouse, European Central Bank. Available at: **https://sdw.ecb.europa.eu/**

We conclude the volatility issue created by the stickiness of the observed rates must be considered in modelling the short rate dynamics. Clearly, Gaussian short rate models do not entail such a feature: a Gaussian term structure model, such as the Vasicek and its Hull-White extension, implies $r(t)$ to have, over an infinitesimal period, the same volatility at each point in time (regardless the point of evaluation). As a consequence, the short rate volatility does not decrease when the short rate approaches zero (or, more generally, the LB we consider.). Therefore, if a Gaussian short rate model is used to model negative interest rates, it cannot embody the stickiness feature in its predictions.

3.2. The ZLB mechanism

Before seeing how the shadow rate approach, originally presented in Black (1995), can solve the problems described above, we present the intuition behind it.

3.2.1. Intuition

Black (1995) specifies the *(ZLB) short rate* to take the maximum value between the *shadow short rate* and a *zero lower bound*. The reason is that nominal short rates are bounded below by zero, or more generally by a lower bound since investors prefer to earn a zero nominal interest rate from holding cash rather than being charged a negative interest rate in whatever investment opportunity they might have.

By formalizing the concept:

$$\underline{r}(t) = max\{ZLB, r(t)\} \tag{3.2}$$

where:

- $\underline{r}(t)$ is the (ZLB) short rate;
- $r(t)$ is the shadow short rate;
- ZLB is the zero lower bound.

While the (ZLB) short rate can be interpreted as the "observable" short rate, the shadow short rate $r(t)$ represents what the short rate would be if the cash option was not available, and it is equivalent to the short rate implied by a given short rate model.[62] From now on, with the term "short rate" we refer to the (ZLB) short rate $\underline{r}(t)$.

As pointed out in Black (1995), given that currency is an option then also the short rate has an option-like profile. In facts, Krippner (2015) provides the following specification of the ZLB mechanism which emphasizes the option component:

$$\underline{r}(t) = r(t) + max\{-r(t), ZLB\}$$

where $max\{-r(t), ZLB\}$ is the payoff of an *instantaneous call option* of holding cash at time t. This is the equivalent to say investors are willing to invest in $r(t)$ irrespectively of its sign. In case $r(t)$ is negative, investors are hedged by the option of holding currency at a zero nominal rate.

A crucial element of the mechanism is the lower bound, that can be assumed to be non-zero. For example, a non-zero lower bound, denoted as LB, can be slightly negative or slightly positive when the mechanism is applied in a euro area context or in a US context,[63] respectively. It may also be treated as a time-dependent random variable, as well as many other possible specifications (see section 3.2.2 for a general overview of lower bound's specifications in the literature).

In this section, for sake of simplicity, we assume the lower bound to be constant, but the same reasonings are valid for whatever type of lower bound we consider. Please note that from now on, for sake of convenience, we will refer to (3.2) simply as "LB mechanism" regardless on whether the lower bound is set at zero or not.

3.2.2. The existence of negative rates in an arbitrage-free economy

Black (1995) proposes the LB mechanism on the premise that, in an arbitrage-free economy, negative rates are not allowed as long as investors can short the asset paying $r(t) < 0$ and hold the proceeds in currency earning a zero-nominal return. Jarrow (2013) argues this point in the context of a Heath–Jarrow–Morton (HJM) arbitrage-free term structure model by showing how

[62] Clearly, what best fits the approach is a Gaussian model. However, square root and log-normally distributed models can be implemented as well by assuming a positive lower bound.
[63] To date, FED's policy rates are very close to zero, but not negative.

storage costs and credit risk makes it too difficult for economic agents to exploit the arbitrage opportunities created by a negative rate, thus eliminating it.

Differently from the standard Heath–Jarrow–Morton (HJM) model, that is frictionless and competitive with ZCB for all conceivable maturities and a money market account paying the risk-free short rate $r(t)$, Jarrow (2013) extends the model by including the possibility to trade cash, together with the presence of consumers, firms, banks and non-bank financial institutions. In such framework, the author assumes consumers cannot short the money market account or any ZCB because of credit risk, a factor that the standard HJM does not consider. This makes it extremely costly for them to implement such a strategy. In addition, he reasonably assumes that firms and financial institutions cannot store cash, as logistic problems would arise as well as theft risk. With such conditions if $r(t)$ happens to be negative, arbitrage opportunities would not exist, implying negative short rates $r(t)$ are compatible with an arbitrage-free model.[64]

Leaving theoretical discussions aside, we now describe how the LB mechanism proposed by Black (1995) is helpful in terms of term structure modelling.

3.2.3. The LB mechanism as a solution for negative interest rate modelling

For what concerns the first issue described in section 3.1, that is the possibility of the shadow short rate $r(t)$ to freely move in a negative region, the lower bound plays the role of an *absorbing barrier* by ruling out any possible realization of the short rate below the lower bound.

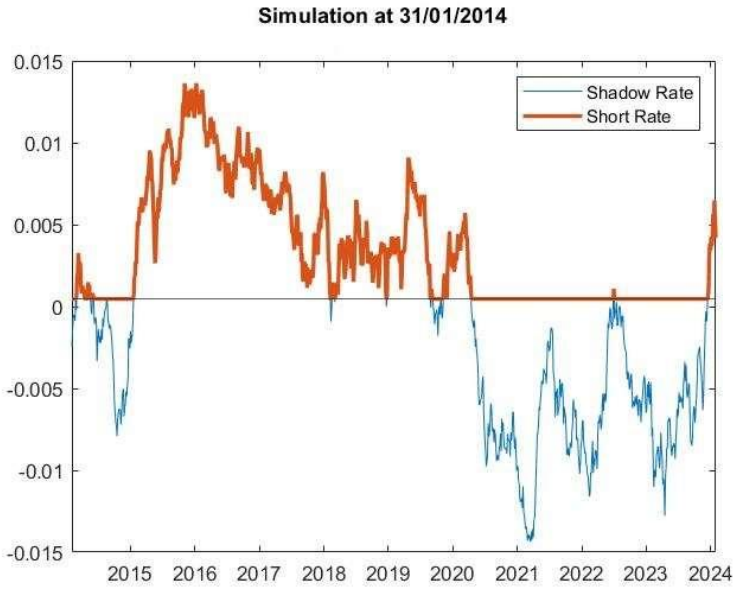

Figure 4. Simulated Short Rate trajectory on the 31st January 2014. LB = 0.0466%.
Constant LB model estimated on 31st January 2014. See appendix B for parameters' estimates.

[64] To show this result Jarrow (2013) makes use of the concept of convenience yields, a decreasing function in the size of an agent's cash holdings.

As we can see in figure 4, if the shadow rate $r(t)$ can take any value, the observed short rate $\underline{r}(t)$ equals the lower bound whenever the barrier absorbs $r(t)$. In other words, $\underline{r}(t) < LB$ cannot occur at any t. The escape from the lower bound will occur as soon as the shadow short rate assumes values greater than LB.

The shadow rate mechanism permits to reproduce the stickiness property of interest rates as well. By assuming the shadow short rate to be described by a Gaussian model, such as the Vasicek or its Hull-White extension, it is clear that all the properties of a Gaussian model are inherited by the shadow rate, including the conditional normal distributions of $r(t)$ at any t. The effect of the lower bound is to prevent any realization of $r(t)$ belonging to the fraction of the normal distributions below the bound, meaning we obtain a censored normal distribution of the short rate $\underline{r}(t)$ at any t. Furthermore, as we can see in figure 5, all the realizations of $r(t)$ at or below a given LB are associated with a probability mass for $\underline{r}(t)$ to be realized at LB.

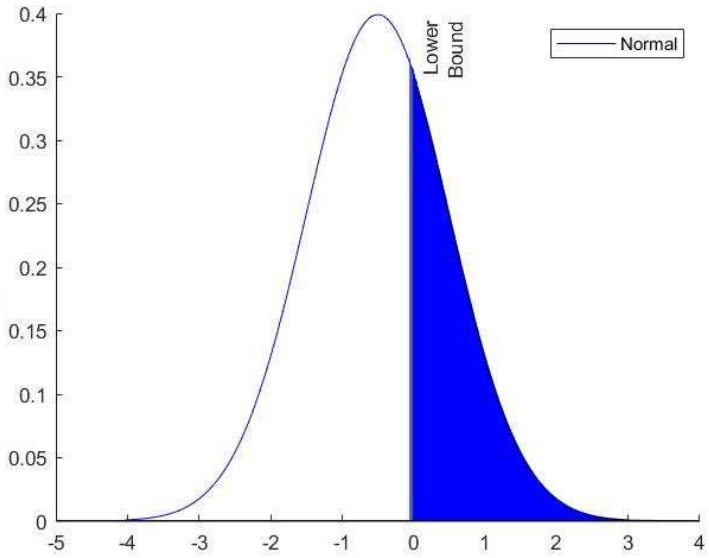

Figure 5. Censored Normal Distribution with probability mass at the Lower Bound.

Clearly, the greater $P(r(t) < 0)$, the tighter the censored distribution of $\underline{r}(t)$, so that $\underline{r}(t)$ is allowed to assume only values very much close to zero. This may be true for very long periods of time if negative realizations of $r(t)$ are very persistent. As a consequence, by means of the continuous-time term structure relationship, Gaussian spot rates $R(t,T)$ will be affected by the negative realitions of $r(t)$, allowing us to replicate the flat shape of the yield curves observed in the last years.[65] In facts, the low volatility of the deposit rates and the overnight rates that we

[65] Clearly, the continuous-time term structure relationship is calculated with respect to the short rate $\underline{r}(t)$. More details are provided in the next chapter.

observe in the market are transmitted into the shorter-maturity interest rates, that tend to be attached to the lower bound for long periods of time. This is also true for longer maturities if expectations on negative deposit rates are persistent.

On top of that, if we consider $r(t)$ to be described by a Gaussian model and we assume a positive mean reversion level, the longer the maturity considered the higher the probabilities of $r(t)$ and thus $\underline{r}(t)$ to take values greater than LB. As indicated by Krippner (2015) the longer maturity interest rates will be less sticky than the shortest ones, simply because $r(t)$ distributions will be much more symmetric at longer maturities relative to shorter maturities. Thus, it is reasonable to expect the yield curve to be upward sloping for very long tenors. Obviously, the mechanism is applicable also in periods which are not characterized by negative rates. A shadow rate model estimated in "normal" circumstances will most probably cause, by construction, the shadow short rate to entail little probabilities of taking negative values, even at short-term maturities. Therefore, the resulting $\underline{r}(t)$ distributions will be very close to the $r(t)$ distributions.

Finally, we must be aware of the main drawback of the mechanism, namely the cost we have to pay for being able to model negative interest rates with this approach is to give up on close-form analytic solutions for ZCB prices and yields, relying instead on numerical solutions. In chapter four we detail the problem and the numerical method we employ.

3.2.4. The lower bound: different specifications

As mentioned before, the lower bound is a crucial element in the LB mechanism. Most of the papers in the literature simply set the lower bound at a constant level. Some examples are Wu and Xia (2016) and Christensen and Glenn D. Rudebusch (2016a), both concerning US data, that set the lower bound to 25 basis points, and to 0 basis point, respectively. The former level was simply the annual interest rate paid on reserves by the FED since 2008 back at the time, while the zero level is justified by the fact that the US treasury yields data they use never violate the zero lower bound. Alternatively, the constant lower bound may be treated as a free parameter to be estimated, such as in Kim and Priebsch (2013).

If a constant lower bound could be a reasonable assumption for US data applications, it does not really fit in a European context, where the several downward adjustments of the DFR over the most recent years suggest a lower bound that is (at least) time dependent. Thus, it is not surprising that models with alternative lower bounds' specifications are more commonly applied to the euro area rather than the US.

Among those models, a time-varying lower bound can be found in Kortela (2016), who shows how from January 1999 to March 2016 the risk-free rates, approximated by OIS rates based on EONIA and government bonds yields of Germany and France, an exogenous time-

varying lower bound outperforms the constant LB model. More specifically, with such a lower bound, we can re-write (3.2) as

$$\underline{r}(t) = max\{LB_t, r(t)\}$$

where the subscript t indicates the time dependence of LB.

In Kortela (2016), LB is defined as an exogenous sequence determined by the data, meaning $LB = \{LB_t\}_{t=1}^{T}$ where LB_t is specified in five different ways:

- $LB_t^n = min\{R_t(\tau), 0\}$ where $R_t(\tau)$ are the observed yields at time t and τ are the maturities included in the sample, that is $\tau = \{0.25, 0.5, 1, 2, 3, 5, 10\}$. Hence, LB_t^n will be the most negative of the observed yields across maturities at time t;
- $LB_t^m = min\{\{R_i(\tau)\}_{i=1}^{t}, 0\}$ where $\{R_i(\tau)\}_{i=1}^{t}$ is the lowest yield in the sample up to time t;
- LB_t^d is the deposit facility rate at time t;
- LB^c is a constant lower bound which firstly considered at negative 0.3 percent for all t, and then at negative 0.4 percent for all t.
- LB_t^e is a sequence of estimated constant LB resulting from a recursive estimation of a shadow rate model in which LB is treated, differently from the other cases, as a free parameter. Mathematically, $LB_t^e = min\{\widehat{LB}_t^e, 0\}$ where $\widehat{LB}_t^e$ is the estimated lower bound considering all the observations up to time t. The shadow rate model with a time-varying lower bound is then estimated using the sequence LB_t^e as an exogenous process.

Another relevant reference for the euro area is Lemke and Vladu (2016) that analyse the yield curve from 1999 to mid-2015 using a combination of OIS rates based on EONIA and spread-adjusted zero rates based on Euribor swaps.[66] They define a discrete-time shadow rate term structure with a constant lower bound being allowed to shift to a new level in specific points in time. In particular, by considering two potential shifting times, that are May 2014 and September 2014, they compare different specifications of LB. In practice, they consider three subperiods, that are January 1999 - April 2014, May 2014 - August 2014 and September 2014 - June 2015, and they impose different restrictions on LB with respect to the three subperiods. The different specifications go from the most flexible one, that is three potential different values of LB, each one for each subperiod, to the most rigid one, that is one constant value for the overall time window. In conclusion, they find the best model is the one ensuring two lower

[66] Calculating the average spread between OIS rates and Euribor swap rates, with the latter being used to extend Euribor maturities over the year, is one of the most common techniques to construct OIS dataset for time periods prior 2005. In facts, OIS rates are not available before 2005.

bound regimes: a constant level of LB for the period January 1999 – August 2014, and a lower LB for the period September 2014 – June 2015.

As we just saw, in most of the literature LB is assumed to be constant, or exogenously determined. The issue is that in such models agents are myopic, that is they do not consider future possible changes in the level of LB. To allow for forward-looking agents, Wu and Xia (2020) employ end-of-month observations of OIS rates based on EONIA from July 2005 to June 2017, with two policy indicators relative to the euro area conditioning the discrete movements of LB. More specifically:

$$\underline{r}(t) = max\{LB_t, r(t)\}$$

where the subscript t indicates the time dependence of LB.

In particular, there are three components determining LB_t: the deposit facility rate, a spread component, Δ_t and Δ_t^l, where the latter two are binary random variables that capture market's expectations of the immediate monetary policy stance and long-term monetary policy stance, respectively. For what concerns the DFR, after observing the ECB's cuts by a constant step of 0.1%, they model their Q-dynamics in such a way LB_t can only move downward,[67] that is

$$\begin{cases} Q_t\left(r_{t+1}^d = r_t^d - 0.1\right) = \alpha_{1,t}^Q \\ Q_t\left(r_{t+1}^d = r_t^d\right) = 1 - \alpha_{1,t}^Q \end{cases} \tag{3.3}$$

where Q_t is the conditional probability under the Q-measures and r_t^d is the deposit rate at time t.

The policy indicator Δ_t capture agents' expectations of the next period's DFR and takes value of 1 if there is a great probability of a cut in the next period, 0 otherwise. The corresponding Q-dynamics are modelled as a two-state Markov chain process, that is

$$\begin{cases} Q_t(\Delta_{t+1} = 0 | \Delta_t = 0) = \alpha_{00,t}^Q \\ Q_t(\Delta_{t+1} = 1 | \Delta_t = 1) = \alpha_{11,t}^Q \end{cases} \tag{3.4}$$

Equation (3.3) can be re-expressed by including the indicator Δ_t:

$$Q_t\left(r_{t+1}^d = r_t^d - 0.1\right) = Q\left(r_{t+1}^d = r_t^d - 0.1 \middle| r_t^d, \Delta_t\right) = \alpha_{1,\Delta_t}^Q, \tag{3.5}$$

[67] This assumption is explained by the authors considering the fact that once a DFR of a given negative level has been reached, investors will not assume the *LB* to be a higher number. On top of that, back to that time, the authors had no market signals of upward movements of the DFR.

Similarly, the policy indicator Δ_t^l assumes value of 1 if there is a great probability of further curs at longer horizons, 0 otherwise. In particular, Δ_t^l is allowed to influence Δ_t, so that we can express (3.4) as

$$\begin{cases} Q_t(\Delta_{t+1} = 0|\Delta_t = 0) = Q\left(\Delta_{t+1} = 0\middle|\Delta_t = 0, \Delta_t^l\right) = \alpha^Q_{00,\Delta_t^l} \\ Q_t(\Delta_{t+1} = 1|\Delta_t = 1) = Q\left(\Delta_{t+1} = 1\middle|\Delta_t = 1, \Delta_t^l\right) = \alpha^Q_{11,\Delta_t^l} \end{cases} \tag{3.6}$$

By finally assuming

$$\begin{cases} Q\left(\Delta_{t+1}^l = 0\middle|\Delta_t^l = 0\right) = \alpha_{00}^{l,Q} \\ Q\left(\Delta_{t+1}^l = 1\middle|\Delta_t^l = 1\right) = \alpha_{11}^{l,Q} \end{cases} \tag{3.7}$$

the lower bound can be expressed as:

$$LB_t \approx \gamma_t r_t^d + (1-\gamma_t) E_t^Q\left(r_{t+1}^d\right)$$

$$= r_t^d - (1-\gamma_t)\alpha_{1,\Delta_t} \times 0.1$$

where γ_t represents the number of days, expressed as a fraction of the month from t to $t+1$, between the end of the current month t and the next ECB's meeting day.[68]

The crucial aspect of this specification is that the combination of (3.5), (3.6) and (3.7) allow the authors to capture various shapes of the observed yield curves, especially for what concerns its short end. Finally, a spread component is considered, given the fact that the deposit rate is always lower than the EONIA and thus the OIS rates considered. After expressing the spread component sp_t as an AR(1) under the risk neutral measures, the lower bound is finally expressed as:

$$LB_t = r_t^d - (1-\gamma_t)\alpha_{1,\Delta_t} \times 0.1 + sp_t$$

A similar set up, that is a regime-switching model, has been previously implemented in Wu and Xia (2017), in which LB_t is affected by a monetary policy component, that is the DFR, and a spread component. The difference with Wu and Xia (2019) concerns the former, the so-called "policy lower bound" component that is permitted to move only by a constant value of 0.1%, but differently from before it can move also upward, or to stay at its current level. A second difference is that, in order to incorporate the persistency of a trend of the DFR and thus of *LB* (i.e. the momentum of the lower bound movements), an indicator Δ_t is used to describe the

[68] A calendar effect is considered given the fact that the ECB's council meeting does not occur necessarily at the end of each month, while the dataset is composed by end-of-month observations.

trend direction: it takes value of 1 for an upward trend, or a value of -1 for a downward trend. In both states, persistency at the current level is allowed.

CHAPTER 4

4. Real time estimation and ex-post estimation: a comparison

In this chapter we estimate a two-factor shadow rate model under two different lower bound specifications, namely a constant and a regime-switching lower bound. This is done by means of the iterated extended Kalman filter with maximum likelihood estimation. Subsequently, for each approach we calculate the model-implied short rate liftoff's timings in the post-2014 period.[69]

4.1. Literature review

Among the ZLB literature, liftoff's timings have been studied mainly for monetary policy analysis. The most common approach, that is well-discussed in Bauer and Rudebusch (2016b), consists in the examination of the simulated liftoff dates distribution. More precisely, a liftoff date, also referred to as "liftoff horizon" is the time at which the short rate is expected to cross a given threshold and to stay above it for at least a pre-specified period of time. Given the strong asymmetry that in most of the cases is obtained in the liftoff horizon distribution, Bauer and Rudebusch (2016b) argue that the median time is an optimal measure of liftoff.

One of the first papers to introduce the concept of liftoff horizon (LOH) was Wu and Xia (2016), however without requiring duration, meaning the short rate to float above the threshold for a given period of time. The same definition of LOH is used in Pericoli and Taboga (2015), meaning the first date at which a threshold is exceeded by the short rate. On the basis of the method of Bauer and Rudebusch (2016b), some of the main results among the literature that compares LOH against different lower bound specifications are the ones of Lemke and Vladu (2016) and Kortela (2016), which represent the most relevant ZLB studies concerning the euro area. In particular, Lemke and Vladu (2016) find the high sensitivity of the LOH to the estimated level of the lower bound in a euro area context, meaning different lower bound specifications lead to substantially different median lift-off-timings, with changes even up to 48 months. This results, contrasts with Kortela (2016), that still with respect to the eurozone provides evidence about the robustness of the LOH measures across different time-varying lower bounds specifications, an evidence that is also obtained by Krippner (2015) relative to US data.

[69] With the term "liftoff" we refer to the upward movement of the short rate from a negative region to a positive one so that the shadow rate, and thus the short rate, takes a positive value.

4.2. Research question

From chapter 1 we know that the big question mark of the most recent years is where the lower bound actually is. Thus, we first want to verify the existence of a time-varying LB as opposed to the idea of a single LB. Additionally, as detailed in the subsection 4.5.4, we recursively estimate a two-factor shadow rate model and we derived its implied LOH under the assumption of a constant LB as if we were doing it real time, that is conditionally on all the information available at each date considered.[70] At the same dates we repeat the recursive estimations for the regime-switching model presented in subsection 4.5.1, that is a shadow rate model whose LB is allowed to switch to a new discrete value at specific points in time.

For simplicity, we refer to the estimation of a regime-switching model as the "ex-post approach", and we compare its performances with the single constant LB model, namely the "real time approach". The rationale behind this terminology is that a regime-switching LB specification, that follows from the idea of a time-varying lower bound, comes after the several ECB's adjustments in the DFR in negative territory that we witnessed in the last years, while the idea of a single LB was commonly agreed before the introduction of the NIRP. In other words, up to 2014 the market could not expect the DFR to be cut several times in negative territory down to the current level of -0.50 percent, that is the idea of a regime-switching LB was not conceivable as it is nowadays. Hence the terminology "ex-post".

Notice that the constant LB specification is what differentiates a real time model from most of the estimates we find in the literature, in which the LOH distribution is analysed after employing a LB specification that has been previously evaluated over the whole sample, typically for macroeconomic analysis.[71] In particular, our real time model estimations concern a not so common risk-management application that makes the topic particularly interesting given that real time decision-making is subject to a lot of noise and uncertainty that a classic ex-post estimation does not consider. Finally, compared to Kortela (2016) and Lemke and Vladu (2016) we dispose of a larger amount of OIS rates over the NIRP period, so that our dataset is made up of interest rates whose dynamics are entirely determined by market forces.[72]

---

[70] In facts, before the introduction of the NIRP the idea of a ZLB was commonly shared. A regime-switching lower bound is instead an assumption which comes after multiple cuts in the DFR. Thus, we think the idea of a single lower bound is reasonable in a real time scenario.

[71] For example, Lemke and Vladu (2016) estimate LOH on the basis of a "preferred" model, that is a two-regime lower bound specification. They also estimate LOH for a model with a constant lower bound, but their data are only up to 2015. Kortela (2016) estimates a shadow rate model in which the time-varying LB is an exogenous sequence previously estimated or pinned down on the basis of what the dataset suggests. Alternatively, we consider the lower bound as a free parameter to estimate.

[72] Lemke and Vladu (2016) employ constructed OIS rates for the period prior 2005 based on an average EURIBOR swaps – OIS rates spread, while Kortela (2016) uses government bonds' rates.

In practice, a real time estimation of the model is particularly relevant for monetary policy analysis, as the LOH provides an indication about the stance of monetary policy perceived by the market. In particular, Kortela (2016) and Krippner (2015) argue that LOH measures can be interpreted as a measure of the likelihood the economic agents give to the possibility of facing negative policy rates in the short and medium-term. Thus, they can be used to guide the stance of monetary policy during NIRP periods. In addition, projections of the yield curves can be made based on what we expected the short rate to be, meaning that a real time simulation of the model can be relevant for all the yield curve-related decisions one can possibly think of. Finally, a real time estimation of the model and related simulations of the short rate under the Q-measures are relevant for valuation purposes as well. However, this is not the main focus of this dissertation, as we forecast liftoff horizons under the P-measures.

4.3. Dataset

We employ Euro OIS rates in line with the vast majority of the post-financial crisis literature. The (risk-free) OIS yield curve that we consider is formed by the following 9 maturities: 1_m, 3_m, 6_m, 1_y, 2_y, 3_y, 5_y, 7_y, 10_y, where the subscripts "m" and "y" indicate months and years, respectively.

The choice of these tenors is quite standard. However, differently from related analysis we include a 1-month tenure, with the aim of enhancing the focus on short term expectations about the policy rate, as suggested by Krippner (2015). Given the fact we recursively estimate the model at the beginning of each year, we think a stronger focus on the short term is coherent with a real time estimation.[73]

For the purpose of estimation by means of an Extended Kalman Filter with Maximum Likelihood we need a dataset which explains how the yield curve evolves overtime. Specifically, we consider end-of-month observations of the yield curve defined above over an interval of 16 years and 2 months, meaning our time window goes from the 31st of August 2005 to the 30th of September 2021, for a total of 194 observations. The interval of time between each observation is obviously one month, as well as the periodicity of our model. Data are provided by Refinitiv Eikon on the 19th of October 2021, whose codes are "OIEUR1M", "OIEUR3M", "OIEUR6M", "OIEUR1Y", "OIEUR2Y", "OIEUR3Y", "OIEUR5Y", "OIEUR7Y" and "OIEU10Y". Our (unusual) starting date is somehow forced by the lack of data for OIS rates relative to long maturities prior august 2005, while the ending date represents the last end-of-month observation at the moment of data gathering.

[73] Clearly, the choice of tenures reflect the scope of the application. We think it is reasonable assuming a risk management application, such as a real time estimation of the model, to be short-term oriented. Additionally, one can think an unconventional monetary policy such as the NIRP to be only temporary.

4.3.1 Dataset analysis

In figure 6 we plot Euro OIS rates for the 1-month, 5-year and 10-year maturities. Along with the downward trend which starts from the global financial crisis, what is really noticeable is a strong correlation, especially between the two longest maturity rates. From the NIRP breakthrough the 1-month OIS rate lies on a level that is essentially the DFR adjusted upward by a little spread.[74] Most importantly, it is evident that if until 2014 the idea of a zero-lower bound was reasonable, from the occurrence of the NIRP the lower bound has changed frequently. In particular, it has always been revised downward, thus supporting the idea that a fixed constant lower bound covering the whole sample clashes in a shadow rate mechanism.

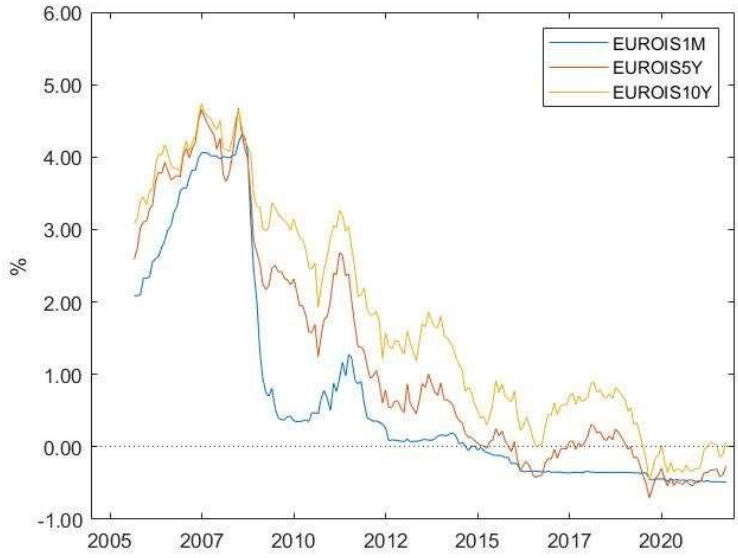

Figure 6. 1-month OIS, 5-year OIS, 10-year OIS: 31/08/2005 – 30/09/2021. End of month observations.
Source: Refinitiv Eikon. Date of access: 19/10/2021.

In figure 7 we plot the yield curve observed on the 31st of January 2006 and on the 29th of January 2021. By considering these two indicative dates we highlight the huge differences in level, slope and curvature in the OIS yield curve before and after the NIRP. While the yield curve in January 2006 starts from a 1-month OIS rate well above 2% and it shows a quite traditional shape, the most recent curve entirely lies in a negative territory, being slightly decreasing until the 3-year maturity and slightly increasing afterwards. The OIS yield curves observed in our dataset are therefore quite heterogenous and affected by the several well-known shocks of the last sixteen years, thus making the estimation quite challenging. However, the shadow rate mechanism allows us to replicate entirely negative yield curves as well.

[74] From the 18th of September 2019 the DFR is set equal to -50 bps per annum: from that date to the last observation at our disposal, the average end-of-month spread between the DFR and the 1-month OIS rate is -3.4 bps.

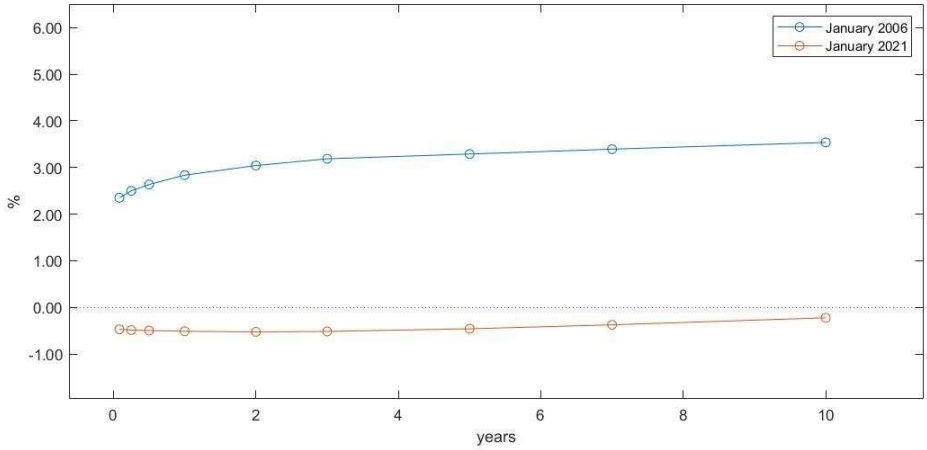

Figure 7. OIS curves on 31st of January 2006 and 29th of January 2021. Maturities: 1m, 3m, 6m, 1y, 2y, 3y, 5y, 7y, 10y.
Source: Refinitiv Eikon. Date of access: 19/10/2021.

Table 1 show the mean, median, standard deviations and the 12-months autocorrelation over the entire sample period, namely August 2005 – Seeptember 2021, of the Euro OIS rates composing the dataset, while in table 2 we represent the correlations of such OIS rates over the same period of time. Notice how the means of OIS rates with maturities up to a year are very close to each other, thus suggesting a flat shape of the short end of the yield curve on average, while the increasing means at longer maturities indicate an upward slope for the long end. The standard deviations are very similar across maturities, meaning that shocks and expectations affected the yield curve in (almost) the same way on average. Finally the autocorrelations are quite high and significant for all tenors, while the correlations between maturities are high, with only the one between 1-month maturity and 10-year maturity being lower 0.90.

	Mean	**Median**	**Std Dev**	**Autocorr 12 months**
1m	0.71194	0.0925	1.4709	0.74264
3m	0.72134	0.087	1.4959	0.74529
6m	0.7385	0.0805	1.5248	0.74858
1y	0.77724	0.08	1.5644	0.76001
2y	0.8619	0.1355	1.5807	0.78762
3y	0.97444	0.256	1.5936	0.80627
5y	1.2261	0.6047	1.597	0.82299
7y	1.4611	0.9628	1.5794	0.82794
10y	1.7534	1.4192	1.5445	0.8262

Table 1. Mean, Median, Std Deviation in percentage points and 12-month lag Autocorrelation for each OIS rate maturity.
All sample period considered.

	1m	3m	6m	1y	2y	3y	5y	7y	10y
1m	1	0.99935	0.99757	0.99306	0.98298	0.97108	0.94596	0.92282	0.8983
3m	0.99935	1	0.99934	0.99609	0.98657	0.97445	0.94891	0.92541	0.90048
6m	0.99757	0.99934	1	0.99849	0.99042	0.97871	0.95336	0.92987	0.90481
1y	0.99306	0.99609	0.99849	1	0.99575	0.98604	0.96278	0.94035	0.91589
2y	0.98298	0.98657	0.99042	0.99575	1	0.99685	0.98159	0.96375	0.94268
3y	0.97108	0.97445	0.97871	0.98604	0.99685	1	0.99317	0.98061	0.96372
5y	0.94596	0.94891	0.95336	0.96278	0.98159	0.99317	1	0.99655	0.98727
7y	0.92282	0.92541	0.92987	0.94035	0.96375	0.98061	0.99655	1	0.99693
10y	0.8983	0.90048	0.90481	0.91589	0.94268	0.96372	0.98727	0.99693	1

Table 2. Correlation table between the observed OIS rates over the whole sample period.

4.4. Model set up

In this section, we first provide a model description in continuous time, and then we detail its discretization for empirical analysis.

4.4.1. The lower bound

Given the difference in lower bound specification between the two approaches, we define the shadow rate model as follow:

$\underline{r}(t) = max\{LB, r(t)\}$, for the real time estimation;

$\underline{r}(t) = max\{LB_t, r(t)\}$, for the ex-post estimation.

For what concerns the real time estimation, we express the lower bound by omitting the subscript t because, in facts, we estimate a constant LB at each re-estimation date, i.e. every year. Instead, under the ex-post scenario, the subscript t allows LB_t to be time-dependent, that is the lower bound is defined over different regimes.

4.4.2. The shadow short rate

In line with our main reference, namely Krippner (2015), we employ the Gaussian specification provided by Dai and Singleton (2002) pp.437-38 for the shadow rate $r(t)$. More specifically, we adopt a standard two-factor Gaussian model in which the instantaneous short rate $r(t)$ is an affine function of two state variables. In matrix notation, we have:

$$r(t) = a_0 + b_0' x(t) \tag{4.0}$$

where $r(t)$ is a scalar, a_0 is a constant, b_0 is a constant 2×1 vector, and $x(t)$ is the 2×1 vector of state variables.

The vector of state variables $x(t)$, under the objective P-measures, evolves according to the following Ornstein-Uhlenbeck vector process:

$$dx(t) = k[\theta - x(t)]dt + \sigma dW^P(t) \tag{4.1}$$

where θ is a constant 2×1 vector representing the long-run mean of the vector of state variables $x(t)$, k is a constant 2×2 matrix of mean reversion coefficients, σ is a constant 2×2 matrix representing the noise coefficients ruling the innovations to $x(t)$. More specifically, σ is composed by the variances and the correlation parameters between the two state variables relative to $dW(t)$, a 2×1 vector of independent Wiener processes, where $dW(t) \sim N(0,1)\sqrt{dt}$.

The dynamics of $x(t)$ under the P-measures are defined as the solution of (4.1), that is

$$x(t+\tau) = \theta + e^{-k\tau}[x(t) - \theta] + \int_t^{t+\tau} e^{-\kappa[\tau-u]}\sigma dW^P(u) \tag{4.2}$$

where τ is the length of the horizon considered from the current time t and $\mathrm{e}^{-k\tau}$ is a matrix exponential.[75]

Under the risk neutral Q-measures, the dynamics of $x(t)$ are defined as

$$dx(t) = k^Q[\theta^Q - x(t)]dt + \sigma dW^Q(t) \tag{4.3}$$

where the mean reversion and long-run parameters include a market price of risk component relative to their P-measure counterparts, while the solution of (4.3) is the Q-measures equivalent of (4.2).

4.4.3. The Gaussian affine term structure of the shadow short rate

To define the standard continuous-time term structure relationship, a crucial element to consider is the *volatility effect* of the short rate on expected returns due to the Jensen's inequality. In this regard, for sake of completeness, we report the expression proposed by Krippner (2015) p.50, pp.63-64, that is

$$VE(\tau) = \int_0^\tau b_0' e^{-k^Q[\tau-s]}\sigma[\sigma' \int_s^\tau e^{-k^{Q\prime}[u-s]} b_0 du]ds. \tag{4.4}$$

By defining the (instantaneous) Gaussian forward rate prevailing at time t under the Q-measures as

$$f(t,\tau) = E^Q[r(t+\tau)|x(t)] - VE(\tau) \tag{4.5}$$

where

$$\begin{aligned} E_t^Q[r(t+\tau)|x(t)] &= a_0 + b_0' E_t^Q[x(t+\tau)|x(t)] \\ &= a_0 + b_0'\left\{\theta^Q + e^{-k^Q\tau}[x(t) - \theta^Q]\right\}, \end{aligned}$$

[75] For analytical purposes, Krippner (2015) applies an eigensystem decomposition of k to express the matrix exponential $\mathrm{e}^{-k\tau}$ in terms of scalar exponentials. For additional details see Krippner (2015), section 3.1.2.

we can express the Gausstian spot interest rate at time t for the horizon τ as

$$R(t,\tau) = \frac{1}{\tau}\int_0^{\tau} f(t,u)du = \frac{1}{\tau}\int_0^{\tau} E_t^Q[r(t+u)|x(t)]du - \frac{1}{\tau}\int_0^{\tau} VE(u)\,du \tag{4.8}$$

Clearly, (4.8) allows us to derive the Gaussian term structure.[76]

4.4.4. The non-linearity issue: a closed form analytic solution

The LB mechanism introduces non-linearity in what it would be a standard Gaussian affine term structure model with the short rate $r(t)$ being affine in the state variables $x(t)$. In this regard, the shadow rate model proposed by Krippner (2015) is very convenient, as it provides continuous-time closed form analytic expressions for the forward rate and thus yields and bond prices in a LB environment.[77] We make use of those closed form expressions, and we refer to forward rates, spot rates and bond prices resulting from a LB mechanism with the additional term LB, namely LB forward rates, LB spot rates and LB bond prices.

By expressing the LB mechanism at time $t+\tau$ emphasising the option component, we have

$$\underline{r}(t+\tau) = r(t+\tau) + max\{LB - r(t+\tau), 0\}\,. \tag{4.9}$$

The Gaussian forward rate, that under the Q-measures is defined as (4.5), can equivalently be expressed by ignoring the volatility effect,[78] so that we have

$$f(t,\tau) = E_{t+\tau}^Q[r(t+\tau)|x(t)] \tag{4.10}$$

where $E_{t+\tau}^Q$ denotes the expected value operator is taken under the $t+\tau$ forward Q measures.

Clearly, (4.10) is still valid if applied with respect to its LB short rate and the LB forward rate counterparts:

$$\underline{f}(t,\tau) = E_{t+\tau}^Q\left[\underline{r}(t+\tau)\middle|x(t)\right]$$

By denoting $\underline{f}(t,\tau)$ as "LB forward rate" (i.e. the Gaussian forward rate bounded below by the lower bound) and by substituting the LB mechanism in (4.9) we obtain:

$$\underline{f}(t,\tau) = E_{t+\tau}^Q\left[\underline{r}(t+\tau)\middle|x(t)\right] \tag{4.10}$$
$$= E_{t+\tau}^Q[r(t+\tau)|x(t)] + E_{t+\tau}^Q[max\{LB - r(t+\tau), 0\}|x(t)]$$

[76] In this chapter and thus in the empirical analysis, when we write "term structure" we refer to the Gaussian interest rates prevailing at t for the interval $[t,T]$ rather than the family of bond prices. However, it is commonly known the standard expression of the continously compounded spot rate $R(t,\tau) = -\frac{\log P(t,\tau)}{\tau}$, which allows to move from spot rates to bond prices.

[77] For additional details see Krippner (2015), section 4.1.

[78] Specifically, Krippner (2015) points out that is more convenient to treat the Gaussian forward rate expression (4.5) under the $t+\tau$ forward Q measures.

$$= f(t,\tau) + z(t,\tau)$$

where $f(t,\tau)$ is the Gaussian forward rate and $z(t,\tau)$ is a *forward rate option effect*.

The closed form solution of $f(t,\tau)$ is equation (4.5) under the Q-measures, equivalently expressed as (4.10) under the $t+\tau$ forward Q measures, while a closed-form analytic expression for $z(t,\tau)$ is derived by Krippner (2015) and it is the crucial element for the tractability of the model. Specifically, the forward rate option effect can be expressed as:

$$z(t,\tau) = [LB - f(t,\tau)]\left(1 - \Phi\left[\frac{f(t,\tau) - LB}{\omega(\tau)}\right]\right) + \omega(\tau)\phi\left[\frac{f(t,\tau) - LB}{\omega(\tau)}\right] \tag{4.11}$$

where $\Phi[\cdot]$ and $\phi[\cdot]$ are the cumulative distribution function (CDF) and the density function (PDF) of the unit normal distribution respectively, and $[\omega(\tau)]^2 = var_t^Q[r(t+\tau)|x(t)]$.[79] Notice how the CDF and the PDF of the unit normal distribution introduce non-linearity in the LB forward rate expression.

Finally, by substituting (4.11) into (4.10) we obtain the closed form solution for the LB forward rate,[80] namely

$$\underline{f}(t,\tau) = LB + [f(t,\tau) - LB] \cdot \Phi\left[\frac{f(t,\tau) - LB}{\omega(\tau)}\right] + \omega(\tau) \cdot \phi\left[\frac{f(t,\tau) - LB}{\omega(\tau)}\right] \tag{4.12}$$

The convergence of $\underline{f}(t,\tau)$ to LB in prolonged periods of negative interest rates is quite straightforward. Let us consider the following limits of the Gaussian forward rate $f(t,\tau)$:

- $\lim_{f(t,\tau)\to -\infty} \Phi\left[\frac{f(t,\tau)-LB}{\omega(\tau)}\right] = 0$
- $\lim_{f(t,\tau)\to -\infty} \phi\left[\frac{f(t,\tau)-LB}{\omega(\tau)}\right] = 0$

It is clear that $\lim_{f(t,\tau)\to -\infty} \underline{f}(t,\tau) = LB$.

At the same time, by considering

- $\lim_{f(t,\tau)\to \infty} \Phi\left[\frac{f(t,\tau)-LB}{\omega(\tau)}\right] = 1$
- $\lim_{f(t,\tau)\to \infty} \phi\left[\frac{f(t,\tau)-LB}{\omega(\tau)}\right] = 0$

we obtain $\lim_{f(t,\tau)\to \infty} \underline{f}(t,\tau) = f(t,\tau)$.

---

[79] The formula is provided by Krippner (2015) at p. 129.
[80] A discrete-time version of (4.12) is proposed by Wu and Xia (2013) and it is quite common in the literature.

Consequently, the LB counterpart of the standard continuous-time term structure relationship can be simply developed as the sum of a Gaussian shadow component, denoted by $R(t,\tau)$, and an option component, denoted by $Z(t,\tau)$:

$$\underline{R}(t,\tau) = \frac{1}{\tau}\int_0^\tau \underline{f}(t,u)du = \frac{1}{\tau}\int_0^\tau f(t,u)du + \frac{1}{\tau}\int_0^\tau z(t,u)\,du = R(t,\tau) + Z(t,\tau) \tag{4.13}$$

where $\underline{R}(t,\tau)$ is the LB spot rate at time t over the horizon τ.

We can express the measurement equation in a LB context as

$$\underline{R_t}^{obs} = \underline{R}_t - \eta_t \tag{4.14}$$

where $\underline{R_t}^{obs}$ represents the 9×1 vector of observed yields at time t for all 9 maturities, $\underline{R}_t$ is the 9×1 vector of predicted yields at time t for all 9 maturities via (4.13), and η_t is the 9×1 vector of the observed yields which are not explained by $\underline{R}_t$.

Finally, LB bond prices, indicated by $\underline{P}(t,\tau)$, can be expressed as

$$\underline{P}(t,\tau) = e^{-\tau\cdot\underline{R}(t,\tau)} = e^{-\tau\cdot R(t,\tau)} \times e^{-\tau\cdot Z(t,\tau)}$$

4.4.5. The model specification and discretization

The models parameters must be calibrated (i.e. restricted) to permit a unique identification. As described in subsection 4.4.2, the two-factor Gaussian model describing the shadow rate has 19 parameters in total, namely the constant a_0, the 2×1 vector b_0, the 2×2 matrix k, the 2×1 vector θ, the 2×2 matrix σ, the 2×2 matrix k^Q and the 2×1 vector θ^Q.

Following the standard specification in the literature, we restrict 9 parametrs so that the remaining 10 are free parameters to estimate. More specifically, we set $a_0 = 0$, b_0 is specified as a 2×1 unit vector, while σ_{12}, k_{11}^Q, k_{12}^Q, k_{21}^Q, θ_{11}^Q, and θ_{21}^Q are set equal to zero.

To sum up, we have

$$a_0 = 0, \quad b_0 = \begin{bmatrix}1\\1\end{bmatrix}$$

$$k = \begin{bmatrix}k_{11} & k_{12}\\ k_{21} & k_{22}\end{bmatrix}, \quad \theta = \begin{bmatrix}\theta_1\\ \theta_2\end{bmatrix}, \quad \sigma = \begin{bmatrix}\sigma_1 & 0\\ \rho_{12}\sigma_2 & \sigma_2\sqrt{1-\rho_{12}^2}\end{bmatrix}$$

$$k^Q = \begin{bmatrix}0 & 0\\ 0 & \phi\end{bmatrix}, \quad \theta^Q = \begin{bmatrix}0\\0\end{bmatrix}.$$

This specification is consistent with a two-factor Nelson and Siegel (1987) model (i.e. ANSM), in particular for the restrictions at zero of a_0 and k_{11}^Q.[81]

Obviously, by introducing a LB mechanism and treating *LB* as a free parameters to estimate, we obtain a two-factor shadow rate model with 20 parameters in total, of which 11 are free to estimate.

Given the state variables vector $x(t) = \begin{bmatrix} x_1(t) \\ x_2(t) \end{bmatrix}$, the specification implies that

$$\begin{aligned} r(t) &= a_0 + b_0' x(t) \\ &= [1,1] \cdot \begin{bmatrix} x_1(t) \\ x_2(t) \end{bmatrix} \\ &= x_1(t) + x_2(t) \end{aligned}$$

Finally, yield curve data are observed at specific (i.e. discrete) points in time, so that we proceed with a discretization of our model. Under the P-measures, equation (4.2) can be expressed in discrete time as

$$\begin{aligned} x(t+\Delta t) &= E_t[x(t+\Delta t)|x(t)] + \int_t^{t+\Delta t} e^{-k[\Delta t - u]} \sigma dW^P(u) \\ &= \theta + e^{-k}\,[x(t) - \theta] + \varepsilon(t+\Delta t) \end{aligned} \tag{4.15}$$

where Δt is the discrete time interval of one month, as the periodicity of the dataset is. Equation (4.15) is equivalent to a first order Gaussian VAR:

$$\begin{aligned} x_t &= \theta + e^{-k\Delta t}(x_{t-1} - \theta) + \varepsilon_t \\ &= \theta + F(x_{t-1} - \theta) + \varepsilon_t \end{aligned} \tag{4.16}$$

where ε_t is the 2×1 vector of innovations to x_t, and the time interval between x_t and x_{t-1} is one month.

4.4.6. Numerical integration

From (4.13) we know that

$$\underline{R}(t,\tau) = \frac{1}{\tau}\int_0^\tau \underline{f}(t,u)du$$

However the CDF and the PDF included in the expression of $\underline{f}(t,u)$ prevent us to find a closed form analytic solution of the integral. As suggested by Krippner (2015), we can rely on a numerical integration of $\underline{f}(t,u)$ based on constant rectangular increments with end-increment

[81] As explained by Krippner (2015) the two zero restrictions on a_0 and k_{11}^Q imply $x_1(t)$ moves as a random walk, while $x_2(t)$ moves as a mean reverting process under the Q-measures. The arbitrage-free Nelson and Siegel (1987) model is in facts a common subclass of Gaussian models.

LB forward rate evaluation. This is done by discretizing the integral, so that we end up expressing $\underline{R}(t,\tau)$ as the mean of end-increment LB forward rates.

More specifically, given a constant time increment $\Delta\tau$ [82] and by expressing $J = \frac{\tau}{\Delta\tau}$, we obtain

$$\underline{R}(t,\tau) = \frac{1}{\tau}\int_0^{\tau} \underline{f}(t,u)du \cong \frac{1}{\tau}\left(\sum_{j=1}^{J} \underline{f}(t,j\Delta\tau)\,\Delta\tau\right)$$
$$= mean\left\{\underline{f}(t,\Delta\tau),\dots,\underline{f}(t,j\Delta\tau)\right\}$$

where $\underline{R}(t,\tau)$ will be referred to as the "LB interest rate function".

Given that $\underline{R}(t,\tau) \cong mean\left\{\underline{f}(t,\Delta\tau),\dots,\underline{f}(t,j\Delta\tau)\right\}$, LB bond prices end up being expressed as

$$\underline{P}(t,\tau) = e^{-\tau\cdot\underline{R}(t,\tau)} \cong e^{-\tau\,[mean\left\{\underline{f}(t,\Delta\tau),\dots,\underline{f}(t,j\Delta\tau)\right\}]}$$

4.5. Model estimation

The state-space representation of the model comprises the measurement equation given by (4.14) and the state equation given by (4.16). Moreover, since we have a nonlinear measurement equation, we must use a nonlinear filtering technique, namely the iterated extended Kalman filter. The nonlinearity requires the calculation of the measurement equation to be done using a first-order Taylor approximation of the LB interest rate function around the best available estimate of $x(t)$. Each iteration of the Kalman filter allows to improve the estimate of $x(t)$ with which we repeat the approximation. This procedure continues either for a pre-determined number of iterations or, as in this dissertation, up to a tolerance condition in the update of $x(t)$. For further details about the estimation algorithm see appendix C.

For the purpose of estimation by means of an Iterated Extended Kalman Filter with Maximum Likelihood estimation an initial guess is needed for each parameter, meaning that we instruct the estimation with an initial set of suitable parameters. Differently from related papers regarding the euro area, we derive a suitable initial set of parameters from the estimation of an ANSM(2) (i.e. without the lower bound). We use the resulting estimates as initial guesses for the estimation of its shadow version.[83] The idea is that since we observed under both approaches a high sensitivity in the shadow model's final parameters relative to their initial guesses, with such method we are able to obtain solid starting values. Finally, in the MATLAB

[82] In practice we use $\Delta\tau = 0.01$.

[83] Such technique is suggested by Christensen and Rudebusch (2016).

codes (Appendix D) we use the "*fminsearch*" function which employs the Nelder-Mead algorithm to maximize the log-likelihood function.[84]

4.5.1. Overall sample estimation

By employing the whole dataset, that is 194 end-of-month observations, we test the idea of a time-varying lower bound. Thus, we estimate a two-factor shadow rate model with a regime-switching lower bound, in the sense that we allow discrete movements in LB at the specific points in time indicated in table 3. Formally, we have

$$\underline{r}(t) = max\{LB_t, r(t)\}, \tag{4.17}$$

where the subscript t denotes the lower bound is time dependent, meaning it is allowed to shift to a new level exactly at the dates of cuts in the DFR. Hence the terminology "regime-switching".

As described in table 3, the dates of cuts are June 2014, September 2014, December 2015, March 2016 and September 2019, and we want to estimate 6 different bound levels with respect to 6 lower bound regimes. We refer to the lower bound values corresponding to each regime as $LB_A, LB_B, LB_C, LB_D, LB_E$ and LB_F, whose initial guesses are the DFR prevailing at the corresponding sub-period. All the other parameters are estimated over the entire time window.

	Time Interval	DFR (Initial Guess for LB)
Regime A	August 2005 - May 2014	0.000
Regime B	June 2014 - August 2014	-0.100
Regime C	September 2014 - November 2015	-0.200
Regime D	December 2015 - February 2016;	-0.300
Regime E	March 2016 - August 2019	-0.400
Regime F	September 2019 - September 2021	-0.500

Table 3. Lower Bound Regimes and corresponding Initial Guesses.

For comparison, we then estimate a two-factor shadow rate model with a single constant lower bound, namely

$$\underline{r}(t) = max\{LB, r(t)\}. \tag{4.18}$$

[84] MATLAB codes are based on the ones provided by Leo Krippner are publicly available at: https://www.rbnz.govt.nz/research-and-publications/research-programme/additional-research/measures-of-the-stance-of-united-states-monetary-policy/matlab-code-for-krippner-2015-shadow-zlb-term-structure-model

As for the initial guess of the lower bound, we use the DFR prevailing at the end of the sample estimation (i.e. -0.50%).

4.5.2. Estimation results

Table 4 shows the parameter estimates for both approaches over the period that goes from August 2005 to September 2021. Calculations of the standard errors are based on the inverse of the Hessian matrix evaluated around the final parameter estimates, that is by taking the square root of its diagonal elements as described in Krippner (2015) pp.74.

For what concerns the lower bound estimations, the two approaches results are in line with each other: the model with a constant lower bound provides a value of -0.5218% for LB, that is very close to the one resulting for LB_F, namely -0.50%. Both reflect the DFR prevailing from September 2019, that is -0.50% indeed. However, the regime-switching mechanism captures the significant downward trend in the value of the lower bound, reflecting the influence exerted by the ECB's decisions, with LB_B, LB_C, LB_D, LB_E, LB_F being statistically significant. Notice LB_A is not statistically different from zero, thus supporting the idea of a constant ZLB prior the NIRP.

Constant LB: Log-likelihood: -9386.39

	Initial Guess	Estimate	Std Error
ϕ	0.1244	0.3473	0.0003
k_{11}	0.0092	0.0206	0.0172
k_{12}	-0.0202	-0.0030	0.0003
k_{21}	0.0651	0.0207	0.0192
k_{22}	0.0163	0.0020	0.0000
θ_1	-0.2189	-0.1036	0.1335
θ_2	0.6186	0.0290	1.5527
σ_1	1.3883	3.4118	0.0011
σ_2	1.5766	3.9099	0.0006
ρ_{12}	-93.7111	-96.9152	0.0000
LB	-0.5000	-0.5218	0.0000

Regime-switching LB: Log-likelihood: 891789.53

	Initial Guess	Estimate	Std Error
ϕ	0.1244	0.1244	0.0000
k_{11}	0.0092	0.0092	0.0000
k_{12}	-0.0202	-0.0202	0.0000
k_{21}	0.0651	0.0651	0.0000
k_{22}	0.0163	0.0163	0.0000
θ_1	-0.2189	-0.2190	0.0000
θ_2	0.6186	0.6186	0.0000
σ_1	1.3883	1.3884	0.0000
σ_2	1.5766	1.6160	0.0000
ρ_{12}	-93.7111	-93.7110	0.0000
LB_A	0.0000	0.0000	0.0129
LB_B	-0.1000	-0.1000	0.0417
LB_C	-0.2000	-0.2025	0.0000
LB_D	-0.3000	-0.3019	0.0000
LB_E	-0.4000	-0.4000	0.0000
LB_F	-0.5000	-0.5000	0.0001

Table 4. Final Parameters of a constant LB model (left panel) and of a regime-switching model (right panel). θ_1, θ_2, σ_1, σ_2, ρ_{12}, LB and the corresponding standard errors are expressed in percentage terms (i.e. multiplied by 100). Initial guesses result from an ANSM(2) estimation.

Additionally, the estimation provides a long run mean for the short rate (i.e. $\theta_1 + \theta_2$) that is not statistically significant under the constant lower bound assumption, while with a regime-switching specification we obtain a long run mean of 0.3996%. Both values are reasonable, considering long term yields have been persistently low as well. By allowing the lower bound to change in time we obtain lower variance coefficients for both state variables, as well as a lower correlation parameter. Regarding the latter, such high values suggest the estimated state variables have (almost) opposite dynamics. Intuitively, this helps in ensuring the flatness of the shadow short rate $r(t)$ with the two factors compensating each other.

The values of the standard errors are worth of mention since under a regime-switching LB they are extremely low for all the model's parameters. This is a curious result, especially if we compare such values with the (still low) standard errors obtained under a constant LB specification. There are different possible explanations behind this results. One of them is that the estimation date, namely September 2021, is two years distant from the last ECB's adjustment in the DFR. This implies that the last 25 end-of-month observations of the Euro OIS curve are not affected by any shock, thus being very similar between them. The incredibly low variability of the dataset may be reflected by the very high values of the standard errors. To give an idea in table 5 we provide the minimum, maximum and the average of the observed OIS rates over the last 25 end-of-months observations, namely from September 2019 to September 2021. However, as we point out in subsection 4.5.5 it has to be noticed that the low variability is not the only determinant of such low standard errors.

	1 month	3 month	6 month	1 year	2 years	3 years	5 years	7 years	10 years
MIN	-0.4863	-0.5064	-0.535	-0.5629	-0.5898	-0.612	-0.574	-0.489	-0.355
MAX	-0.44	-0.4441	-0.4444	-0.4464	-0.4278	-0.406	-0.2675	-0.129	0.071
MEAN	-0.4657	-0.4740	-0.4837	-0.4993	-0.5093	-0.5076	-0.4333	-0.3394	-0.1802

Table 5. Minimum, maximum and mean of end-of-month Euro OIS rates at each maturity. Time window: August 2015 – September 2021.

For what concerns the goodness of fit, table 6 and table 7 show the regime-switching model and the constant LB model provide root mean squared errors (RMSE) and mean absolute errors (MAE) that are in line with each other for most maturities but for the long-end of the yield curve, namely for the 7-year and 10-year maturities, where the regime-switching model seems to have a poor predictive power.[85] However, the standard deviation for the 10-year maturity is much more contained under a regime-switching LB, as well as the standard deviations

[85] The poor fit at the extremes of the yield curve is somehow expected under both models. Krippner (2015) specifies a better goodness of fit at the very short end and the very long end of the yield curve can be achieved by exploiting the extra flexibility offered by a three-factor shadow rate model.

corresponding to the maturities below the year, suggesting a much better fit to the short end of the yield curve. At the same time, the standard deviations of the 1-year, 2-year and 3-year maturities, are larger under a regime-switching LB compared to a constant LB model.

Constant LB

	1 month	3 month	6 month	1 year	2 year	3 year	5 year	7 year	10 year
RMSE	13.13	6.66	0.34	8.25	12.66	11.94	6.36	1.10	12.06
MAE	9.32	4.72	0.03	5.92	9.41	9.09	4.85	0.42	10.46
STD DEV*	34.33	25.23	14.35	3.86	4.70	4.35	6.29	12.66	51.84

Table 6. RMSE, MAE and STD DEV. All values are in basis points (i.e. multiplied by 10000). The STD DEV* represents the standard deviation estimated by the iterated extended Kalman filter for each maturity. Time window August 2005 – September 2021.

Regime-Switching LB

	1 month	3 month	6 month	1 year	2 year	3 year	5 year	7 year	10 year
RMSE	12.44	6.47	1.99	8.72	13.44	12.55	5.56	12.35	28.78
MAE	9.26	5.05	0.38	7.24	11.77	10.88	2.66	10.67	24.83
STD DEV*	12.38	6.30	0.01	7.83	12.99	13.46	3.17	13.46	33.71

Table 7. RMSE, MAE and STD DEV*. All values are in basis points (i.e. multiplied by 10000). The STD DEV* represents the standard deviation parameters, for each maturity, resulting from estimation. Time window August 2005 – September 2021.

4.5.3. Cumulative estimations: real time scenario and ex-post scenario

From the previous estimations it is clear the constant LB model does not provide us with information regarding the evolution of the time-varying lower bound. However, in real time estimation and forecasting we do not dispose of information regarding the future evolution of the bound, as we did not when negative rates were adopted by the ECB. Let us analyse how the two approaches perform by setting ourselves at the beginning of each year starting from January 2014. Thus, we calculate the model implied LOH under both approaches and compare differences.

Notice the update frequency of one year is a good compromise between a very-short term update, which is not needed considering policy rates do not change frequently, and a longer-term update, which could make us lose some new market information. Thus, considering the governing council meeting of the ECB schedules its meeting every three month, we decided to employ a one-year update. Additionally, we adopt a cumulative estimation method, so that at each time we re-estimate the model we add the last 12 end-of-month observations.[86] By implementing a cumulative window rather than a rolling window we are able to exploit the whole variability of the dataset up to each estimation date, especially in those periods in which OIS rates are extremely stable. Finally, the choice of January 2014 as starting date comes from

[86] The approach is similar to Christensen and Rudebusch (2016) that implement a (cumulative) weekly re-estimation using US treasury yields.

two reasons. First, the estimate in January 2014 will be based on 102 end-of-month observations, providing a solid initial estimate. Second, estimating the model in January 2014 sets us exactly 6 months before the first negative cut, allowing us to check whether the market anticipated negative cuts over the year.

We organize the real time estimation as follow: starting from January 2014, we re-estimate the two-factor shadow rate model with a constant lower bound, formally expressed as (4.18), at a yearly frequency up to January 2021, for a total of eight real time estimations. The choice of a constant lower bound for the real time estimation comes from the commonly agreed idea of a ZLB prior the NIRP. We therefore carry on this idea over time, meaning after the cuts in negative territory. However, by updating the shadow rate model we actually question the value of the bound every 12 months.[87] As for the real time estimation, we re-estimate the regime-switching model in (4.17) at the same dates conditionally on information available at each date. In facts, the difference with the real time scenario is the LB mechanism in (4.17) is an information we dispose of after evaluating the entire time window. More specifically, when we re-estimate the model by adding new observations which include a date of a cut in the DFR, we allow the bound to switch to a new value. As a consequence, the shadow rate models estimated under the two approaches in January 2014 are equivalent. The lower bound specifications, and thus the estimations start to diverge from January 2015 onwards. Table 8 sums up the lower bound specifications under the two scenarios.

Estimation Window	**Real Time Estimation** $\underline{r}(t) = max\{LB, r(t)\}$	**Ex-post Estimation** $\underline{r}(t) = max\{LB_t, r(t)\}.$
August 2005 – January 2014	$LB^{(1)}$	$LB_t = LB_A{}^{(1)}$
August 2005 – January 2015	$LB^{(1)}$	$LB_t = \{LB_A, LB_B, LB_C{}^{(2)}\}$
August 2005 – January 2016	$LB^{(1)}$	$LB_t = \{LB_A, LB_B, LB_C, LB_D{}^{(3)}\}$
August 2005 – January 2017	$LB^{(1)}$	$LB_t = \{LB_A, LB_B, LB_C, LB_D, LB_E{}^{(4)}\}$
August 2005 – January 2018	$LB^{(1)}$	$LB_t = \{LB_A, LB_B, LB_C, LB_D, LB_E{}^{(5)}\}$
August 2005 – January 2019	$LB^{(1)}$	$LB_t = \{LB_A, LB_B, LB_C, LB_D, LB_E{}^{(6)}\}$
August 2005 – January 2020	$LB^{(1)}$	$LB_t = \{LB_A, LB_B, LB_C, LB_D, LD_E, LB_F{}^{(7)}\}$
August 2005 – January 2021	$LB^{(1)}$	$LB_t = \{LB_A, LB_B, LB_C, LB_D, LD_E, LB_F{}^{(8)}\}$

Table 8 Lower bound specifications under a real time scenario and an ex-post scenario.
Notes: (1) LB is estimated over the entire corresponding window.
(2) Regime C starts in September 2014 up to January 2015.
(3) Regime D starts in December 2015 up to January 2016.
(4) Regime E starts in March 2016 up to January 2017.
(5) Regime E starts in March 2016 up to January 2018.
(6) Regime E starts in March 2016 up to January 2019.
(7) Regime F starts in September 2019 up to January 2020.
(8) Regime F starts in September 2019 up to January 2021.

[87] Technically we are assuming a constant lower bound, but to some extent by re-estimating the model we derive an estimated sequence of constant lower bounds.

4.5.4. Estimation results

The results of our estimations are reported in the Appendix (B). For comparison, here we plot parameters' estimates under the two scenarios to analyse differences and parameters stability over time.

Figure 8 shows the series of real time estimates of a constant lower bound closely resembles the bound values assumed by a regime-switching model estimated in January 2021. The real time lower bound in 2014 is slightly positive, while is it not significant under the ex-post scenario. Additionally, a clear downward trend leads to a real time estimate in January 2021 of -0.5315%, and a slightly higher value of -0.4965% for the last regime lower bound at the same estimation date. However, despite minor differences, the two approaches are in line with each other, reproducing the adjustments in the DFR quite precisely. Obviously, allowing the bound to switch at the DFR cut dates in the ex-post approach means updating the bound specification as soon as the cut occurs, while under a real time yearly re-estimation we incorporate market information with some degree of delay. However, this problem could be improved with a more frequent real time re-estimation to immediately capture current market perceptions.

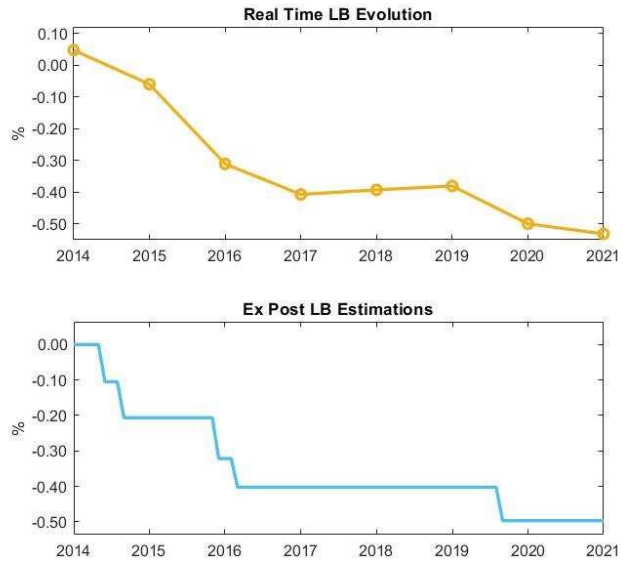

Figure 8. Panel 1: dotted points represent the estimated real time *LB* in January of each year.
Panel 2: estimated LB regimes under an ex-post estimation in January 2021.

For what concerns mean reversion values, i.e. the elements of the matrix k, figure 9 shows a poor parameters stability under both approaches, especially in the first half of the window. Each speed of reversion coefficient assumes similar values under both scenarios, with the real time estimates showing slightly more persistence, that is lower estimated values. Noticeably, in January 2017 a regime-switching specification leads to substantially different estimates for k_{12}, $k_{21}$and k_{22}.

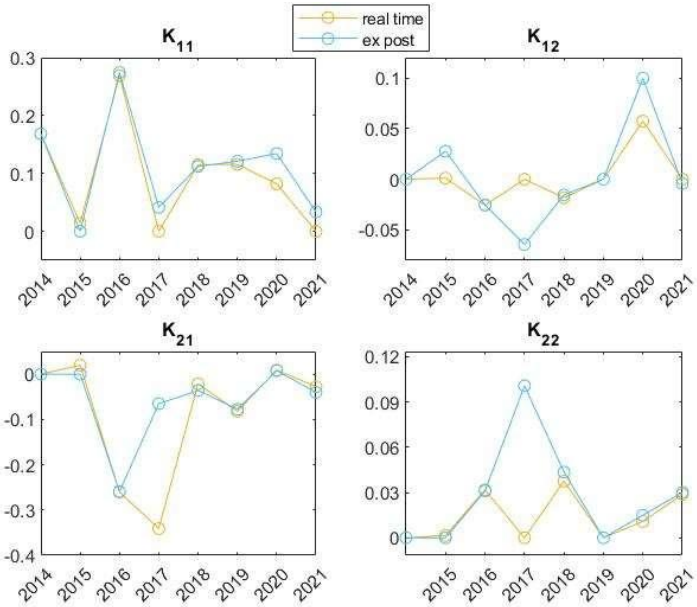

Figure 9. Mean reversion parameters k_{11}, k_{12},k_{21} and k_{22} estimated under a real time and ex-post scenario. Estimated values which are not significant are set equal to zero.

Generally, mean reversion parameters seems to achieve stability from January 2018, meaning over a period which is not characterized by DFR cuts, with the only exception of September 2019, a cut that seems to be reflected by the little adjustments in the 2020 estimates of k_{11} and k_{12}. In facts, from the January 2018 updates, re-estimations of both models lead to changes in parameters values that are smoother than the ones we witness before 2018. This is reasonable if we consider that 4 cuts out of 5 occurred before January 2017.

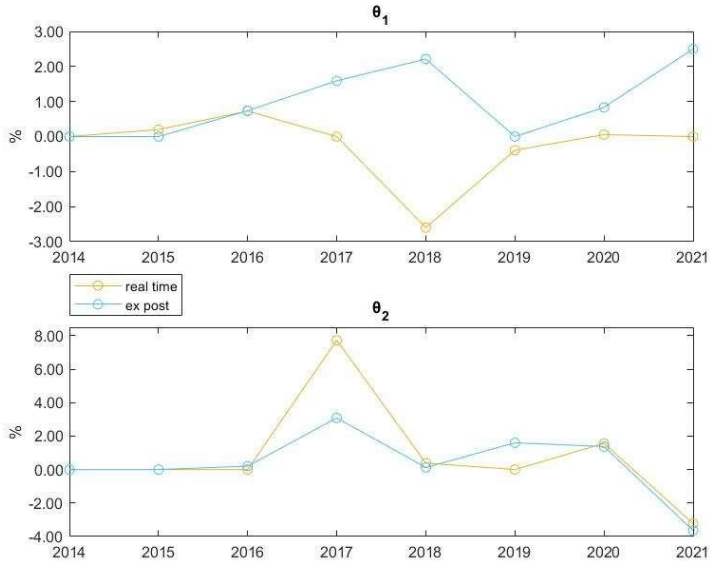

Figure 10. Long run mean parameters of the state variables $x_1(t)$ and $x_2(t)$, namely θ_1 and θ_2 respectively, estimated under a real time and ex-post scenario. Estimated values which are not significant are set equal to zero.

In Figure 10 we plot the estimated long run means of the two state variables. In this case, poor stability is observed for both θ_1 and θ_2 under a real time scenario, while updates are flatter when we employ a regime-switching mechanism. Estimates are quite similar with the exception of 2017 and 2018. However, what is important is actually the combined effect of θ_1 and θ_2, i.e. their sum, that is equivalent to the long run mean of the shadow short rate $r(t)$. In figure 11 we can see the long expectation of $r(t)$ moves in the same direction each time the model is updated under both scenarios, with the only exception of January 2019. However, magnitudes are quite different, as well as the sign in estimated means in 2018 and in 2019. Finally, except for the estimates in 2017, long run means float around zero.[88]

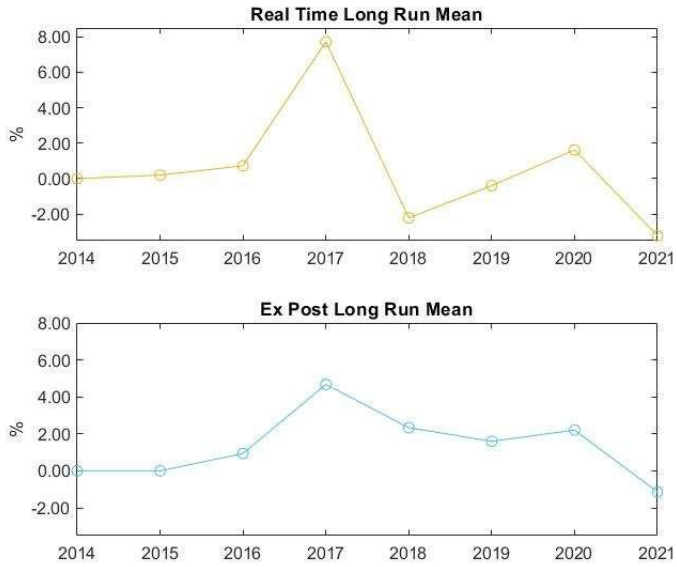

Figure 11. Long run mean of shadow short rate $r(t)$ estimated under a real time and ex-post scenario.

These results, and the fact that the long run mean does not decline as the LB does, are not surprising for two reasons. First, also related analysis in the literature, such as the one of Lemke and Vladu (2016) and Kortlea (2016), show parameters estimated under the P-measures are less accurate than the ones under the Q-measures.[89] Second, Krippner (2015) proposes the shadow short rate $r(t)$, and thus its long run mean, as an indicator of monetary policy stance, meaning it may reflect long-term market expectations regarding future central bank decisions. In this perspective, $r(t)$ moving in the same direction at each update but in 2019, suggests expectations

[88] The average estimated long run mean is -0.47% and 0.85% under a real time estimation and ex-post estimation, respectively.

[89] In this regard, Lemke and Vladu (2016) specifies the reason is that estimates under the P-measures do not exploit the full data cross section observed at a given point in time as estimates under the Q-measures do. For example, the 2017 estimate of θ_2 is 0.0772 (i.e. 7.72%) against a standard error of 0.0342, meaning it is just slightly significant.

under the two scenarios are captured in a similar way. However, further analysis are needed, and the sole indication provided by long run mean must be treated with care given the poor accuracy issue mentioned above.

As for the long run means, in figure 12 we see how estimated volatility coefficients are always similar under the two scenarios, but still showing remarkable differences in 2017 and in 2018. As before, a regime-switching mechanism permits to obtain more stable parameters. Irrespectively of the lower bound specification, we obtain similar magnitudes for $\sigma_1$and σ_2. This is not surprising given the high correlation parameters (i.e. ρ_{12}) that we obtain under both approaches. Such values of σ_1 and σ_2, together with a high value of ρ_{12} guarantee the estimated series of $x_1(t)$ and $x_2(t)$ to reproduce the flatness property of the observed yields.

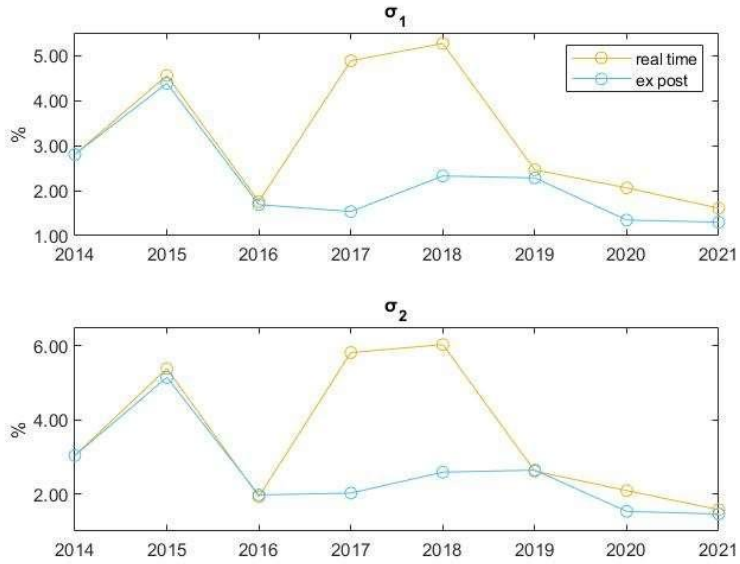

Figure 12. Volatility coefficients $\sigma_1$and σ_2 estimated under a real time and ex-post scenario.
Estimated values which are not significant are set equal to zero.

Finally, in figure 13 we plot ϕ that is the speed of reversion of the state variable $x_2(t)$ under the Q-measures. Again, the regime-switching specification allows smoother changes in the value of ϕ, and the estimated values show substantial differences in 2017 and 2018.

To sum up, it seems the two approaches provide different estimates in 2017 and 2018. Curiously, if we consider the time distance between each re-estimation date and the previous DFR cut, then 2017 and 2018, together with 2019, represent the more distant re-estimation dates from the previous rate cut.[90] However, it may also be the case that recursive differences in

[90] The last cut we observe prior January 2017 is 9 months before, that is March 2016, and the following one occurs only in September 2019.

parameter estimates observed in the same years may actually compensate each other, so that both models are, on overall, similar.

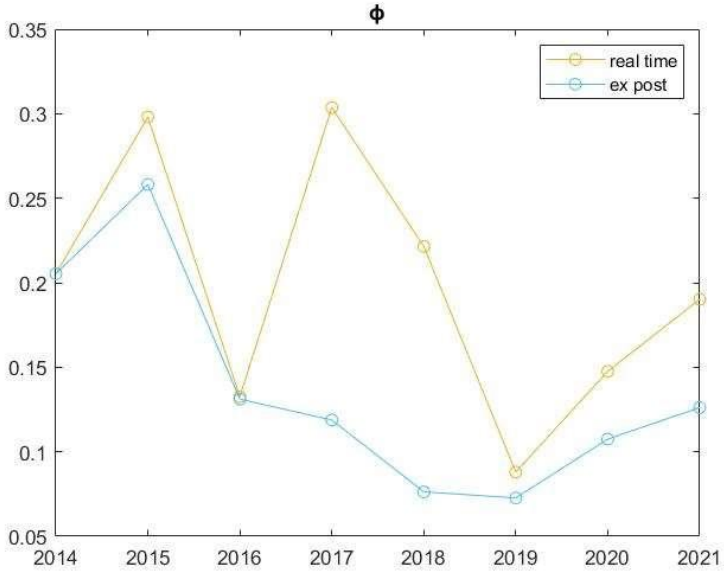

Figure 13. Mean reversion parameter ϕ estimated under a real time and ex-post scenario.

To conclude, it has to be noticed how estimation results in appendix (B) show similar final parameter estimates compared to their corresponding initial guesses. This is particularly true for a regime-switching model from the 3rd cumulative window (i.e. 2005-2016) onwards, while it is not always the case for a constant LB model. Additionally, we have already pointed out in section 4.5.2 that, for what concerns the values obtained for the standard errors, the low variability of the dataset may be an important determinant. As we can see in table 9, in which we provide the standard deviations of the observed yields at each estimation date (i.e. up to that date, from the introduction of the NIRP volatility has dramatically decreased. However, an additional point must be made: by looking at the standard errors obtained at the different estimation dates in appendix (B), we do not observe relevant and systematic differences between the two LB specifications. Moreover, although the distance of the estimation date from the date of the previous DFR cut impacts on the variability of the dataset, this cannot be the only explanation of such values of the standard errors. In facts, standard errors are definitely lower for most parameters under a regime-switching LB in January 2016, with a cut happening only in December 2015, as well as in January 2017 with the cut happening in March 2016. Additionally, the estimate of January 2019, that is almost three years later the previous DFR cut date (i.e. March 2016) does not lead to extremely low standard errors as for the estimates of January 2021 and the one of section 4.5.2 (i.e. September 2021). In other words, the distance of the estimation dates from the DFR cut dates do not necessarily lead to low values of the

standard errors. Another factor that could possibly explain such results is the fact that we employ the estimates of a Gaussian model, that is ANSM(2), as initial guesses for the shadow rate model estimation. This means that in facts we are estimating parameters twice, and what we generally observe, especially from the estimate of January 2016 onwards, is the final parameters estimates being very close to their initial guesses.

	1-month	3-month	6-month	1-year	2-year	3-year	5-year	7-year	10-year
2014	1.5241	1.5487	1.5720	1.5873	1.5280	1.4609	1.3136	1.1804	1.0501
2015	1.5201	1.5456	1.5717	1.5953	1.5578	1.5132	1.4056	1.2970	1.1783
2016	1.5206	1.5475	1.5760	1.6054	1.5845	1.5563	1.4782	1.3901	1.2886
2017	1.5256	1.5524	1.5819	1.6162	1.6103	1.5982	1.5508	1.4829	1.3937
2018	1.5201	1.5461	1.5751	1.6103	1.6090	1.6011	1.5629	1.5021	1.4171
2019	1.5079	1.5332	1.5616	1.5975	1.5981	1.5911	1.5557	1.4996	1.4203
2020	1.4943	1.5199	1.5490	1.5871	1.5950	1.5967	1.5778	1.5373	1.4747
2021	1.4808	1.5062	1.5355	1.5751	1.5892	1.5992	1.5968	1.5736	1.5324

	1-month	3-month	6-month	1-year	2-year	3-year	5-year	7-year	10-year
Pre-June 2014	1.5207	1.5460	1.5706	1.5896	1.5393	1.4803	1.3439	1.2151	1.0747
Post-June 2014	0.1437	0.1452	0.1467	0.1516	0.1671	0.1996	0.2721	0.3406	0.4196

Table 9. Euro OIS rates volatilities at each estimation date (panel 1).
Euro OIS rates volatilites prior and after June 2014 (panel 2).
Time window: August 2005 – January 2021.

4.5.5. A parallel analysis: the importance of updating the LB

In order to doublecheck the importance of treating the LB as a free parameter to estimate and to be regularly updated, we carry out a recoursive estimation of a model in which the LB is set to the value estimated over the entire time window in section 4.5.2 under the constant LB model. Formally, we have

$$\underline{r}(t) = max\{LB, r(t)\},$$

where LB = -0.5218% at each re-estimation date.

As expected, the estimation is quite problematic. First of all, not allowing the LB to be updated overtime implies a larger computational burden in carrying out such estimates. In particular, it dramatically increases the time required by the estimation algorithm to reach convergence, that is to provide estimates of the model's parameters (see appendix C for more details on the iterated extended Kalman filter with maximum likelihood estimation). This issue makes it impossible to obtain estimates for some re-estimation dates with our current hardware. Additionally, for those time windows for which we are able to reach convergence, we obtain

an extremely high mean reversion parameter under the Q-measures (i.e. ϕ) and very low mean reversion parameters under the P-measures (i.e. k_{11}, k_{12}, k_{21}, k_{22}). The long run mean of $r(t)$ assumes, for some estimation dates, extremely positive values as well as extremely negative values for some others. As a consequence, these results imply a very poor goodness of fit.

This further analysis strengthens the hypothesis of a time-varying LB, thus the importance to allow the model to update the LB value overtime. In other words, even though the LB value has been previously estimated and it is significantly negative, the fact that we do not allow the update implies practical problems in the estimation and it dramatically decreases the model's predictive power.

4.6. The liftoff horizon

In this section, we calculate the LOH at each estimation date under both scenarios. The difference is that with a real time approach the LOH reflects the set of all the available information up to the estimation dates. Contrarily, LOH calculated with an ex-post estimation of the model are obtained on the basis of a model's specification previously evaluated by exploiting all the dataset at our disposal.

In line with the literature, we define the liftoff measure at current time t as LOH_t, that is the median future point in time in which the short rate is expected to cross a given threshold and to float above it for at least a given time. We repeat the following procedure for all eight estimation dates, so that we obtain eight LOH measures under each approach: by employing the parameter estimates obtained in the previous section, we use a Monte Carlo simulation to derive $J = 10000$ short rate paths over a 10-year horizon under the P-measures,[91] and we find the first point in time at which each simulated short rate crosses a threshold of 0.10% and stays above it for at least K months. [92]

By expressing with $LOH_{t,j}$ the liftoff horizon at the current time t of the j^{th} simulated path, we have

$$LOH_{t,j} = \inf\{\hat{\tau} \mid r(t+s) > 0.001, \text{ for } s = \hat{\tau}, \hat{\tau}+1, \ldots, \hat{\tau}+K-1\} \qquad (4.19)$$

where K is equal to 3, 6 and 12 months.

At time t, each J^{th} simulated path provides a $LOH_{t,j}$, and the resulting LOH_t will be the median of such distribution. Given the extreme flatness of the observed yields, differently from related

[91] We use only parameters that are statistically significant.

[92] We use a slightly positive threshold since we have slightly positive LB estimates for January 2014. In addition, this choice gives more accuracy to the LOH estimates relative to a simple zero threshold.

studies,[93] we choose to consider different values of K so that, to some extent, we derive different degrees of accuracy for LOH_t.[94]

Concerning the simulation, the choice of employing estimated parameters under the P-measures is to capture real world expectations about the ECB's decisions. Notice that under the ex-post scenario, at each simulation date we assume the future values of the LB to be the ones we previously estimated over the entire sample period. In other words, with respect to the simulation date, the future movements of the LB are the ones estimated in section 4.5.2 and presented in table 5, with the LB value to shift exactly at the dates of change in regime. For example, for the simulation date of January 2014, the LB value is assumed to change in June 2014, September 2014, December 2015, March 2016 and September 2019 and to take the corresponding regime's estimated LB value. The same reasoning goes for the simulation date of January 2015, with the LB value to change in December 2015, March 2016 and September 2019, and so on for the following simulation dates. However, this is not a sensitive assumption: by calculating LOH_t with respect to a threshold and not with respect to the LB, the value of the latter per se' has little importance. Finally, any estimated $LOH_{t,j}$ exceeding 10 years is recorded at the maximum value of 10 years. Consequently, this is valid also for LOH_t as well as the resulting standard deviations.[95]

4.6.1. Model-implied liftoff horizons

As we can see in table 10, in January 2014, while the DFR was at 0 percent, the model-implied liftoff measure for LOH_{2014} is equal to 3.75 years for $K = 3$ months under a real time scenario. Higher values of K imply higher values for LOH_{2014}, thus suggesting the 3.75 years estimate to be quite weak. Although we cannot say anything regarding expectations of a cut in negative territory, it seems market participants expect the zero-rate policy to last for years. At the same time, uncertainty is substantial, as standard deviations are around 4 years for whatever K. Results are very similar under the ex-post scenario being the two models equivalent in 2014.

The difference in lower bound specification leads to different estimates starting from January 2015: under a real time scenario the estimated values of LOH_{2015} under all K suggest solid expectations of a liftoff in positive territory in the following 2 or 3 years, with less variability relative to 2014. In particular, a LOH_{2015} equal to 3.74 years for with $K = 1$ year is very

[93] Lemke and Vladu (2016), Kortela (2016), Pericoli and Taboga (2015) and Wu and Xia (2016) do not derive multiple measures of LOH for different duration requirements.

[94] Kortela (2016) considers a 6-month period, while Lemke and Vladu (2016) one year period.

[95] We think it makes little sense to consider such long liftoff's dates. A 10-year LOH would be interpreted as the market does not expect upward adjustments in DFR any soon.

indicative of the market perception of a temporary NIRP. Under the ex-post scenario, liftoff estimates for LOH_{2015} are higher for all values of K, as well as their standard deviations.[96]

Liftoff estimates from 2016 to 2019 under both scenarios imply very little probabilities given by market agents to a DFR upward adjustment any time soon. Notice, this corresponds to the longest period over which the ECB did not revise its decisions: the DFR was kept at -0.40% from March 2016 to September 2019, before being cut even further to -0.50%.

	REAL TIME SCENARIO(1)			**EX-POST SCENARIO(1)**		
	3 months	6 months	1 year	3 months	6 months	1 year
2014	3.75	5.63	8.25	3.94	5.73	8.38
StdDev(2)	(4.14)	(4.07)	(3.93)	(4.15)	(4.07)	(3.94)
2015	2.02	(2.67)	3.74	3.96	6.83	10
StdDev(2)	(3.76)	(3.83)	(3.89)	(4.08)	(4.02)	(3.75)
2016	10	10	10	10	10	10
StdDev(2)	(3.46)	(3.30)	(3.09)	(3.47)	(3.32)	(3.11)
2017	10	10	10	8.69	10	10
StdDev(2)	(3.47)	(3.29)	(3.18)	(2.70)	(2.61)	(2.49)
2018	5.77	7.48	10	6.64	7.93	10
StdDev(2)	(4.03)	(3.94)	(3.82)	(3.70)	(3.59)	(3.45)
2019	10	10	10	10	10	10
StdDev(2)	(3.48)	(3.31)	(3.07)	(2.79)	(2.61)	(2.40)
2020	2.89	3.32	3.93	2.15	2.46	2.83
StdDev(2)	(3.05)	(3.15)	(3.28)	(2.43)	(2.59)	(2.81)
2021	10	10	10	10	10	10
StdDev(2)	(2.74)	(2.40)	(2.03)	(1.75)	(1.52)	(1.26)
Sept.2021	3.98	5.50	8.01	8.63	10	10
StdDev(2)	(3.97)	(3.93)	(3.82)	(3.51)	(3.40)	(3.25)

Table 10. LOH calculations and standard deviations under the real time and ex-post scenarios.
10000 simulated short rate paths under the P-measures. LOH measures are median dates expressed in years.
Notes: (1) LOH exceeding 10 years have been set equal to 10 years.
(2) LOH exceeding 10 years have been set equal to 10 years in the StdDev calculation.

Curiously, market agents seem to start questioning the NIRP duration in January 2020: under both scenarios measures of LOH_{2020} indicate the market to expect an increase in the short rate in the following 2 or 3 years, probably not taking into account the pandemic effects yet, as one might deduce by ECB (2020c).[97] Under the ex-post scenario, estimates are less uncertain for all K, as indicated by the lower standard deviations. However, in January 2021 liftoff measures do not seem to reflect expectations about a short rate increase any soon. Intuitively, a reasonable

[96] For $LOH_{2015} = 10$ years with $K = 1$ year we obtain a standard deviation of 3.75 years. However, most values of the liftoff's distribution exceed 10 years, thus making such standard deviation meaningless.
[97] In the press conference of 23 January 2020 there were no references to possible effects of Covid 19. See ECB (2020c)

explanation may be the expansionary policies implemented to sustain the eurozone during the pandemic as ECB (2021a) suggest.[98]

Finally, under a real time scenario, liftoff measures in September 2021 seem to ease the idea of a long-term NIRP implied by the estimates of the beginning of the year, probably reflecting, among other factors, the more recent increase in inflation rate.[99] However, the regime-switching model does not revise the January 2021 estimates, except for a slight downward adjustment in $LOH_{Sep\,2021}$ for $K = 3$ months. Volatilities still suggest a widespread uncertainty.

	Differences in LOH measures		
	3 months	6 months	1 year
2014	0.19	0.10	0.13
2015	1.94	4.16	6.26
2016	0	0	0
2017	1.31	0	0
2018	0.87	0.45	0
2019	0	0	0
2020	0.74	0.86	1.10
2021	0	0	0
Sept.2021	4.65	4.50	1.99

Table 11. Differences in absolute terms in LOH measures.
Values expressed in years.

The LOH measures we obtain under the two approaches are generally in line with each other. From table 11, that shows the difference in LOH measures for each date and for every K, we see remarkable differences only in January 2015 and September 2021. For all the other estimation dates LOH measures differ by a magnitude within the year, but for 2017 that is 1.31 years for $K = 3$ months. Additionally, the two models seem to agree in forecasting a long-term implementation of the NIRP in the period 2016-2019.

Notice the high liftoff estimates that we derived from 2016 to 2019, as well as 2021, are not surprising: by setting a threshold of 0.10% we require the short rate to overcome such positive level for at least K months. In other words, we are actually evaluating the horizon after which market participants expect the NIRP to finish rather than a simple liftoff from the current lower bound (i.e. the current DFR). As shown in the following section, the market participants reasonably expects a series of gradual upward adjustments in the DFR. In particular, if the short rate is stuck at negative levels such as -0.30%, -0.40% and -0.50%, as it is in those years, if

[98] ECB (2021) was conducted between 7 and 11 January 2021 indicates inflations expectations to be 0.9%, 1.3% and 1.5% for 2021, 2022 and 2023 respectively. Additionally, survey participants expect the ECB's main policy rates to remain unchanged until at least 2023.
[99] See Eurostat (2021).

there are no clear signals of an ECB move, the time required to cross the threshold may be substantial, thus such a jump is logically not contemplated by the market.

4.6.2. Comparison of liftoff horizon measures with survey evidence

Given the observation provided above, we compare our model-implied estimates of LOH with real market expectations. For this purpose, we use the most recent ECB Survey of Monetary Analysts (SMA),[100] which report, among the others, survey's participants answers relative to the expected size of the next increase in DFR, as well as the expected timing of the next increase. Although the two answers may affect each other, we will focus on the median of the answer's distributions. Unfortunately, surveys' results are publicly available only from June 2021, so that we are forced to employ the ones of June 2021 and September 2021. Their corresponding survey periods are from 25 May 2021 to 28 May 2021 and from 23 August to 27 August 2021, respectively. In line with the survey periods, the simulation dates we consider are the 31st of May 2021 and the 31st of August 2021. As before, we simulate using parameters under the P-measures, which have been estimated given all the available information up the simulation date.

Notice that both surveys provides us with an expected median size of the next DFR increase being equal to 10 basis points. This suggest the market expects a gradual upward adjustment in the DFR by the ECB. As a consequence, for the purpose of this comparison, LOH estimates are derived with respect to a threshold of -0.45%. Such a threshold allows us to focus on the liftoff from the current estimated lower bound, that in 2021, as we saw in section 4.4.2, is basically equivalent to -0.50%.

Formally,

$$LOH_{t,j} = \inf\{\hat{\tau} \mid r(t+s) > -0.0045, \text{ for } s = \hat{\tau}, \hat{\tau}+1, \ldots, \hat{\tau}+K-1\} \qquad (4.19)$$

where K is equal to 3, 6 and 12 months.

At time t, each J^{th} simulated path provides a $LOH_{t,j}$, and the resulting LOH_t will be the median of such distribution.

It has to be noticed that, if on the one hand we are able to forecast a liftoff horizon from the current level of the DFR, we cannot say anything about its size, while the answers of the survey's partecipants in terms of timing and size may affect each other. Given this remark, it is curious to test what our models suggest at least from a timing point of view, considering also the fact that expectations about the size of the ECB's adjustments are embodied in the observed OIS rates that we use for the exercise. Results are in table 12.

[100] See ECB's website for additional details: https://www.ecb.europa.eu/stats/ecb_surveys/sma/html/index.en.html

	REAL TIME SCENARIO			EX-POST SCENARIO		
	3 months	6 months	1 year	3 months	6 months	1 year
31 May 2021	1.37	2.11	3.38	4.23	5.77	8.42
StdDev(1)	(3.71)	(3.87)	(3.99)	(3.98)	(3.93)	(3.82)
31 August 2021	2.16	3.04	4.51	9.72	10	10
StdDev(1)	(3.74)	(3.84)	(3.90)	(2.69)	(2.59)	(2.47)

Table 12. LOH and standard deviations under the real time and ex-post scenario.
10000 simulated short rate paths under the P-measures. LOH measures are median dates expressed in years.
Notes: (1) LOH exceeding 10 years have been set equal to 10 years in the StdDev calculation.

As the results obtained in the previous subsection, the standard deviations of the LOH distribution are quite large, reflecting the widespread uncertainty of the market regarding the timing ECB's decisions. This makes it difficult to express a judgement regarding the accuracy of such measures. However, the model-implied LOH estimates that we obtain seem to be in line with real market expectations. In particular, for what concerns measures of $LOH_{May\ 21}$, ECB (2021b) indicated the expected median timing of the next DFR increase to be May 2024, meaning 3 years later. Our real time model seems to replicate this forecast: the most solid LOH estimate, that is the one with $K = 1$ year, is 3.38 years. In other words, our model forecasts an upward adjustment from the current level of the DFR of -0.50% in 3.38 years. Even though we cannot say anything about the size of the increase, our estimate is in line with the market expectations in terms of timing. Additionally, under a duration requirement of $K = 6$ months we obtain an estimate of 2.11 years, in line with the 25th percentile of the SMA, that is $LOH_{May\ 21}$ being September 2023. As in table 10, standard deviations take values from 3.70 up to 4 years, reflecting a wide LOH distribution. On the other hand, the regime-switching model seems to be less sensitive to market expectations, providing us with an estimate of 8.49 years for K =1 year, 5.77 years for $K = 6$ months and 4.23 years for $K = 3$ months.

Similarly, relative to liftoff's expectations in August 2021, ECB (2021c) indicates the median size of the next DFR increase to be 10 basis points, with the expected median timing being December 2024, that is 3.33 years later. Also in this case, by considering the most accurate $LOH_{Aug\ 21}$ estimates, namely for $K = 6$ months and for $K = 1$ year, the real time model provides similar liftoff horizons, that are 3.04 years and 4.51 years, respectively. Under an ex-post scenario horizons are again overestimated to the extent that the model does not foresee any upward adjustment any soon.

Differently from LOH measures with respect to a positive threshold, estimates regarding an upward adjustment in the DFR are quite different under the two approaches, especially in August 2021. Although, we cannot reach further conclusion on the basis of two surveys, differences in table 13 suggest a possible sensitivity relative to the lower bound specification

that we generally do not observe in table 11. A similar result is provided by Lemke and Vladu (2016), that observe changes up to 48 months in liftoff measures across models with different lower bound specifications. Additionally, the interquartile range of their estimated LOH distributions float between 3 and 7 years under their preferred (regime-switching) model, that is in line with our standard deviations.

	Differences in LOH measures		
	3 months	6 months	1 year
31 May 2021	2.86	3.66	5.04
31 August 2021	7.56	6.96	5.49

Table 13. Differences in absolute terms in LOH measures.
Values expressed in years.

Finally, we consider ECB pre-meeting poll results provided by Reuters: figure 14 clearly shows how, from 2013 up to 2021, polls' participants never expected an upward adjustment in the deposit rate, that is maximum expectations about the level of the deposit rate are always equivalent to the current DFR value. However, median poll results (i.e. the blue line) shows how participants anticipated all ECB's cuts in negative territory but the one in September 2014. Although Reuters polls only refer to the immediate ECB governing council's meeting and do not include long-term forecasts, there is a clear downward trend in DFR real expectations that correlates with the actual cuts. Over the same period, regardless the scenario considered, table 9 shows that our LOH estimates predict short rates to turn back positive in the medium term (i.e. in no less than 5 years), with the exceptions of the most optimistic forecasts, namely 2014, 2015, 2020 and September 2021 in which LOH estimates are in any case no less than 2 years. Thus, our results seem to be coherent with the general economic sentiment, especially over the period 2016 – 2019, in which everyone seems to agree on the current deposit rate level, while our estimates suggest the market to not foresee the end of the NIRP any time soon.

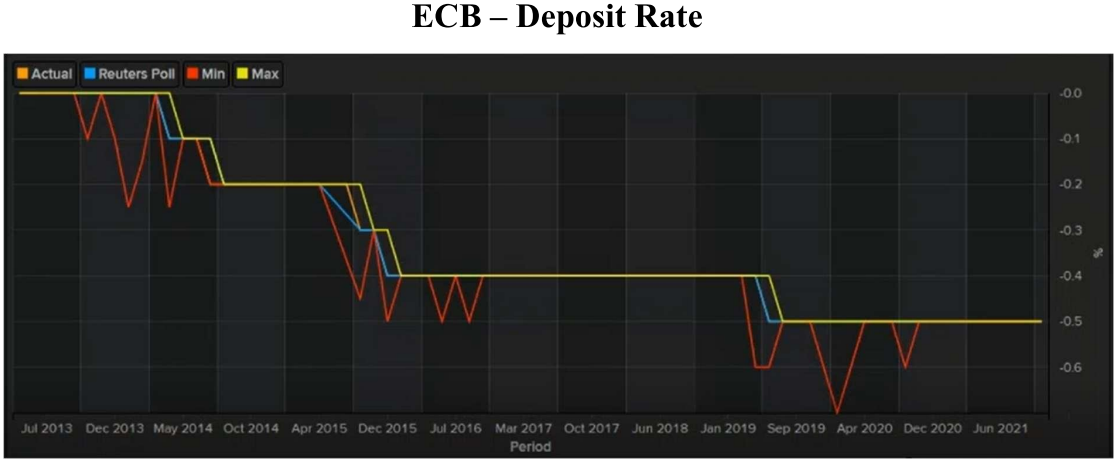

Figure 14. Actual DFR and pre-meeting poll results (median) 2013 – 2021, included minimum and maximum poll answers. Source: Reuters.

4.7. Goodness of fit

In table 14 we report the average for each maturity of the RMSE, MAE and the standard deviations resulting from the two models estimates. As pointed out in section 4.4.2, the poor fit at the extremes of the yield curve, namely 1-month and 10-year maturities is expected from a two-factor model. However, a regime-switching LB specification does not seem to provide a better fit to the observed yields: all the indicators are, on average, slightly higher relative to the constant LB model, but for the long-end of the yield curve in which the fit provided by a regime-switching model is substantially worse. Moreover, the lower standard deviations we observe for the 1-month, 2-month and 3-month maturities do not seem to compensate the worse fit the model generally provides.

By observing the estimates on a standalone basis (see appendix B), we note that for the period 2005-2015 a regime-switching LB specification allows to obtain a slightly better fit: in tables A7 and A8, for all maturities but 6-month and 7-year maturities, RMSE and MAE are slightly lower than with a constant lower bound. Also the estimated STD DEV suggest a better fit to the observe yields for most maturities under a regime-switching model. Over the period 2005-2016 the regime-switching model starts providing a worse fit: in tables A11 and A12, RMSE and MAE are slightly higher for all maturities but 7-year and 10-year, with no significant differences in terms of estimated STD DEV. However, in the periods 2005-2017 and 2005-2018, the fit provided by the regime-switching models start being substantially worse than constant LB as all the indicators suggest, especially for maturities above 2 years. Finally, from the window 2005-2019 onwards, RMSE, MAE and STD DEV are very similar, especially for the period 2005-2019, while still being slightly higher under an ex-post scenario for the remaining windows.

Real Time Scenario: Constant LB

	1m	3m	6m	1y	2y	3y	5y	7y	10y
RMSE	14.35	7.31	0.22	9.09	13.83	12.95	5.70	3.77	15.47
MAE	10.85	5.68	0.03	7.30	11.70	11.09	4.68	3.11	13.17
STD DEV	16.74	9.12	1.73	8.59	12.61	12.17	5.93	5.64	20.92

Ex-Post Scenario: Regime-Switching LB

	1m	3m	6m	1y	2y	3y	5y	7y	10y
RMSE	14.35	7.39	1.19	9.53	14.99	14.44	6.60	6.31	20.93
MAE	11.03	5.90	0.24	8.04	13.17	12.65	5.09	5.24	17.56
STD DEV	14.29	7.23	0.22	9.16	14.96	14.47	6.24	6.48	23.59

Table 14. Average RMSE, MAE and STD DEV for each maturity.
All cumulative windows considered, included the one on the overall sample. All values are in basis points.

Under both models it seems there is a problem in fitting the observed yields at the long-end of the yield curve. In this regard we recall the fact that we use three maturities below the year, namely 1-month, 3-month, 6-month maturities, to accentuate the focus of the models on the short term. This choice could generally explain the poor predictive power of long maturities. However, the problem is observed with more frequency under a regime-switching LB, in particular for the estimates of January 2017 and January 2018. Thus, it seems that by allowing the lower bound to switch downward, the model loses additional predictive power for what concerns longer maturities.

CHAPTER 5

5. Conclusions

After having established the existence of a time-varying lower bound, we found that including historical information regarding shifts in LB in a two-factor model through a regime-switching specification does not allow to significantly improve the model performance, at least in a context of a recursive model estimation. Although it guarantees more stable parameters, a regime-switching mechanisms provides parameter estimates that are not particularly different compared to a single LB specification where the value of the bound is re-estimated and thus updated at each estimation date. Additionally, the goodness of fit of its predicted yield curves appears to be in line with the one under a single LB specification. However, as pointed out by Hull (2014) the quality of the goodness of fit may not be particularly relevant for a real time estimation aimed at scenario analysis over the long term, that is the current term structure may not be particularly important.

More specifically, a sequence of estimated single LB closely resembles the estimated LB regimes values, allowing a single LB model to incorporate the current market perceptions about the value of the LB. Additionally, mean reversion parameters and long run mean estimates do not seem to be affected by the lower bound specification when employing the same initial guesses. However, we observed differences in estimates at two dates, namely 2017 and 2018, but the fact this is true for all parameters suggests differences may compensate each other, so that the two models have similar predictive power on overall.

For what concerns liftoffs to a positive region, forecasts under the two approaches seem broadly in line with each other: with the exceptions of 2 estimation dates out of 9 (i.e. January 2015 and September 2021) at which LOH measures vary significantly, we observe little sensitivity against LB specifications for whatever K we require. When they greatly differ, LOH estimates vary up to 6.36 years for $K = 1$ year and around 60 months for $K = 3$ and $K = 6$ months, in line with Lemke and Vladu (2016) that found differences up to 48 months for $K = 1$ year with a three-factor model. For all the remaining dates we do not observe systematic differences, meaning that LOH are quite robust to LB specification.

However, the additional estimates of LOH with respect to the current DFR are instead sensitive to the LB specification. Thus, it is difficult to reach a conclusion regarding a preferred specification for what concerns LOH forecasts, as in facts, up to date, we are still facing a DFR of -0.50%. What we observe is that LOH measures under a regime-switching LB seem more "cautious" and seem to reflect less real market expectations, at least according to surveys. A

possible explanation is that a downward regime-switching mechanism accentuate the influence of the downward trend in rates on parameter estimates compared to parameters of a constant LB model. In other words, the short rate may be strongly instructed to stick to the LB, thus requiring more time to permit a liftoff. A possible explanation is that by emplyoing cumulative windows rather than a rolling window the weights of new observations on the estimation results is less relevant. This could explain the reluctance of the model in forecasting a LOH any time soon. However, we employ cumulative windows also for the estimation of the constant LB model, the regime-switching specification could be the element playing a big role in delaying LOH forecasts.

Finally, differently from Christensen and Rudebusch (2016a) that found differences in parameter estimates of a standard Gaussian model compared to its shadow rate representation, we find that with a consistent number of observations, parameters resulting from the estimation of an ANSM(2) mirror the final estimates of its shadow version, as well as LB estimates closely resemble the DFR. Thus, a regime-switching specification seems to allow a shortcut in model estimation reducing the computational burden and thus the estimation time required by a full shadow rate model. However, this is not valid for a constant LB specification.

APPENDIX A: The affine term structure

We present the definition and a (partial) derivation of an affine term structure as according to Björk (2009). This result is extremely important for the analytical tractability of the Vasicek and Hull-White models.

Definition A. Suppose to have a generic short rate model, whose dynamics under the Q-measures are:

$$dr(t) = \mu\big(t, r(t)\big)dt + \sigma\big(t, r(t)\big)dW(t), \tag{A1}$$

where

$$\mu(t, r) = \alpha(t)r + \beta(t),$$

and

$$\sigma(t, r) = \sqrt{\gamma(t)r + \delta(t)}.$$

Then the model admits an ATS form, meaning $P(t,T) = exp\{A(t,T) - B(t,T)r(t)\}$ where $A(t,T)$ and $B(t,T)$ are the deterministic functions and solutions of

$$\begin{cases} B_t(t,T) + \alpha(t)B(t,T) - \dfrac{1}{2}\gamma(t)B^2(t,T) = -1, \\ B(T,T) = 0. \end{cases} \tag{A2}$$

$$\begin{cases} A_t(t,T) = \beta(t)B(t,T) - \dfrac{1}{2}\delta(t)B^2(t,T), \\ A(T,T) = 0. \end{cases} \tag{A3}$$

Proof: Assume the model in (A1) admits an ATS form: $F^T(t, r(t)) = exp\{A(t,T) - B(t,T)r(t)\}$. Considering term structure equation (2.15) must be solved by $F^T(t, r(t))$, after deriving the partial derivatives F_t^T, F_r^T, F_{rr}^T, and plugging them in (2.15) we obtain

$$A_t(t,T) - \{1 + B_t(t,T)\}r - \mu(t,r)B(t,T) + \frac{1}{2}\sigma^2(t,r)B^2(t,T) = 0 \tag{A4}$$

with the boundary value of (2.15) implying

$$\begin{cases} A(T,T) = 0, \\ B(T,T) = 0. \end{cases} \tag{A5}$$

If (A4) and (A5) are satisfied, then the ATS exist. In particular, as Björk (2009) points out, there will be choices of $\mu(t,r)$ and $\sigma(t,r)$ which, under some conditions, ensure the $A(t,T)$ and $B(t,T)$ exist such that (A4) is satisfied.

These conditions are obtained by assuming an affine form for $\mu(t,r)$ and $\sigma(t,r)$, that is

$$\begin{cases} \mu(t,r) = \alpha(t)r + \beta(t), \\ \sigma(t,r) = \sqrt{\gamma(t)r + \delta(t).} \end{cases}$$

so that (A4) is a separable differential equation that can be re-written as

$$A_t(t,T) - \beta(t)B(t,T) + \frac{1}{2}\delta(t)B^2(t,T) - \left\{1 + B_t(t,T) + \alpha(t)B(t,T) - \frac{1}{2}\gamma(t)B^2(t,T)\right\}r = 0 \tag{A6}$$

Given that (A6) holds for all t, T and r, we can fix t and T. Now (A6) holds for every r, making us conclude that its coefficient must be equal to zero, that is

$$B_t(t,T) + \alpha(t)B(t,T) - \tfrac{1}{2}\gamma(t)B^2(t,T) = -1, \tag{A7}$$

and, consequently,

$$A_t(t,T) = \beta(t)B(t,T) - \frac{1}{2}\delta(t)B^2(t,T). \tag{A8}$$

Thus, we conclude $A(t,T)$ and $B(t,T)$ must satisfy (A5), as well as (A8) and (A7), respectively. As stated above, this is a partial derivation. It must be remarked $\mu(t,r)$ and $\sigma(t,r)$ do not have to be necessarily affine to guarantee an ATS to be admitted. However, affinity is a necessary condition for a model to admit an ATS when $\mu(r)$ and $\sigma(r)$ are not dependent on time.

APPENDIX B: Estimation Results

1st window 2005 - 2014:

2005-2014 Constant LB: Log-likelihood: -4780.43

	Initial Guess	Estimate	Std Error
ϕ	0.1203	0.2053	0.0085
k_{11}	0.1285	0.1683	0.0154
k_{12}	0.0422	0.0405	0.1343
k_{21}	-0.0799	-0.0782	0.1364
k_{22}	0.0097	0.0104	0.0749
θ_1	0.4123	0.1015	0.1974
θ_2	0.0341	0.0194	0.0547
σ_1	1.8104	2.8029	0.0034
σ_2	2.1134	3.0381	0.0064
ρ_{12}	-94.7277	-96.1682	0.2614
LB	0.0000	0.0466	0.0000

Table A1. Final Parameters of a constant LB model. θ_1, θ_2, σ_1, σ_2, ρ_{12}, LB and the corresponding standard errors are expressed in percentage terms (i.e. multiplied by 100).

2005-2014 Regime-switching LB
Log-likelihood: -4780.43

	Initial Guess	Estimate	Std Error
ϕ	0.1203	0.2053	0.0085
k_{11}	0.1285	0.1683	0.0154
k_{12}	0.0422	0.0405	0.1343
k_{21}	-0.0799	-0.0782	0.1364
k_{22}	0.0097	0.0104	0.0749
θ_1	0.4123	0.1015	0.1974
θ_2	0.0341	0.0194	0.0547
σ_1	1.8104	2.8029	0.0034
σ_2	2.1134	3.0381	0.0064
ρ_{12}	-94.7277	-96.1682	0.2614
LB_A	0.0000	0.0466	0.0000

Table A2. Final Parameters of a regime-switching model. θ_1, θ_2, σ_1, σ_2, ρ_{12}, LB and the corresponding standard errors are expressed in percentage terms (i.e. multiplied by 100).

	RMSE	MAE	STD DEV*
1 m	17.00	13.35	18.57
3 m	8.69	7.12	8.05
6 m	0.10	0.02	0.23
1 y	10.86	9.23	11.14
2 y	17.05	14.95	15.33
3 y	16.41	14.40	16.96
5 y	8.26	6.95	8.33
7 y	0.03	0.01	0.25
10 y	9.20	7.64	8.62

Table A3. RMSE, MAE and STD DEV. All values are in basis points (i.e. multiplied by 10000). The STD DEV* represents the standard deviation parameters, for each maturity, resulting from estimation.

	RMSE	MAE	STD DEV*
1 m	17.00	13.35	18.57
3 m	8.69	7.12	8.05
6 m	0.10	0.02	0.23
1 y	10.86	9.23	11.14
2 y	17.05	14.95	15.33
3 y	16.41	14.40	16.96
5 y	8.26	6.95	8.33
7 y	0.03	0.01	0.25
10 y	9.20	7.64	8.62

Table A4. RMSE, MAE and STD DEV. All values are in basis points (i.e. multiplied by 10000). The STD DEV* represents the standard deviation parameters, for each maturity, resulting from estimation.

2nd window 2005 - 2015:

2005-2015 Constant LB: Log-likelihood: -5421.10

	Initial Guess	Estimate	Std Error
ϕ	0.1287	0.2980	0.0046
k_{11}	0.0043	0.0141	0.0000
k_{12}	-0.0078	0.0011	0.0001
k_{21}	-0.0205	0.0197	0.0001
k_{22}	0.0375	0.0016	0.0000
θ_1	0.0848	0.2001	0.0621
θ_2	1.0099	4.8177	6.3133
σ_1	1.4556	4.5527	0.0000
σ_2	1.7322	5.3806	0.0000
ρ_{12}	-91.8250	-98.8342	0.1726
LB	-0.2000	-0.0606	0.0201

Table A5. Final Parameters of a constant LB model. θ_1, θ_2, σ_1, σ_2, ρ_{12}, LB and the corresponding standard errors are expressed in percentage terms (i.e. multiplied by 100).

2005-2015 Regime-switching LB

Log-likelihood: -5458.22

	Initial Guess	Estimate	Std Error
ϕ	0.1287	0.2582	0.0002
k_{11}	0.0043	0.0030	0.0156
k_{12}	-0.0078	0.0277	0.0054
k_{21}	-0.0205	-0.0117	0.0161
k_{22}	0.0375	0.0041	0.0158
θ_1	0.0848	0.2554	2.3770
θ_2	1.0099	0.5836	0.4691
σ_1	1.4556	4.3788	0.0156
σ_2	1.7322	5.1435	0.0416
ρ_{12}	-91.8250	-99.2175	0.0527
LB_A	0.0000	0.0626	0.0072
LB_B	-0.1000	0.0111	0.0187
LB_C	-0.2000	-0.0680	0.0297

Table A6. Final Parameters of a regime-switching model. θ_1, θ_2, σ_1, σ_2, ρ_{12}, lower bounds and the corresponding standard errors are expressed in percentage terms (i.e. multiplied by 100).

	RMSE	MAE	STD DEV*
1 m	16.54	13.31	16.48
3 m	8.27	6.71	8.85
6 m	0.09	0.01	0.05
1 y	9.77	7.72	9.85
2 y	13.65	11.37	13.24
3 y	12.51	10.76	12.51
5 y	6.38	5.59	5.95
7 y	0.02	0.01	0.27
10 y	8.63	7.09	8.88

Table A7. RMSE, MAE and STD DEV (all wrt residuals p.55. All values are in basis points (i.e. multiplied by 10000). The STD DEV* represents the standard deviation parameters i.e. the std dev of the residuals p.55, for each maturity, resulting

	RMSE	MAE	STD DEV*
1 m	15.89	12.01	15.52
3 m	7.98	6.20	7.96
6 m	0.45	0.23	0.91
1 y	9.72	7.59	9.71
2 y	13.62	11.14	14.65
3 y	12.36	10.41	12.40
5 y	6.29	5.35	6.39
7 y	0.03	0.01	0.21
10 y	7.08	5.65	7.03

Table A8. RMSE, MAE and STD DEV. All values are in basis points (i.e. multiplied by 10000). The STD DEV* represents the standard deviation parameters, for each maturity, resulting from estimation.

3rd window 2005 – 2016:

2005-2016 Constant LB: Log-likelihood: -5836.81

	Initial Guess	Estimate	Std Error
ϕ	0.1305	0.1326	0.0000
k_{11}	0.2712	0.2690	0.0071
k_{12}	-0.0261	-0.0258	0.0000
k_{21}	-0.2632	-0.2606	0.0111
k_{22}	0.0314	0.0317	0.0014
θ_1	0.7225	0.7273	0.0000
θ_2	0.1992	0.1986	0.9178
σ_1	1.7255	1.7565	0.0016
σ_2	1.9635	1.9285	0.0000
ρ_{12}	-93.9670	-94.0421	0.0014
LB	-0.3000	-0.3114	0.0000

Table A9. Final Parameters of a constant LB model. θ_1, θ_2, σ_1, σ_2, ρ_{12}, LB and the corresponding standard errors are expressed in percentage terms (i.e. multiplied by 100).

2005-2016 Regime-switching LB

Log-likelihood: -5838.42

	Initial Guess	Estimate	Std Error
ϕ	0.1305	0.1311	0.0004
k_{11}	0.2712	0.2743	0.0000
k_{12}	-0.0261	-0.0254	0.0000
k_{21}	-0.2632	-0.2592	0.0000
k_{22}	0.0314	0.0311	0.0000
θ_1	0.7225	0.7383	0.0219
θ_2	0.1992	0.2030	0.0000
σ_1	1.7255	1.6891	0.0000
σ_2	1.9635	1.9768	0.0105
ρ_{12}	-93.9670	-94.0106	0.0456
LB_A	0.0000	0.0126	0.0047
LB_B	-0.1000	-0.1010	0.0917
LB_C	-0.2000	-0.1976	0.0000
LB_D	-0.3000	-0.3114	0.0000

Table A10. Final Parameters of a regime-switching model. θ_1, θ_2, σ_1, σ_2, ρ_{12}, lower bounds and the corresponding standard errors are expressed in percentage terms (i.e. multiplied by 100).

	RMSE	MAE	STD DEV*
1 m	15.00	11.80	14.60
3 m	7.69	6.30	7.82
6 m	0.58	0.05	0.01
1 y	9.60	8.24	9.45
2 y	14.43	12.96	14.29
3 y	12.53	11.20	12.58
5 y	0.66	0.06	0.13
7 y	14.17	12.30	14.78
10 y	32.01	27.54	35.71

Table A11. RMSE, MAE and STD DEV. All values are in basis points (i.e. multiplied by 10000). The STD DEV* represents the standard deviation parameters, for each maturity, resulting from estimation.

	RMSE	MAE	STD DEV*
1 m	15.28	12.23	15.11
3 m	7.83	6.49	7.73
6 m	1.07	0.15	0.01
1 y	9.74	8.42	8.85
2 y	14.55	13.11	13.43
3 y	12.60	11.30	12.78
5 y	1.02	0.14	0.14
7 y	14.01	12.19	15.11
10 y	31.66	27.19	36.19

Table A12. RMSE, MAE and STD DEV. All values are in basis points (i.e. multiplied by 10000). The STD DEV* represents the standard deviation parameters, for each maturity, resulting from estimation.

4th window 2005 - 2017:

2005-2017 Constant LB: Log-likelihood: -6660.87

	Initial Guess	Estimate	Std Error
ϕ	0.1208	0.3036	0.0023
k_{11}	0.0402	0.1076	0.0774
k_{12}	-0.0639	0.0322	0.0459
k_{21}	-0.0675	-0.3411	0.0003
k_{22}	0.1075	-0.0923	0.0776
θ_1	1.7946	-2.6070	4.1632
θ_2	2.7896	7.7220	3.4157
σ_1	1.7984	4.8792	0.1124
σ_2	2.0384	5.8125	0.0553
ρ_{12}	-94.9796	-98.9723	0.1746
LB	-0.4000	-0.4074	0.0124

Table A13. Final Parameters of a constant LB model. θ_1, θ_2, σ_1, σ_2, ρ_{12}, LB and the corresponding standard errors are expressed in percentage terms (i.e. multiplied by 100).

2005-2017 Regime-switching LB

Log-likelihood: -94.4215

	Initial Guess	Estimate	Std Error
ϕ	0.1208	0.1188	0.0000
k_{11}	0.0402	0.0416	0.0000
k_{12}	-0.0639	-0.0644	0.0000
k_{21}	-0.0675	-0.0650	0.0000
k_{22}	0.1075	0.1008	0.0000
θ_1	1.7946	1.5925	0.0002
θ_2	2.7896	3.0823	0.0001
σ_1	1.7984	1.5347	0.0001
σ_2	2.0384	2.0257	0.0000
ρ_{12}	-94.9796	-94.9455	0.0005
LB_A	0.0000	-0.0067	0.0129
LB_B	-0.1000	-0.1018	0.0585
LB_C	-0.2000	-0.1986	0.0001
LB_D	-0.3000	-0.3418	0.0001
LB_E	-0.4000	-0.3557	0.0002

Table A14. Final Parameters of a regime-switching model. θ_1, θ_2, σ_1, σ_2, ρ_{12}, lower bounds and the corresponding standard errors are expressed in percentage terms (i.e. multiplied by 100).

	RMSE	MAE	STD DEV*
1 m	14.15	10.22	14.14
3 m	7.14	5.26	7.08
6 m	0.00	0.00	0.05
1 y	8.34	6.13	8.39
2 y	10.66	8.43	10.58
3 y	8.30	6.87	8.56
5 y	1.82	1.40	3.33
7 y	5.10	4.21	5.97
10 y	12.65	10.77	13.08

Table A15. RMSE, MAE and STD DEV. All values are in basis points (i.e. multiplied by 10000). The STD DEV* represents the standard deviation parameters, for each maturity, resulting from estimation.

	RMSE	MAE	STD DEV*
1 m	14.83	11.65	13.76
3 m	7.60	6.17	7.61
6 m	1.10	0.23	0.06
1 y	9.53	8.17	8.67
2 y	14.37	12.76	16.24
3 y	12.60	11.12	12.32
5 y	1.64	0.63	0.98
7 y	14.43	12.30	11.50
10 y	34.03	28.70	40.05

Table A16. RMSE, MAE and STD DEV. All values are in basis points (i.e. multiplied by 10000). The STD DEV* represents the standard deviation parameters, for each maturity, resulting from estimation.

5th window 2005 - 2018:

2005-2018 Constant LB: Log-likelihood: -7317.18

	Initial Guess	Estimate	Std Error
ϕ	0.0765	0.2214	0.0001
k_{11}	0.1117	0.1151	0.0000
k_{12}	-0.0153	-0.0183	0.0000
k_{21}	-0.0368	-0.0214	0.0000
k_{22}	0.0436	0.0375	0.0000
θ_1	2.2014	-2.5991	0.0047
θ_2	0.1246	0.3848	0.0001
σ_1	2.3138	5.2636	0.0178
σ_2	2.5679	6.0275	0.0629
ρ_{12}	-97.6825	-99.3918	0.0486
LB	-0.4000	-0.3930	0.0164

Table A17. Final Parameters of a constant LB model. θ_1, θ_2, σ_1, σ_2, ρ_{12}, LB and the corresponding standard errors are expressed in percentage terms (i.e. multiplied by 100).

2005-2018 Regime-switching LB

Log-likelihood: -4798.39

	Initial Guess	Estimate	Std Error
ϕ	0.0765	0.0763	0.0000
k_{11}	0.1117	0.1121	0.0000
k_{12}	-0.0153	-0.0155	0.0000
k_{21}	-0.0368	-0.0359	0.0000
k_{22}	0.0436	0.0435	0.0000
θ_1	2.2014	2.2126	0.0001
θ_2	0.1246	0.1241	0.0001
σ_1	2.3138	2.3248	0.0001
σ_2	2.5679	2.5909	0.0001
ρ_{12}	-97.6825	-97.6938	0.0001
LB_A	0.0000	0.0051	0.0161
LB_B	-0.1000	-0.1010	0.0625
LB_C	-0.2000	-0.2005	0.0002
LB_D	-0.3000	-0.3031	0.0004
LB_E	-0.4000	-0.3970	0.0003

Table A18. Final Parameters of a regime-switching model. θ_1, θ_2, σ_1, σ_2, ρ_{12}, lower bounds and the corresponding standard errors are expressed in percentage terms (i.e. multiplied by 100).

	RMSE	MAE	STD DEV*
1 m	13.69	9.85	13.75
3 m	6.96	5.07	7.16
6 m	0.07	0.02	0.34
1 y	8.48	6.21	8.55
2 y	12.16	9.44	12.11
3 y	11.21	9.02	11.18
5 y	5.90	4.87	5.93
7 y	0.00	0.00	0.13
10 y	7.94	6.63	7.92

Table A19. RMSE, MAE and STD DEV. All values are in basis points (i.e. multiplied by 10000). The STD DEV* represents the standard deviation parameters, for each maturity, resulting from estimation.

	RMSE	MAE	STD DEV*
1 m	14.11	11.00	14.00
3 m	7.33	5.93	7.18
6 m	1.26	0.20	0.14
1 y	9.71	8.43	9.46
2 y	16.49	14.84	16.24
3 y	17.36	15.52	17.66
5 y	10.69	9.39	11.10
7 y	0.63	0.12	0.53
10 y	16.80	13.48	18.64

Table A20. RMSE, MAE and STD DEV. All values are in basis points (i.e. multiplied by 10000). The STD DEV* represents the standard deviation parameters, for each maturity, resulting from estimation.

6th window 2005 - 2019:

2005-2019 Constant LB: Log-likelihood: -7720.92

	Initial Guess	Estimate	Std Error
ϕ	0.0723	0.0880	0.0002
k_{11}	0.1207	0.1157	0.0000
k_{12}	0.0058	0.0057	0.0788
k_{21}	-0.0811	-0.0821	0.0000
k_{22}	0.0161	0.0160	0.0747
θ_1	-0.4059	-0.3900	0.0000
θ_2	1.5733	1.5457	1.6343
σ_1	2.3725	2.4601	0.0224
σ_2	2.6168	2.6186	0.0211
ρ_{12}	-98.0001	-98.0052	0.0238
LB	-0.4000	-0.3808	0.0084

Table A21. Final Parameters of a constant LB model. θ_1, θ_2, σ_1, σ_2, ρ_{12}, LB and the corresponding standard errors are expressed in percentage terms (i.e. multiplied by 100).

2005-2019 Regime-switching LB

Log-likelihood: -6937.10

	Initial Guess	**Estimate**	**Std Error**
ϕ	0.0723	0.0727	0.0021
k_{11}	0.1207	0.1212	0.0072
k_{12}	0.0058	0.0059	0.0730
k_{21}	-0.0811	-0.0775	0.0000
k_{22}	0.0161	0.0161	0.0730
θ_1	-0.4059	-0.3954	0.7226
θ_2	1.5733	1.5981	0.0001
σ_1	2.3725	2.2814	0.0133
σ_2	2.6168	2.6441	0.0000
ρ_{12}	-98.0001	-98.0028	0.2089
LB_A	0.0000	0.0071	0.0236
LB_B	-0.1000	-0.1010	0.0693
LB_C	-0.2000	-0.2103	0.0001
LB_D	-0.3000	-0.3181	0.0019
LB_E	-0.4000	-0.3575	0.0005

Table A22. Final Parameters of a regime-switching model. θ_1, θ_2, σ_1, σ_2, ρ_{12}, lower bounds and the corresponding standard errors are expressed in percentage terms (i.e. multiplied by 100).

	RMSE	**MAE**	**STD DEV***
1 m	13.40	9.92	13.52
3 m	6.95	5.41	6.81
6 m	0.13	0.03	0.27
1 y	9.17	7.80	9.12
2 y	15.77	14.00	15.72
3 y	16.56	14.55	17.33
5 y	10.03	8.62	10.96
7 y	0.04	0.00	0.08
10 y	15.17	12.23	18.42

Table A23. RMSE, MAE and STD DEV. All values are in basis points (i.e. multiplied by 10000). The STD DEV* represents the standard deviation parameters, for each maturity, resulting from estimation.

	RMSE	**MAE**	**STD DEV***
1 m	13.50	9.73	13.16
3 m	6.99	5.25	7.03
6 m	1.11	0.23	0.31
1 y	9.17	7.54	8.93
2 y	15.46	13.13	15.96
3 y	16.20	13.61	17.05
5 y	9.85	8.21	11.03
7 y	0.65	0.05	0.09
10 y	15.99	12.23	17.68

Table A24. RMSE, MAE and STD DEV. All values are in basis points (i.e. multiplied by 10000). The STD DEV* represents the standard deviation parameters, for each maturity, resulting from estimation.

7th window 2005 - 2020:

2005-2020 Constant LB: Log-likelihood: -8237.89

	Initial Guess	Estimate	Std Error
ϕ	0.1072	0.1476	0.0006
k_{11}	0.1343	0.0821	0.0004
k_{12}	0.1008	0.0574	0.0053
k_{21}	0.0076	0.0092	0.0002
k_{22}	0.0149	0.0109	0.0052
θ_1	0.8372	0.0566	0.0000
θ_2	1.3740	1.5645	0.0032
σ_1	1.3426	2.0608	0.0019
σ_2	1.5262	2.0941	0.0001
ρ_{12}	-92.7555	-97.5259	0.0920
LB	-0.5000	-0.4996	0.0024

Table A25. Final Parameters of a constant LB model. θ_1, θ_2, σ_1, σ_2, ρ_{12}, LB and the corresponding standard errors are expressed in percentage terms (i.e. multiplied by 100).

2005-2020 Regime-switching LB

Log-likelihood: -4228.49

	Initial Guess	Estimate	Std Error
ϕ	0.1072	0.1075	0.0000
k_{11}	0.1343	0.1343	0.0006
k_{12}	0.1008	0.0996	0.0009
k_{21}	0.0076	0.0076	0.0006
k_{22}	0.0149	0.0150	0.0009
θ_1	0.8372	0.8342	0.0099
θ_2	1.3740	1.3750	0.0081
σ_1	1.3426	1.3460	0.0001
σ_2	1.5262	1.5321	0.0014
ρ_{12}	-92.7555	-92.7782	0.0000
LB_A	0.0000	-0.0003	0.0148
LB_B	-0.1000	-0.0997	0.0582
LB_C	-0.2000	-0.2006	0.0003
LB_D	-0.3000	-0.3055	0.0006
LB_E	-0.4000	-0.4112	0.0002
LB_F	-0.5000	-0.4997	0.0034

Table A26. Final Parameters of a regime-switching model. θ_1, θ_2, σ_1, σ_2, ρ_{12}, lower bounds and the corresponding standard errors are expressed in percentage terms (i.e. multiplied by 100).

	RMSE	MAE	STD DEV*
1 m	13.50	10.44	13.34
3 m	6.97	5.57	5.45
6 m	0.43	0.04	0.21
1 y	9.16	7.82	8.81
2 y	15.69	13.96	15.56
3 y	16.24	14.37	15.33
5 y	9.52	8.28	8.68
7 y	1.13	0.36	1.65
10 y	13.40	11.60	12.26

Table A27. RMSE, MAE and STD DEV. All values are in basis points (i.e. multiplied by 10000). The STD DEV* represents the standard deviation parameters, for each maturity, resulting from estimation.

	RMSE	MAE	STD DEV*
1 m	13.40	10.46	13.40
3 m	7.01	5.71	6.85
6 m	1.68	0.31	0.25
1 y	9.51	8.32	9.52
2 y	16.23	14.75	16.84
3 y	17.09	15.39	15.79
5 y	10.61	9.26	11.10
7 y	2.35	1.17	2.82
10 y	15.61	13.07	17.76

Table A28. RMSE, MAE and STD DEV. All values are in basis points (i.e. multiplied by 10000). The STD DEV* represents the standard deviation parameters, for each maturity, resulting from estimation.

8th window 2005 - 2021:

2005-2021 Constant LB: Log-likelihood: -8846.44

	Initial Guess	Estimate	Std Error
ϕ	0.1294	0.1902	0.0101
k_{11}	0.0341	0.0129	0.0084
k_{12}	-0.0043	-0.0051	0.0064
k_{21}	-0.0401	-0.0277	0.0056
k_{22}	0.0303	0.0288	0.0009
θ_1	2.5519	2.1264	1.1626
θ_2	-3.6151	-3.2233	1.2877
σ_1	1.2824	1.6092	0.0321
σ_2	1.4649	1.5796	0.0000
ρ_{12}	-91.9531	-94.6035	0.4245
LB	-0.5000	-0.5316	0.0046

Table A29. Final Parameters of a constant LB model. θ_1, θ_2, σ_1, σ_2, ρ_{12}, LB and the corresponding standard errors are expressed in percentage terms (i.e. multiplied by 100).

2005-2021 Regime-switching LB

Log-likelihood: 85671.59

	Initial Guess	Estimate	Std Error
ϕ	0.1294	0.1262	0.0000
k_{11}	0.0341	0.0336	0.0000
k_{12}	-0.0043	-0.0043	0.0000
k_{21}	-0.0401	-0.0401	0.0000
k_{22}	0.0303	0.0301	0.0000
θ_1	2.5519	2.4996	0.0000
θ_2	-3.6151	-3.6398	0.0000
σ_1	1.2824	1.2996	0.0000
σ_2	1.4649	1.4631	0.0000
ρ_{12}	-91.9531	-91.7861	0.0000
LB_A	0.0000	0.0022	0.0403
LB_B	-0.1000	-0.1049	0.0454
LB_C	-0.2000	-0.2064	0.0000
LB_D	-0.3000	-0.3214	0.0000
LB_E	-0.4000	-0.4023	0.0000
LB_F	-0.5000	-0.4965	0.0001

Table A30. Final Parameters of a regime-switching model. θ_1, θ_2, σ_1, σ_2, ρ_{12}, lower bounds and the corresponding standard errors are expressed in percentage terms (i.e. multiplied by 100).

	RMSE	MAE	STD DEV*
1 m	12.72	9.38	11.95
3 m	6.49	4.95	5.67
6 m	0.26	0.03	0.04
1 y	8.15	6.64	8.18
2 y	12.43	10.74	12.00
3 y	10.88	9.50	10.75
5 y	2.38	1.54	3.79
7 y	12.34	10.70	15.00
10 y	28.20	24.57	31.50

Table A31. RMSE, MAE and STD DEV. All values are in basis points (i.e. multiplied by 10000). The STD DEV* represents the standard deviation parameters, for each maturity, resulting from estimation.

	RMSE	MAE	STD DEV*
1 m	12.68	9.59	12.75
3 m	6.58	5.21	6.34
6 m	1.95	0.39	0.03
1 y	8.85	7.45	8.36
2 y	13.67	12.10	12.97
3 y	12.78	11.18	11.83
5 y	5.49	3.18	3.94
7 y	12.35	10.67	14.35
10 y	29.21	25.27	32.62

Table A32. RMSE, MAE and STD DEV. All values are in basis points (i.e. multiplied by 10000). The STD DEV* represents the standard deviation parameters, for each maturity, resulting from estimation.

APPENDIX C: Kalman Filter with Maximum Likelihood Algorithm

In this appendix we provide the main intuitions about the functioning of the estimation algorithm implemented in the MATLAB codes. The Kalman filter is applied via maximum likelihood, meaning that we maximize the log-likelihood value of observing the OIS rates at each observation date. Moreover, the presence of non-linearity requires the use of nonlinear filtering technique, that is the iterated extended Kalman filter (i.e. IEKF). We address the reader to Krippner (2015) for a detailed explanation about each single step of the estimation algorithm.

A Kalman filter is an optimal estimation algorithm, which allows to estimate an unobservable process making use of an observable one, under the assumption that the former affects the latter. In particular, the filter, upon a comparison with the observable process, uses the measurement errors obtained at a given point in time from the estimates of the unobservable process to update and improve them. In this way we are able to get the best estimates of the unobservable process from what we can observe instead. In our case, we utilize the Kalman Filter in the estimation of a shadow rate model whose shadow rate is described by gaussian dynamics. A shadow rate model describes the short rate $r(t)$, something that is unobservable in reality, while what we observe in reality are yields of ZCB (i.e. OIS rates). Thus, our unobservable process is the short rate $r(t)$, and therefore the state variables $x(t)$, while our observable process concerns OIS rates. The filter will then make use of the information we get from the measurement errors obtained to improve its predictive power.

A Kalman Filter estimation requires a *state equation* that describes how the state variables $x(t)$, and thus $r(t)$ evolve overtime, and a *measurement equation* which tells us how the state variables explain the observed OIS rates at each observation time, that is from $t = 1$ to T. The latter is a function of the state variables $x(t)$ and residuals, namely the measurement errors, which are the key for the proper functioning of the algorithm.

The full estimations of the shadow rate models presented in the dissertation provide, as outputs, the estimated time series of state variables, as well as estimates of the parameters of the models. To implement such estimation, repeated applications of the Kalman filter are required. In figure C1 we provide a broad scheme of how the estimation works. The optimization algorithm is composed by two blocks: the implementation of the IEKF and the maximization of the log-likelihood function. For additional details see Krippner (2015), sections 3.2.2, 3.2.3, 4.2.2 and 4.2.3.

Full Estimation with Kalman Filter via MLE

Optimization Algorithm

IEKF algorithm

1. Setup and estimation constraints

2. State initialization

3. Kalman Recursion:

For t = 1 : T

3.1. Prior state estimates
3.2. Measurement/posterior state estimates
Iterations up to tolerance condition
3.3. Posterior state estimates

next t

Maximize: $log\text{-}L\left(\left\{\underline{R_1}, \dots, \underline{R_T}\right\}, \mathbb{A}\right)$

Tolerance condition

Figure C1. Algorithm of a Full Estimation by means of the Iterated Extended Kalman Filter wth MLE.

The first step of the IEKF algorithm requires the set up (i.e. the evaluation) of parameters vectors and matrices needed for estimation. The evaluations are subject to particular constraints which are required for a smooth functioning of the algorithm.

Obviously, the IEKF requires some starting values. In step 2, we proceed to define the starting values for the state variable vector $x(t)$ and its variance, that typically are identified in the unconditional expectation and the variance of the state equation, respectively.[101]

The Kalman recursion is made up of three steps, that are applied to all the observed OIS curves from $t = 1$ to T. Notice that for each time t, multiple iterations of the Kalman filter are implemented in step 3.2, hence the name IEKF.

In step 3.1, for $t = 1$ the algorithm uses the parameters set up in step 1 and the starting values from step 2 to calculate *projections*, also called *prior estimates*, of the state vector $x(t)$ and its variance. The prior estimates will be then updated thanks to the information we extract in step 3.2, so that we derive the so called *posterior state estimates*. Subsequently, from $t = 2$ up to T the algorithm uses as prior state estimates the posterior state estimates obtained from $t - 1$. In

[101] For additional details see Krippner (2015), section 3.2.1.

facts, the main difference between the two estimates is that the prior ones are not optimal, as they only reflect the previous time information.

The crucial step of the algorithm is 3.2, where the measurement equation comes into place. In particular, the model-predicted yield curve for time t is compared with the t-observed OIS curve. However, the nonlinearity issue requires to derive the predicted OIS curve at time t via first-order Taylor approximation of the LB interest rate function around the best available estimate of $x(t)$. Furthermore, for each time t, the initial best estimate is the projection of $x(t)$ from step 3.1. However, the information provided by the measurement errors obtained from the measurement equation are fundamental to improve the initial best estimate (i.e. the prior estimate). More specifically, residuals at time t are used to derive an essential element of the IEKF, namely the *Kalman gain matrix*, which includes the new information needed to update the prior estimates of the state variable vector $x(t)$ (in step 3.2) and its variance. (in step 3.3) The initial best estimate is then updated, so that we obtain a (temporary) posterior estimate of $x(t)$ (i.e. a (new) best estimate) around which we repeat the first-order Taylor approximation of the Krippner interest rate function thus the comparison between the model-predicted yield curve at time t and the t-observed OIS curve. As before, the residuals obtained with the (new) best estimate of $x(t)$ are used to improve such estimate. To sum up, each iteration of the Kalman filter improves the estimate of $x(t)$ which is in turn used to repeat the comparison. The process repeats up to a tolerance condition in the update of $x(t)$.

Finally, step 3.3 defines the posterior estimate of $x(t)$, which has been derived in the previous step, and most importantly the posterior estimate of its variance. This is done by using the prior estimate of the variance, as well as the information coming from step 3.2. Posterior estimates are now optimal, since they reflect both the information coming from the previous time step as well as information from the current t, and will be used as starting values for $t+1$. The Kalman recursion repeats up to time T.

The second block of the optimization algorithm requires the maximization of the log-likelihood function, namely $log\text{-}L\left(\left\{\underline{R_1}^{obs}, \dots, \underline{R_T}^{obs}\right\}, \mathbb{A}\right)$ where $\underline{R_t}^{obs}$ represents the 9×1 vector of observed yields at time t for all 9 maturities, and $\mathbb{A}$ is the set of free parameters and fixed (i.e. specified) parameters of the model, that are required by the IEKF algorithm for estimation, included the lower bound. Notice that $log\text{-}L\left(\left\{\underline{R_1}^{obs}, \dots, \underline{R_T}^{obs}\right\}, \mathbb{A}\right)$ is a function of elements obtained by the IEKF algorithm.[102] Moreover, once the IEKF algorithm repeats the

[102] Specifically, the IEKF is employed at each time step to maximize the time-corresponding log-likelihood function. However, the total log-likelihood function $log\text{-}L\left(\left\{\underline{R_1}^{obs}, \dots, \underline{R_T}^{obs}\right\}, \mathbb{A}\right)$ will be the sum of each time log-likelihood function.

above-mentioned procedure up to time T those elements, such as the residuals and the projected variances of the state variable vector $x(t)$ are passed to the second block for maximization, which leads to a new parameter set $\mathbb{A}$ that is sent back to step 1 of the IEKF algorithm. Notice that, regardless of the parameter set A passed back to the IEKF algorithm, the constraints in step 1 prevent the IEKF to deliver infinite or imaginary values that could lead to potential fail of the algorithm. The procedure repeats until a convergence condition is satisfied, meaning when an additional implementation of the algorithm will not increase the value of the log-likelihood function more than a pre-specified threshold. Once convergence is reached, the set of parameters $\mathbb{A}$ are the final parameters estimates.

In conclusion, the algorithm provides as outputs the estimated set of parameters $\mathbb{A}$, the estimated time series of state variable vector $x(t)$ and the corresponding variances.

APPENDIX D: MATLAB Codes

The following codes are based on the ones of Leo Krippner, which are publicy available at: https://www.rbnz.govt.nz/research-and-publications/research-programme/additional-research/measures-of-the-stance-of-united-states-monetary-policy/matlab-code-for-krippner-2015-shadow-zlb-term-structure-model. However, some of them have been modified for the purpose of this dissertation. Thus, we provide their modified versions with comments along the code's scripts. Please notice that the codes of the functions "AAC_KAGM_SingleLoop", "AAD_KAGM_R_and_dR_dx", "AAE_KAGM_f_and_df_dx", "G", "normdist", "AAF_FiniteDifferenceHessian" and "AAL_CommonSaveName" are original codes from Leo Krippner. They have been reported for a matter of completeness along with related comments. Page numbers along the scripts refer to Krippner (2015). The Monte Carlo simulations and the LOH estimates codes have been written from scratch.

Here, we provide the codes employed for the estimation of the constant LB model and the regime-switching model over the entire sample period. However, they can be easily modified to estimate the models on a different time window, i.e. for the recursive estimations, by selecting the time window of interest within the code. The same goes for the Monte Carlo simulations and LOH estimates codes for the constant LB and regime-switching models which report the simulations dates of August and May 2021, respectively. The MATLAB codes implemented for the derivation of the initial guesses, namely for the estimation of an ANSM(2), are not reported, but they can be found at the link above.

Constant lower bound model

Main code

```
clc
clear
global Max_IEKF_Count
global Max_IEKF_Point

format short
% format long

restoredefaultpath;

% Model is K-ANSM(2), with lower bound free parameter to estimate
% There are 11 free parameter to estimate + 9 Measurement equation std dev:
% 1. rL.
% 2. KappaQ2; Bounded below by zero.
% 3. KappaP11;
% 4. KappaP12
% 5. KappaP21
% 6. KappaP22
% 7. ThetaP1
% 8. ThetaP2
% 9. Sigma1; Bounded below by zero.
% 10. Sigma2; Bounded below by zero.
% 11. Rho12; Bounded by +/- 1.
% In addition:
% 12-20. Measurement equation std deviations

% Hyperparameters.
N=2; % FIXED: Number of factors.
dTau=0.01; % OPTION: Spacing for TauGrid, used to numerically obtain R.
KappaP_Constraint='Direct'; % FIXED: KappaP matrix values are set directly,
    % (but subject to an eigenvalue constraint in
'AAC_EKF_CAB_GATSM_SingleLoop').
ZLB_Imposed=1; % FIXED: 0=ANSM(2) or 1=K-ANSM(2).
DailyIterations=200; % OPTION: Sets number of iterations between interim
saves.
IEKF_Count=-1e-5; % OPTION: EKF if 0, IEKF steps if >0, tolerance if <0
(e.g. -1e-5).
FinalNaturalParametersGiven=0; % OPTION: Full estimation if 0 (the
Optimization toolbox is required),
    % partial estimation with given parameters if 1 (not used).
HessianRequired=1; % OPTION: Omits Hessian and standard errors if 0,
calculates them if 1.

%% Import Euro_OIS_Dataset
Country='Euro_OIS_Dataset';
DataFileName='Euro_OIS_Dataset';
[DataImported,TextImported]=xlsread('Euro_OIS_Dataset.xlsx');
DataFrequency='Monthly';
FirstDay=datenum('31-Aug-2005'); % Start of dataset
LastDay=datenum('30-Sep-2021'); % End of dataset
SampleMaturities=DataImported(1,1:end); %extract maturities from
DataImported
MonthlyYieldCurveData=DataImported(2:end,1:end); %extract yields from
DataImported
MonthlyDateIndex=datenum(TextImported,'dd/mm/yyyy'); %extract dates from
TextImported

%% Set starting parameters
```

```
%These lines manually set parameters from "ANSM(2)" estimation
FinalNaturalParameters=[-0.0050 0.12443578  0.00923884  -0.020230345
0.065148363 0.016258272 -0.002189487    0.006185622 0.0138829   0.015765896
-0.937110655    0.00123762  0.000629684 1.16E-06    0.00078304  0.001299465
0.001338296 3.17E-04    1.35E-03    0.003371196];
InitialNaturalParameters=FinalNaturalParameters;

%Set Dt e Iterations (for fminsearch function) and transpose maturities
Dt=1/12;
Iterations=DailyIterations*21; %may be used in fminsearch
Tau_K=SampleMaturities';

%% Select window of interest
FirstDayRolling=datenum('31-Aug-2005');
LastDayRolling=datenum('30-Sep-2021');
CutoffFirst=find(MonthlyDateIndex==FirstDayRolling);
CutoffLast=find(MonthlyDateIndex==LastDayRolling);
MonthlyDateIndex=MonthlyDateIndex(CutoffFirst:CutoffLast,:);
MonthlyYieldCurveData=MonthlyYieldCurveData(CutoffFirst:CutoffLast,:);
YieldCurveDateIndex=MonthlyDateIndex; %rename MontlhylDateIndex in
YieldCurveDateIndex
YieldCurveData=MonthlyYieldCurveData; %rename MonthlyYieldCurveData in
YieldCurveData

%% Estimation.

if FinalNaturalParametersGiven==1 %original code line to enable partial
estimation
%  No partial estimation in our case
else  %full estimation
    disp(['Estimating K-AFNSM(2) for ',Country,' using ',...
        num2str(SampleMaturities(1)),'-',num2str(SampleMaturities(end)),'
year data at ',...
        DataFrequency,' frequency for period ',...
        datestr(YieldCurveDateIndex(1)),' to
',datestr(YieldCurveDateIndex(end))])
    Exitflag=0;
    while Exitflag==0
    if strcmp(KappaP_Constraint,'Direct')
        InitialParameters=InitialNaturalParameters;
        InitialParameters(11)=fzero(@(x)x/(1+abs(x))-
InitialNaturalParameters(11),1);
    elseif strcmp(KappaP_Constraint,'S/A')
        disp('Nothing here.')
    end

    % Extended Kalman filter estimation.
    Time0=now();
    FINAL=0;
    Max_IEKF_Count=0;
    Max_IEKF_Point=0;
    [x_T,FinalParameters,Fval,Exitflag,Output]= ...

AAB_KAGM_Estimation_NelderMead(YieldCurveData,Tau_K,N,InitialParameters,Dt,
dTau,KappaP_Constraint,ZLB_Imposed,IEKF_Count,FINAL,Iterations);
    Time1=now();

    if strcmp(KappaP_Constraint,'Direct')
        % Values from KF are "proxies" in p.71 we have to convert them
        % Take the absolute value of Sigma parameters.
        FinalNaturalParameters=FinalParameters;
        FinalNaturalParameters(9)=abs(FinalParameters(9)); %mechanism p.73
```

```
        FinalNaturalParameters(10)=abs(FinalParameters(10)); %mechanism
p.73
        % Convert correlation parameters into correlations.

FinalNaturalParameters(11)=FinalParameters(11)/(1+abs(FinalParameters(11)))
; %mechanism p.73
        FinalNaturalParameters(12:end)=abs(FinalParameters(12:end));
        % Calculate the state equation quantities based on parameter
values.
        KappaQ=[0,0;0,FinalNaturalParameters(2)];

KappaP=[FinalNaturalParameters(3),FinalNaturalParameters(4);FinalNaturalPar
ameters(5),FinalNaturalParameters(6)];
        [V,D]=eig(KappaP);
        d1=D(1,1);
        d2=D(2,2);
        if any([real(d1),real(d2)]<0)
            if real(d1)<0
                d1=complex(1e-6,imag(d1)); %to ensure F<1, See p.72
            end
            if real(d2)<0
               d2=complex(1e-6,imag(d2));  %to ensure F<1, See p.72
            end
            D=diag([d1,d2]);
            KappaP=real(V*D/V);
            FinalNaturalParameters(3)=KappaP(1,1);
            FinalNaturalParameters(4)=KappaP(1,2);
            FinalNaturalParameters(5)=KappaP(2,1);
            FinalNaturalParameters(6)=KappaP(2,2);
        end
    elseif strcmp(KappaP_Constraint,'S/A')
        disp('Nothing here')
    end
    rL=FinalNaturalParameters(1);
    KappaQ2=FinalNaturalParameters(2);

KappaP=[FinalNaturalParameters(3),FinalNaturalParameters(4);FinalNaturalPar
ameters(5),FinalNaturalParameters(6)];
    ThetaP=[FinalNaturalParameters(7);FinalNaturalParameters(8)];
    Sigma1=FinalNaturalParameters(9);
    Sigma2=FinalNaturalParameters(10);
    Rho12=FinalNaturalParameters(11);

    % disp(Exitflag)
    disp([Max_IEKF_Point,Max_IEKF_Count])
    format long
    disp(Fval)
    format short
    disp(FinalNaturalParameters(1:10))
    format short
    TextImported=TextImported(CutoffFirst:CutoffLast,:)
    date=TextImported(:,1);
    dates=datetime(date);
    dates=datenum(dates);
    plotyy(dates,x_T',dates,sum(x_T)')
    formatIn = 'yyyy';
    datetick('x',formatIn);
    ylim('manual');
    xlim('padded')
    pause(0.1)

    % Reset InitialNaturalParameters for next iteration (if ExitFlag of
fminsearch = 0).
```

```
    InitialNaturalParameters=FinalNaturalParameters;
    end
end

%% Diagnostics and output.
% Calculate Hessian and standard errors for parameters, if required.
if HessianRequired==1
    % Calculate Hessian and standard errors for natural model parameters.
    fHandle=@AAC_KAGM_SingleLoop;
    FINAL=1;

NaturalHessian=AAF_FiniteDifferenceHessian(fHandle,FinalNaturalParameters,1
e-
10,YieldCurveData,Tau_K,N,Dt,dTau,KappaP_Constraint,ZLB_Imposed,IEKF_Count,
FINAL);
    NaturalParameterStandardErrors=sqrt(abs(diag(inv(NaturalHessian))))';
else
    NaturalParameterStandardErrors=-
9.999*ones(1,length(FinalNaturalParameters));
end

% Display output.
clc
dTime=Time1-Time0;
disp([num2str(dTime*24),' hours (=',num2str(dTime*24*60),' minutes',')'])
disp(Output)
disp(Exitflag)
format long
disp(Fval)
format short
disp([InitialNaturalParameters(1:10);FinalNaturalParameters(1:10);...
    NaturalParameterStandardErrors(1:10)])

%% t-stat and residuals
clc
tstat=(FinalNaturalParameters./NaturalParameterStandardErrors);
format long
disp(tstat)

KappaQ=[0,0;0,KappaQ2];
disp([KappaP,eig(KappaP),KappaQ-KappaP])

[T,K]=size(YieldCurveData);
Residuals=NaN(T,K);
PlotCurves=1;
for t=1:T
    YieldCurveData_t=YieldCurveData(t,:)';

Fitted_R_t=AAD_KAGM_R_and_dR_dx(x_T(:,t),rL,KappaQ2,Sigma1,Sigma2,Rho12,Tau
_K,dTau,ZLB_Imposed);
    if PlotCurves==1
        plot1=plot(Tau_K,100*Fitted_R_t,Tau_K,YieldCurveData_t);
        set(plot1(2),'Marker','o','LineStyle','none');
        ylim([-2 10]);
        pause(0.3)
    end
    Residual_t=0.01*YieldCurveData_t-Fitted_R_t;
    Residuals(t,:)=Residual_t;
    %disp(t)
end
RMSE_Residuals=sqrt(sum(Residuals.*Residuals)/T);
disp([mean(Residuals);RMSE_Residuals])
ABS_residuals=abs(Residuals);
```

```
MAE_Residuals=sum(ABS_residuals)/T;

%Scatter Index
format long;
AverageY=mean(YieldCurveData);
AverageY=AverageY*0.01;
SI=(RMSE_Residuals./AverageY)*100;

% Save final output in MatLab file.
SaveName=AAL_CommonSaveName(DataFileName,ZLB_Imposed,IEKF_Count,SampleMatur
ities,N,DataFrequency,FINAL,-10);
disp(SaveName)

% Save final output in MatLab file.
save(SaveName)

disp('end');
```

The "Nelder Mead" function (AAB_KAGM_Estimation_NelderMead)

```
function [x_T,FinalParameters,Fval,Exitflag,Output]=...

AAB_KAGM_Estimation_NelderMead(R_data,Tau_K,N,InitialParameters,Dt,dTau,Kap
paP_Constraint,ZLB_Imposed,IEKF_Count,FINAL,Iterations)

Parameters=InitialParameters;
Options=optimset('Display','iter','MaxFunEvals',1e30,'TolFun',1e-
2,'TolX',1e-2,'MaxIter',1e30); % Set tolerances for the fminsearch function
[FinalParameters,Fval,Exitflag,Output]=fminsearch(@EKF_function,Parameters,
Options);
    function EKF_logL=EKF_function(Parameters)

[EKF_logL,x_T]=AAC_KAGM_SingleLoop(R_data,Tau_K,N,Parameters,Dt,dTau,KappaP
_Constraint,ZLB_Imposed,IEKF_Count,FINAL);
    end
end
```

The Kalman Filter function (AAC_KAGM_SingleLoop)

```
% The code follows the pseudo algorithm in appendix C.

function
[EKF_logL,x_T]=AAC_KAGM_SingleLoop(R_data,Tau_K,N,Parameters,Dt,dTau,KappaP
_Constraint,ZLB_Imposed,IEKF_Count,FINAL)
% Extended Kalman filter for the CAB-AFNSM(2).
global Max_IEKF_Count
global Max_IEKF_Point

if FINAL==1
%
[EKF_logL,x_T]=AAC_EKF_CAB_GATSM_SingleLoop_FINAL(R_data,Tau_K,N,Parameters
,Dt,dTau,KappaP_Constraint,ZLB_Imposed,IEKF_Count,FINAL);
%     return
    % The parameters are in their natural form, including Rho values.
    rL=Parameters(1);
    KappaQ2=Parameters(2);
    KappaP=[Parameters(3),Parameters(4);Parameters(5),Parameters(6)];
    ThetaP=[Parameters(7);Parameters(8)];
    Sigma1=abs(Parameters(9));
    Sigma2=abs(Parameters(10));
    Rho12=Parameters(11);
else
```

```
    % The parameters are in one of their restricted forms.
    if strcmp(KappaP_Constraint,'Direct')
        rL=Parameters(1);
        KappaQ2=Parameters(2);
        KappaP=[Parameters(3),Parameters(4);Parameters(5),Parameters(6)];
        ThetaP=[Parameters(7);Parameters(8)];
        Sigma1=abs(Parameters(9));
        Sigma2=abs(Parameters(10));
        Rho12=Parameters(11)/(1+abs(Parameters(11)));
    else
        KappaQ2=Parameters(1);
        L=[Parameters(2),0;Parameters(3),Parameters(4)];
        A=[0,Parameters(5);-Parameters(5),0];
        KappaP=L*L'+A;
        ThetaP=[Parameters(6);Parameters(7)];
        Sigma1=abs(Parameters(8));
        Sigma2=abs(Parameters(9));
        Rho12=Parameters(10)/(1+abs(Parameters(10)));
    end
end

SIGMA=[ Sigma1      ,0                      ;...
        Rho12*Sigma2,Sigma2*sqrt(1-Rho12^2)];
OMEGA=SIGMA*SIGMA';

Sigma_Nu=Parameters(12:end);

[T,K]=size(R_data);
KT=K*T;

% Extended Kalman filter items.
x_T=NaN(N,T);
P_T=NaN(N,N,T);

% Calculate the state equation quantities based on parameter values.
[V,D]=eig(KappaP); %Eigen decomposition of K, See p.66
d1=D(1,1);
d2=D(2,2);
if any([real(d1),real(d2)]<0)
    if real(d1)<0
        d1=complex(1e-6,imag(d1)); %to ensure F<1 See p.72
    end
    if real(d2)<0
       d2=complex(1e-6,imag(d2));     %to ensure F<1
    end
    D=diag([d1,d2]);
    KappaP=real(V*D/V);
end
F=expm(-KappaP*Dt);
if any(abs(eig(F))>1)
    error('SingleLoop:argChk','abs(eig(F))>1')
end

Q=[ G(2*d1,Dt),G(d1+d2,Dt);
    0         ,G(2*d2,Dt)];
Q=Q+transpose(triu(Q,1));
% NOTE: Use TRANSPOSE, because ' gives congugate transpose.
U=V\OMEGA/transpose(V);
Q=U.*Q;
Q=V*Q*transpose(V);
Q=real(Q);

% The measurement equation quantities depend on the state variables, and
```

```
% so have to be re-calculated at each step of  the Kalman filter.

% Starting the Recursion.
% Unconditional mean and variance of state variable vector.
x_Plus=ThetaP;
P_Plus=[ 0.5/d1, 1/(d1+d2);...
         0     , 0.5/d2   ];
P_Plus=P_Plus+transpose(triu(P_Plus,1));
P_Plus=U.*P_Plus;
P_Plus=V*P_Plus*transpose(V);
P_Plus=real(P_Plus);

%IEKF_Count=2;
logL=0;
% Extended Kalman filter if IEKF_Count=0, iterated EKF with fixed
% IEKF_Count iterations if IEKF_Count>0, and iterated EKF with fixed
% tolerance abs(IEKF_Count) if IEKF_Count<0.
if IEKF_Count<0
    x_Tolerance=abs(IEKF_Count);
    IEKF_Count=20;
end
for t=1:T
    % Forecast step.
    x_Minus=(eye(N)-F)*ThetaP+F*x_Plus;
    P_Minus=F*P_Plus*F'+Q;

    % Update step.
    % Observations for time t.
    y_Obs=0.01*R_data(t,:)';
    y_Missing=isnan(y_Obs);
    y_Obs=y_Obs(~y_Missing);
    R=diag(Sigma_Nu(~y_Missing).^2); %R = ?_n eq.3.31, see step 3.2 p. 121

    x_Plus_i_Minus_1=x_Minus; %Initial set up, see step 3.2. p.121
    x_Plus_i0=x_Minus;
    for i=1:1+IEKF_Count
        % EKF and IEKF iterations
        % Following Simon (2006), p. 409 and pp. 411-12.
        % Note that the EKF step is the i=1 iteration. To see this, note
        % that x_Minus - x_Plus_i0 = 0 in eq. 13.64.
        % y_t_Hat=h(x_Minus,0), i.e. fitted values of y_t given x_Minus.
        % Ht=dR/dX(x_Minus), i.e. the Jacobian given x_Minus.

[y_Hat,H_i]=AAD_KAGM_R_and_dR_dx(x_Plus_i0,rL,KappaQ2,Sigma1,Sigma2,Rho12,T
au_K,dTau,ZLB_Imposed);
        y_Hat=y_Hat(~y_Missing);
        H_i=H_i(~y_Missing,:);
        HPHR_i=(H_i*P_Minus*H_i'+R); %HPHR_i = M_t,i in step 3.2 p.121
        K_i=P_Minus*H_i'/HPHR_i; %kalman gain matrix
        w_i=y_Obs-y_Hat-H_i*(x_Minus-x_Plus_i0);
        x_Plus_i1=x_Minus+K_i*w_i; %current temporary posterior estimate
        if IEKF_Count==20
            % Using tolerance, so check for convergence.
            if i>15
                % Large number of iterations, so print output to screen.
                disp([num2str(t),' ',num2str(i-1),' ',num2str(x_Plus_i1'),'
',num2str(x_Plus_i0'),' ',num2str(x_Plus_i1'-x_Plus_i0')])
            end
            if all(abs(x_Plus_i1-x_Plus_i0)<x_Tolerance) % Exit condition
in step 3.2. p.121
                % Difference from last update within tolerance, so exit.
                break
            end
```

```
            if all(abs(x_Plus_i1-x_Plus_i_Minus_1)<x_Tolerance)
                % Allows for numerical cycling between i+1, i, i-1 updates.
                % Difference from i-1 update within tolerance, so exit.
                x_Plus_i1=0.5*(x_Plus_i1+x_Plus_i0);
                break
            end
        end
        % Record these values to allow testing for convergence.
        x_Plus_i_Minus_1=x_Plus_i0;
        x_Plus_i0=x_Plus_i1;
    end

    % Calculate final posterior values and record values.
    x_Plus=x_Plus_i1;
    P_Plus=(eye(N)-K_i*H_i)*P_Minus;
    x_T(:,t)=x_Plus;
    P_T(:,:,t)=P_Plus;
    logL=logL+log(det(HPHR_i))+w_i'/HPHR_i*w_i;

    % Hold IEKF count.
    if i-1>Max_IEKF_Count
        Max_IEKF_Count=i-1;
        Max_IEKF_Point=t;
    end
    %disp([num2str(t),' ',num2str(i-1),' ',num2str(x_Plus_i1'-x_Plus_i0')])
%     format long
%     str = sprintf('%s %s %3.10f',t,i,logL);
%     disp(str);
%     disp([num2str(t),' ',num2str(i-1),' ',num2str(logL)])
%    disp([num2str(t),' ',num2str(i-1),' ',sprintf('%3.16f',logL)])
    %std_SSR(t)=sqrt([1,1]*P_T(:,:,t)*[1;1]);
end

% log likelihood value to maximize.
EKF_logL=-0.5*KT*log(2*pi)-0.5*logL;
% Negate the log likelihood value because fminunc minimizes.
EKF_logL=-EKF_logL;

disp([EKF_logL*1e-3,Parameters(1:10),Rho12])%,real(eig(KappaP))']);
set(0,'DefaultFigureWindowStyle','docked')
plot([x_T',sum(x_T)'])
pause(0.01)

end
```

LB interest rate calculation (AAD_KAGM_R_and_dR_dx)

```
function
[CAB_GATSM_R,CAB_GATSM_dR_dx]=AAD_KAGM_R_and_dR_dx(x_t,rL,KappaQ2,Sigma1,Si
gma2,Rho12,Tau_K,dTau,ZLB_Imposed)

Tau_K_T=round(Tau_K/dTau); %Tau_K = tenors expressed in years
                           %dTau = constant time to maturity increment
                           %Tau_K_T = tenors expressed "in terms of
increments"
                           %This is done because we are going to derive
forwards and spot rates at each point of the taugrid

TauMax=max(Tau_K);
TauGrid=(0:dTau:TauMax)';

%with the next function we simply calculate the forwards
```

```
[CAB_GATSM_f,CAB_GATSM_df_dx]=AAE_KAGM_f_and_df_dx(x_t,rL,KappaQ2,Sigma1,Si
gma2,Rho12,TauGrid,ZLB_Imposed);
% [CAB_GATSM_f12,~]=AAE_CAB_GATSM_f_and_df_dx(x_t-
[0.000001;0],KappaQ,ThetaQ,SIGMA,TauGrid);
%
[CAB_GATSM_f13,~]=AAE_CAB_GATSM_f_and_df_dx(x_t+[0.000001;0],KappaQ,ThetaQ,
SIGMA,TauGrid);
% [CAB_GATSM_f22,~]=AAE_CAB_GATSM_f_and_df_dx(x_t-
[0;0.000001],KappaQ,ThetaQ,SIGMA,TauGrid);
%
[CAB_GATSM_f23,~]=AAE_CAB_GATSM_f_and_df_dx(x_t+[0;0.000001],KappaQ,ThetaQ,
SIGMA,TauGrid);
% Test=[(CAB_GATSM_f13-CAB_GATSM_f12)/(2*0.000001),(CAB_GATSM_f23-
CAB_GATSM_f22)/(2*0.000001)];

%Now, with the calculated forward, we derive the relevant R(t,T) as the
mean of the sum of the forwards up to
%each point of interest

%With the next two lines we calculate R(t,T) at each point in time of the
taugrid
%See eq.4.25 p.122
CAB_GATSM_R=cumsum(CAB_GATSM_f); %cumulative sum of forwards
CAB_GATSM_R=CAB_GATSM_R./(1:length(CAB_GATSM_f))'; %divide from 1 to 1001,
so we obtain the means at each point in time

%With the next two lines we do the same for the Jacobian, but considering
%that df/dx is a matrix (CAB_GATSM_R of lines 23, 24 is a vector)
%See eq.4.32 p.124
CAB_GATSM_dR_dx=cumsum(CAB_GATSM_df_dx);
CAB_GATSM_dR_dx=CAB_GATSM_dR_dx./repmat((1:length(CAB_GATSM_df_dx))',1,2);
%repmat Horizontally stack the column vector (1:length(CAB_GATSM_df_dx))'
two times

% Record required results in matrix.
CAB_GATSM_R=CAB_GATSM_R(Tau_K_T); %eq. 4.25: TauGrid determines the
positions in the vector of the relevant maturities
CAB_GATSM_dR_dx=CAB_GATSM_dR_dx(Tau_K_T,:); %eq. 4.32 TauGrid determines
the positions in the matrix of the relevant maturities

%since spot rates R e dR/dx (for jacobian) are calculated in each point in
time of the tau grid, we extract the relevant ones with Tau_K_T

end
```

LB forward rate calculation (AAE_KAGM_f_and_df_dx)

```
function
[CAB_GATSM_f,CAB_GATSM_df_dx]=AAE_KAGM_f_and_df_dx(x_t,rL,KappaQ2,Sigma1,Si
gma2,Rho12,TauGrid,ZLB_Imposed)

g1=ones(length(TauGrid),1);
G1=TauGrid;
g2=exp(-KappaQ2*TauGrid);
G2=(1-g2)/KappaQ2; %eq 4.40 p.128

% Expected path of short rate.
SR=x_t(1)*g1+x_t(2)*g2; %eq 3.37 p.62 (that is first part of formula 4.39
p.128)
%expectation is taken at current time "t", but we obtain the expectation
%over all the future points in time indicated by TauGrid

% Volatility effect. NB: "tau" in formula 4.39 is the equivalent of G1
```

```
VE=-0.5*Sigma1^2*G1.*G1-0.5*Sigma2^2*G2.*G2-Rho12*Sigma1*Sigma2*G1.*G2;
%see eq.4.39 p.128
%also here we obtain VE's evaluated at current time "t", over all the
%possible future points in time indicated by TauGrid

% Forward rate. %eq 4.39 p.128
GATSM_f=SR+VE; %plus sign because we expressed it negative in the first
place
%so that we obtain forward rates evaluated at current time "t", over all
%the possible future points in time indicated by TauGrid

%so far we have calculated just the shadow component f(t,tau), now we
%calculate the option component f_(t,tau)

if ZLB_Imposed==1
    % Calculate annualized option volatility, Omega.
    G_11=TauGrid;
    G_22=(1-exp(-2*KappaQ2*TauGrid))/(2*KappaQ2); %4.40 p.128 evaluated in
2*?
    G_12=G2; %eq.4.40 p.128 evaluated in ?
    Omega=sqrt(Sigma1^2*G_11+Sigma2^2*G_22+2*Rho12*Sigma1*Sigma2*G_12);
%eq.4.47 p.129

    % Calculate cumulative normal probabilities for N(0,1) distribution.
    d=(GATSM_f-rL)./Omega; %cdf eq. 4.45 p.129
    normsdist_erf_d=normsdist_erf(d);

    % Calculate gradiant and CAB_GATSM_f
    CAB_GATSM_df_dx=[g1.*normsdist_erf_d,g2.*normsdist_erf_d]; %Eq.4.56
p.132 for the jacobian
    CAB_GATSM_f=rL+(GATSM_f-rL).*normsdist_erf_d+exp(-
0.5*d.*d).*Omega/sqrt(2*pi);  %eq. 4.45 p.129
else
    % ZLB not imposed, so just constant gradiant and GATSM_f.
    CAB_GATSM_df_dx=[g1,g2];
    CAB_GATSM_f=GATSM_f;
end

% format long
% disp(normsdist_erf_d(end))
% if normsdist_erf_d(end)<0.9
% end

end
```

“G” function

```
function G_Phi_Tau=G(Phi,Tau)

if Phi<=0
    G_Phi_Tau=Tau;
else
    invPhi=1/Phi;
    PhiTau=Phi*Tau;
    ExpNegPhiTau=exp(-PhiTau);
    G_Phi_Tau=invPhi*(1-ExpNegPhiTau);
end
```

Normal distribution function (normsdist)

```
function normsdist=normsdist_erf(x)

%erf_x=erf(x/sqrt(2));

normsdist=0.5*(1+erf(x/sqrt(2))); %calculate CDF of [f(t,tau) -
rL]/omega(tau)=(GATSM_f-rL)./Omega
% The cumulative distribution function (CDF) of the normal, or Gaussian,
distribution with standard deviation ? and mean ? is
%
% ?(x)=0.5*(1+erf((x??)/(?*sqrt(2)) the CDF of the normal distribution with
?=0 and ?=1
end
```

Hessian matrix calculation (AAF_FiniteDifferenceHessian)

```
function Hessian =
AAF_FiniteDifferenceHessian(Function,x,minDiff,R_data,Tau_K,N,Dt,dTau,Kappa
P_Constraint,ZLB_Imposed,IEKF_Count,FINAL)
%NaturalHessian=AAF_FiniteDifferenceHessian(fHandle,FinalNaturalParameters,
1e-
10,YieldCurveData,Tau_K,N,Dt,dTau,KappaP_Constraint,ZLB_Imposed,IEKF_Count,
FINAL);
%output: NaturalHessian

% FINDIFFHESSIAN calculates the numerical Hessian of funfcn evaluated at
% the parameter set x (FinalNaturalParameters) using finite differences.
% Adapted from MatLab code in fminusub, line 431-548.

numberOfVariables=length(x);
f=feval(Function,R_data,Tau_K,N,x,Dt,dTau,KappaP_Constraint,ZLB_Imposed,IEK
F_Count,FINAL);
Hessian = zeros(numberOfVariables);

% Define stepsize
CHG = eps^(1/4)*sign(x).*max(abs(x),1);
% Make sure step size lies within DiffMinChange and DiffMaxChange
CHG = sign(CHG+eps).*max(abs(CHG),minDiff);

% Calculate the upper triangle of the finite difference Hessian element
% by element, using only function values. The forward difference formula
% we use is
%
% Hessian(i,j) = 1/(h(i)*h(j)) * [f(x+h(i)*ei+h(j)*ej) - f(x+h(i)*ei)
%                           - f(x+h(j)*ej) + f(x)]                    (2)
%
% The 3rd term in (2) is common within each column of Hessian and thus
% can be reused. We first calculate that term for each column and store
% it in the row vector fplus_array.
fplus_array = zeros(1,numberOfVariables);

for j = 1:numberOfVariables
    xplus = x;
    xplus(j) = x(j) + CHG(j);
    % evaluate
    %(R_data,Lambda,ParamFix,x_Fixed,ParamFree,x_Free,Dt,Tau,EA)

fplus=feval(Function,R_data,Tau_K,N,xplus,Dt,dTau,KappaP_Constraint,ZLB_Imp
osed,IEKF_Count,FINAL);
    fplus_array(j) = fplus;
end
```

```
for i = 1:numberOfVariables
    % For each row, calculate the 2nd term in (4). This term is common to
    % the whole row and thus it can be reused within the current row: we
    % store it in fplus_i.
    xplus = x;
    xplus(i) = x(i) + CHG(i);
    % evaluate

fplus_i=feval(Function,R_data,Tau_K,N,xplus,Dt,dTau,KappaP_Constraint,ZLB_I
mposed,IEKF_Count,FINAL);

    for j = i:numberOfVariables   % start from i: only upper triangle
      % Calculate the 1st term in (2); this term is unique for each element
      % of Hessian and thus it cannot be reused.
      xplus = x;
      xplus(i) = x(i) + CHG(i);
      xplus(j) = xplus(j) + CHG(j);
      % evaluate

fplus=feval(Function,R_data,Tau_K,N,xplus,Dt,dTau,KappaP_Constraint,ZLB_Imp
osed,IEKF_Count,FINAL);
      Hessian(i,j) = (fplus - fplus_i - fplus_array(j) +
f)/(CHG(i)*CHG(j));
    end
end
% Fill in the lower triangle of the Hessian
Hessian = Hessian + triu(Hessian,1)';

end
```

Save function (AAL_CommonSaveName)

```
function
SaveName=AAL_CommonSaveName(DataFileName,ZLB_Imposed,IEKF_Count,SampleMatur
ities,N,DataFrequency,FINAL,rL)
%UNTITLED Summary of this function goes here
%   Detailed explanation goes here

% global rL

% Time stamp for file names.
TimeStamp=datestr(now(),'_yyyy_mm_dd_HH_MM_SS');
if ZLB_Imposed==0
    ModelType='ANSM';
else
    ModelType='KANSM';
end
if FINAL==1
    FinalOrInterim='Final';
else
    FinalOrInterim='Interim';
end
if IEKF_Count<0
    IEKFString=['_E',num2str(log10(-IEKF_Count))];
else
    IEKFString=num2str(IEKF_Count);
End
```

Regime-switching model

The functions called within the code's script which are not reported are in common with the constant LB model estimation code. Here, the main difference is in "AAC_KAGM_SingleLoop" which have been properly modified to allow the LB to switch to new values at given points in time.

Main code

```
clc
clear
global Max_IEKF_Count
global Max_IEKF_Point

format short
% format long

restoredefaultpath;

% Model is K-ANSM(2), with lower bound free parameter to estimate
% There are 11 free parameter to estimate + 9 Measurement equation std dev:
% 1. rL.
% 2. KappaQ2; Bounded below by zero.
% 3. KappaP11;
% 4. KappaP12
% 5. KappaP21
% 6. KappaP22
% 7. ThetaP1
% 8. ThetaP2
% 9. Sigma1; Bounded below by zero.
% 10. Sigma2; Bounded below by zero.
% 11. Rho12; Bounded by +/- 1.
% In addition:
% 12-20. Measurement equation std deviations

% Hyperparameters.
N=2; % FIXED: Number of factors.
dTau=0.01; % OPTION: Spacing for TauGrid, used to numerically obtain R.
KappaP_Constraint='Direct'; % FIXED: KappaP matrix values are set directly,
    % (but subject to an eigenvalue constraint in
'AAC_EKF_CAB_GATSM_SingleLoop').
ZLB_Imposed=1; % FIXED: 0=ANSM(2) or 1=K-ANSM(2).
DailyIterations=200; % OPTION: Sets number of iterations between interim
saves.
IEKF_Count=-1e-5; % OPTION: EKF if 0, IEKF steps if >0, tolerance if <0
(e.g. -1e-5).
FinalNaturalParametersGiven=0; % OPTION: Full estimation if 0 (the
Optimization toolbox is required),
    % partial estimation with given parameters if 1.
HessianRequired=1; % OPTION: Omits Hessian and standard errors if 0,
calculates them if 1.

%% Import Euro_OIS_Dataset
Country='Euro_OIS_Dataset';
DataFileName='Euro_OIS_Dataset';
[DataImported,TextImported]=xlsread('Euro_OIS_Dataset.xlsx');
DataFrequency='Monthly';
FirstDay=datenum('31-Aug-2005'); % Start of dataset
LastDay=datenum('30-Sep-2021'); % End of dataset
```

```
SampleMaturities=DataImported(1,1:end); %extract maturities from
DataImported
MonthlyYieldCurveData=DataImported(2:end,1:end); %extract yields from
DataImported
MonthlyDateIndex=datenum(TextImported,'dd/mm/yyyy'); %extract dates from
TextImported

%% Select window of interest
FirstDayRolling=datenum('31-Aug-2005');
LastDayRolling=datenum('30-Sep-2021');
CutoffFirst=find(MonthlyDateIndex==FirstDayRolling);
CutoffLast=find(MonthlyDateIndex==LastDayRolling);
MonthlyDateIndex=MonthlyDateIndex(CutoffFirst:CutoffLast,:);
MonthlyYieldCurveData=MonthlyYieldCurveData(CutoffFirst:CutoffLast,:);
YieldCurveDateIndex=MonthlyDateIndex; %rename MontlhylDateIndex in
YieldCurveDateIndex
YieldCurveData=MonthlyYieldCurveData; %rename MonthlyYieldCurveData in
YieldCurveData

%% Set starting parameters
%These lines set parameters from "ANSM" estimation
load(['ANSM_results','.mat'],'FinalNaturalParameters');
FinalNaturalParameters=[0 FinalNaturalParameters(:,:) -0.1/100 -0.2/100 -
0.3/100 -0.4/100 -0.5/100]; %add guesses on LB values over LB regimes
InitialNaturalParameters=FinalNaturalParameters;

%Setto Dt e Iterations
Dt=1/12;
Iterations=DailyIterations*21; %may be used in fminsearch
Tau_K=SampleMaturities';

%% Estimation.
if FinalNaturalParametersGiven==1 %original code line to enable partial
estimation
%     No partial estimation for us
else
    % Estimate final parameters.
    disp(['Estimating K-AFNSM(2) for ',Country,' using ',...
        num2str(SampleMaturities(1)),'-',num2str(SampleMaturities(end)),'
year data at ',...
        DataFrequency,' frequency for period ',...
        datestr(YieldCurveDateIndex(1)),' to
',datestr(YieldCurveDateIndex(end))])
    Exitflag=0;
    while Exitflag==0
    if strcmp(KappaP_Constraint,'Direct')
        InitialParameters=InitialNaturalParameters;
        InitialParameters(11)=fzero(@(x)x/(1+abs(x))-
InitialNaturalParameters(11),1); %modified
    elseif strcmp(KappaP_Constraint,'S/A')
        disp('Nothing here.')
    end

    % Extended Kalman filter estimation.
    Time0=now();
    FINAL=0;
    Max_IEKF_Count=0;
    Max_IEKF_Point=0;
    [x_T,FinalParameters,Fval,Exitflag,Output]= ...

AAB_KAGM_Estimation_NelderMead(YieldCurveData,Tau_K,N,InitialParameters,Dt,
dTau,KappaP_Constraint,ZLB_Imposed,IEKF_Count,FINAL,Iterations);
    Time1=now();
```

```
    if strcmp(KappaP_Constraint,'Direct')
        %Values from KF are "proxies" (p.71) we have to convert them
        % Take the absolute value of Sigma parameters.
        FinalNaturalParameters=FinalParameters;
        FinalNaturalParameters(9)=abs(FinalParameters(9)); %mechanism p.73
        FinalNaturalParameters(10)=abs(FinalParameters(10)); %mechanism
p.73
        % Convert correlation parameters into correlations.

FinalNaturalParameters(11)=FinalParameters(11)/(1+abs(FinalParameters(11)))
; %mechanism p.73
        FinalNaturalParameters(12:20)=abs(FinalParameters(12:20));
        % Calculate the state equation quantities based on parameter
values.
        KappaQ=[0,0;0,FinalNaturalParameters(2)];

KappaP=[FinalNaturalParameters(3),FinalNaturalParameters(4);FinalNaturalPar
ameters(5),FinalNaturalParameters(6)];
        [V,D]=eig(KappaP);
        d1=D(1,1);
        d2=D(2,2);
        if any([real(d1),real(d2)]<0)
            if real(d1)<0
                d1=complex(1e-6,imag(d1)); %to ensure F<1, See p.72
            end
            if real(d2)<0
               d2=complex(1e-6,imag(d2));  %to ensure F<1, See p.72
            end
            D=diag([d1,d2]);
            KappaP=real(V*D/V);
            FinalNaturalParameters(3)=KappaP(1,1);
            FinalNaturalParameters(4)=KappaP(1,2);
            FinalNaturalParameters(5)=KappaP(2,1);
            FinalNaturalParameters(6)=KappaP(2,2);
        end
    elseif strcmp(KappaP_Constraint,'S/A')
        disp('Nothing here')
    end
    rL=FinalNaturalParameters(1);
    rL2=FinalNaturalParameters(21);
    rL3=FinalNaturalParameters(22);
    rL4=FinalNaturalParameters(23);
    rL5=FinalNaturalParameters(24);
    rL6=FinalNaturalParameters(25);
    KappaQ2=FinalNaturalParameters(2);

KappaP=[FinalNaturalParameters(3),FinalNaturalParameters(4);FinalNaturalPar
ameters(5),FinalNaturalParameters(6)];
    ThetaP=[FinalNaturalParameters(7);FinalNaturalParameters(8)];
    Sigma1=FinalNaturalParameters(9);
    Sigma2=FinalNaturalParameters(10);
    Rho12=FinalNaturalParameters(11);

    % disp(Exitflag)
    disp([Max_IEKF_Point,Max_IEKF_Count])
    format long
    disp(Fval)
    format short
    disp(FinalNaturalParameters(1:21))
    format short

    TextImported=TextImported(CutoffFirst:CutoffLast,:)
```

```
    date=TextImported(:,1);
    dates=datetime(date);
    dates=datenum(dates);
    plotyy(dates,x_T',dates,sum(x_T)')
    formatIn = 'yyyy';
    datetick('x',formatIn);
    ylim('manual');
    xlim('padded')
    pause(0.1)

    % Reset InitialNaturalParameters for next iteration (if ExitFlag of
fminsearch = 0).
    InitialNaturalParameters=FinalNaturalParameters;
    end
end

%% Diagnostics and output.
% Calculate Hessian and standard errors for parameters, if required.
if HessianRequired==1
    % Calculate Hessian and standard errors for natural model parameters.
    fHandle=@AAC_KAGM_SingleLoop;
    FINAL=1;

NaturalHessian=AAF_FiniteDifferenceHessian(fHandle,FinalNaturalParameters,1
e-
10,YieldCurveData,Tau_K,N,Dt,dTau,KappaP_Constraint,ZLB_Imposed,IEKF_Count,
FINAL);
    NaturalParameterStandardErrors=sqrt(abs(diag(inv(NaturalHessian))))';
else
    NaturalParameterStandardErrors=-
9.999*ones(1,length(FinalNaturalParameters));
end

% Display output.
clc
dTime=Time1-Time0;
disp([num2str(dTime*24),' hours (=',num2str(dTime*24*60),' minutes',')'])
disp(Output)
disp(Exitflag)
format long
disp(Fval)
format short
disp([InitialNaturalParameters(1:10);FinalNaturalParameters(1:10);...
    NaturalParameterStandardErrors(1:10)])

%% t-stat and RMSE
clc
tstat=(FinalNaturalParameters./NaturalParameterStandardErrors);
format long
disp(tstat)

KappaQ=[0,0;0,KappaQ2];
disp([KappaP,eig(KappaP),KappaQ-KappaP])

[T,K]=size(YieldCurveData);
Residuals=NaN(T,K);
PlotCurves=1; %plot curves considering the different LB regimes
for t=1:T
    YieldCurveData_t=YieldCurveData(t,:)';
    if t<=106

Fitted_R_t=AAD_KAGM_R_and_dR_dx(x_T(:,t),rL,KappaQ2,Sigma1,Sigma2,Rho12,Tau
_K,dTau,ZLB_Imposed);
```

```
    else if t<=109

Fitted_R_t=AAD_KAGM_R_and_dR_dx(x_T(:,t),rL2,KappaQ2,Sigma1,Sigma2,Rho12,Ta
u_K,dTau,ZLB_Imposed);
        else if t<=124

Fitted_R_t=AAD_KAGM_R_and_dR_dx(x_T(:,t),rL3,KappaQ2,Sigma1,Sigma2,Rho12,Ta
u_K,dTau,ZLB_Imposed);
                else if t<=127

Fitted_R_t=AAD_KAGM_R_and_dR_dx(x_T(:,t),rL4,KappaQ2,Sigma1,Sigma2,Rho12,Ta
u_K,dTau,ZLB_Imposed);
                    else if t<=169

Fitted_R_t=AAD_KAGM_R_and_dR_dx(x_T(:,t),rL5,KappaQ2,Sigma1,Sigma2,Rho12,Ta
u_K,dTau,ZLB_Imposed);
                        else

Fitted_R_t=AAD_KAGM_R_and_dR_dx(x_T(:,t),rL6,KappaQ2,Sigma1,Sigma2,Rho12,Ta
u_K,dTau,ZLB_Imposed);
                        end
                    end
            end
        end
    end

    if PlotCurves==1
        plot1=plot(Tau_K,100*Fitted_R_t,Tau_K,YieldCurveData_t);
        set(plot1(2),'Marker','o','LineStyle','none');
        ylim([-2 10]);
        pause(0.3)
    end
    Residual_t=0.01*YieldCurveData_t-Fitted_R_t;
    Residuals(t,:)=Residual_t;
    %disp(t)
end
RMSE_Residuals=sqrt(sum(Residuals.*Residuals)/T);
disp([mean(Residuals);RMSE_Residuals])
ABS_residuals=abs(Residuals);
MAE_Residuals=sum(ABS_residuals)/T;

%Scatter Index
format long;
AverageY=mean(YieldCurveData);
AverageY=AverageY*0.01;
SI=(RMSE_Residuals./AverageY)*100;

% Save final output in MatLab file.
SaveName=AAL_CommonSaveName(DataFileName,ZLB_Imposed,IEKF_Count,SampleMatur
ities,N,DataFrequency,FINAL,-10);
disp(SaveName)

% Save final output in MatLab file.
save(SaveName)

disp('end');
```

Kalman Filter function (AAC_KAGM_SingleLoop)

```
function
[EKF_logL,x_T]=AAC_KAGM_SingleLoop(R_data,Tau_K,N,Parameters,Dt,dTau,KappaP
_Constraint,ZLB_Imposed,IEKF_Count,FINAL)
% Extended Kalman filter for the CAB-AFNSM(2).
global Max_IEKF_Count
global Max_IEKF_Point

if FINAL==1
%
[EKF_logL,x_T]=AAC_EKF_CAB_GATSM_SingleLoop_FINAL(R_data,Tau_K,N,Parameters
,Dt,dTau,KappaP_Constraint,ZLB_Imposed,IEKF_Count,FINAL);
%     return
    % The parameters are in their natural form, including Rho values.
    rL=Parameters(1);
    KappaQ2=Parameters(2);
    KappaP=[Parameters(3),Parameters(4);Parameters(5),Parameters(6)];
    ThetaP=[Parameters(7);Parameters(8)];
    Sigma1=abs(Parameters(9));
    Sigma2=abs(Parameters(10));
    Rho12=Parameters(11);
    rL2=Parameters(21);
    rL3=Parameters(22);
    rL4=Parameters(23);
    rL5=Parameters(24);
    rL6=Parameters(25);
else
    % The parameters are in one of their restricted forms.
    if strcmp(KappaP_Constraint,'Direct')
        rL=Parameters(1);
        KappaQ2=Parameters(2);
        KappaP=[Parameters(3),Parameters(4);Parameters(5),Parameters(6)];
        ThetaP=[Parameters(7);Parameters(8)];
        Sigma1=abs(Parameters(9));
        Sigma2=abs(Parameters(10));
        Rho12=Parameters(11)/(1+abs(Parameters(11)));
        rL2=Parameters(21);
        rL3=Parameters(22);
        rL4=Parameters(23);
        rL5=Parameters(24);
        rL6=Parameters(25);
    else
        KappaQ2=Parameters(1);
        L=[Parameters(2),0;Parameters(3),Parameters(4)];
        A=[0,Parameters(5);-Parameters(5),0];
        KappaP=L*L'+A;
        ThetaP=[Parameters(6);Parameters(7)];
        Sigma1=abs(Parameters(8));
        Sigma2=abs(Parameters(9));
        Rho12=Parameters(10)/(1+abs(Parameters(10)));
    end
end

SIGMA=[ Sigma1      ,0                      ;...
        Rho12*Sigma2,Sigma2*sqrt(1-Rho12^2)];
OMEGA=SIGMA*SIGMA';
Sigma_Nu=Parameters(12:20);

[T,K]=size(R_data);
KT=K*T;

% Extended Kalman filter items.
```

```
x_T=NaN(N,T);
P_T=NaN(N,N,T);

% Calculate the state equation quantities based on parameter values.
[V,D]=eig(KappaP);
d1=D(1,1);
d2=D(2,2);
if any([real(d1),real(d2)]<0)
    if real(d1)<0
        d1=complex(1e-6,imag(d1));
    end
    if real(d2)<0
       d2=complex(1e-6,imag(d2));
    end
    D=diag([d1,d2]);
    KappaP=real(V*D/V);
end
F=expm(-KappaP*Dt);
if any(abs(eig(F))>1)
    error('SingleLoop:argChk','abs(eig(F))>1')
end

Q=[ G(2*d1,Dt),G(d1+d2,Dt);
    0         ,G(2*d2,Dt)];
Q=Q+transpose(triu(Q,1));
% NOTE: Use TRANSPOSE, because ' gives congugate transpose.
U=V\OMEGA/transpose(V);
Q=U.*Q;
Q=V*Q*transpose(V);
Q=real(Q);

% The measurement equation quantities depend on the state variables, and
% so have to be re-calculated at each step of  the Kalman filter.

% Starting the Recursion.
% Unconditional mean and variance of state variable vector.
x_Plus=ThetaP;
P_Plus=[ 0.5/d1, 1/(d1+d2);...
         0     , 0.5/d2   ];
P_Plus=P_Plus+transpose(triu(P_Plus,1));
P_Plus=U.*P_Plus;
P_Plus=V*P_Plus*transpose(V);
P_Plus=real(P_Plus);

%IEKF_Count=2;
logL=0;
% Extended Kalman filter if IEKF_Count=0, iterated EKF with fixed
% IEKF_Count iterations if IEKF_Count>0, and iterated EKF with fixed
% tolerance abs(IEKF_Count) if IEKF_Count<0.
if IEKF_Count<0
    x_Tolerance=abs(IEKF_Count);
    IEKF_Count=20;
end
for t=1:T
    % Forecast step.
    x_Minus=(eye(N)-F)*ThetaP+F*x_Plus;
    P_Minus=F*P_Plus*F'+Q;

    % Update step.
    % Observations for time t.
    y_Obs=0.01*R_data(t,:)';
    y_Missing=isnan(y_Obs);
    y_Obs=y_Obs(~y_Missing);
```

```
    R=diag(Sigma_Nu(~y_Missing).^2);

    x_Plus_i_Minus_1=x_Minus;
    x_Plus_i0=x_Minus;
    for i=1:1+IEKF_Count
        % EKF and IEKF iterations
        % Following Simon (2006), p. 409 and pp. 411-12.
        % Note that the EKF step is the i=1 iteration. To see this, note
        % that x_Minus - x_Plus_i0 = 0 in eq. 13.64.
        % y_t_Hat=h(x_Minus,0), i.e. fitted values of y_t given x_Minus.
        % Ht=dR/dX(x_Minus), i.e. the Jacobian given x_Minus.

        %To allow for estimation of different LB values with shifts in
specific dates:
        if t<=106 %until May 2014 (included) --> first LB regime

[y_Hat,H_i]=AAD_KAGM_R_and_dR_dx(x_Plus_i0,rL,KappaQ2,Sigma1,Sigma2,Rho12,T
au_K,dTau,ZLB_Imposed);
        else if t<=109 %until Aug 2014 (included) --> second LB regime

[y_Hat,H_i]=AAD_KAGM_R_and_dR_dx(x_Plus_i0,rL2,KappaQ2,Sigma1,Sigma2,Rho12,
Tau_K,dTau,ZLB_Imposed);
        else if t<=124 %until Nov 2015 (included) --> third LB regime

[y_Hat,H_i]=AAD_KAGM_R_and_dR_dx(x_Plus_i0,rL3,KappaQ2,Sigma1,Sigma2,Rho12,
Tau_K,dTau,ZLB_Imposed);
            else if t<=127 %until Feb 2016 (included) --> fourth LB regime

[y_Hat,H_i]=AAD_KAGM_R_and_dR_dx(x_Plus_i0,rL4,KappaQ2,Sigma1,Sigma2,Rho12,
Tau_K,dTau,ZLB_Imposed);
                else if t<=169 %until Aug 2019 (included) --> fifth LB
regime

[y_Hat,H_i]=AAD_KAGM_R_and_dR_dx(x_Plus_i0,rL5,KappaQ2,Sigma1,Sigma2,Rho12,
Tau_K,dTau,ZLB_Imposed);
                    else %until Sep 2021 (included) --> sixth LB regime

[y_Hat,H_i]=AAD_KAGM_R_and_dR_dx(x_Plus_i0,rL6,KappaQ2,Sigma1,Sigma2,Rho12,
Tau_K,dTau,ZLB_Imposed);
                    end
                end
            end
            end
        end
        y_Hat=y_Hat(~y_Missing);
        H_i=H_i(~y_Missing,:);
        HPHR_i=(H_i*P_Minus*H_i'+R);
        K_i=P_Minus*H_i'/HPHR_i;
        w_i=y_Obs-y_Hat-H_i*(x_Minus-x_Plus_i0);
        x_Plus_i1=x_Minus+K_i*w_i;
        if IEKF_Count==20
            % Using tolerance, so check for convergence.
            if i>15
                % Large number of iterations, so print output to screen.
                disp([num2str(t),' ',num2str(i-1),' ',num2str(x_Plus_i1'),'
',num2str(x_Plus_i0'),' ',num2str(x_Plus_i1'-x_Plus_i0')])
            end
            if all(abs(x_Plus_i1-x_Plus_i0)<x_Tolerance)
                % Difference from last update within tolerance, so exit.
                break
            end
            if all(abs(x_Plus_i1-x_Plus_i_Minus_1)<x_Tolerance)
                % Allows for numerical cycling between i+1, i, i-1 updates.
```

```
                % Difference from i-1 update within tolerance, so exit.
                x_Plus_i1=0.5*(x_Plus_i1+x_Plus_i0);
                break
            end
        end
        % Record these values to allow testing for convergence.
        x_Plus_i_Minus_1=x_Plus_i0;
        x_Plus_i0=x_Plus_i1;
    end

    % Calculate final posterior values and record values.
    x_Plus=x_Plus_i1;
    P_Plus=(eye(N)-K_i*H_i)*P_Minus;
    x_T(:,t)=x_Plus;
    P_T(:,:,t)=P_Plus;
    logL=logL+log(det(HPHR_i))+w_i'/HPHR_i*w_i;

    % Hold IEKF count.
    if i-1>Max_IEKF_Count
        Max_IEKF_Count=i-1;
        Max_IEKF_Point=t;
    end
    %disp([num2str(t),' ',num2str(i-1),' ',num2str(x_Plus_i1'-x_Plus_i0')])
%     format long
%     str = sprintf('%s %s %3.10f',t,i,logL);
%     disp(str);
%     disp([num2str(t),' ',num2str(i-1),' ',num2str(logL)])
%    disp([num2str(t),' ',num2str(i-1),' ',sprintf('%3.16f',logL)])
    %std_SSR(t)=sqrt([1,1]*P_T(:,:,t)*[1;1]);
end

% log likelihood value to maximize.
EKF_logL=-0.5*KT*log(2*pi)-0.5*logL;
% Negate the log likelihood value because fminunc minimizes.
EKF_logL=-EKF_logL;

disp([EKF_logL*1e-3,Parameters(1:10),Rho12])%,real(eig(KappaP))']);
set(0,'DefaultFigureWindowStyle','docked')
plot([x_T',sum(x_T)'])
pause(0.01)

end
```

Monte Carlo simulation and LOH forecasts

Constant LB model

```
%% MONTE CARLO SIMULATION and LOH CALCULATION %%

clc
clear
close all

%UPLOAD estimation results at the date of interest
workspace_name='AUGUST 2021_K_ANSM_realtime';
load([workspace_name,'.mat']);

%Selection of parameters statistically significant
tstat_abs=abs(tstat);
cutoff=1.96;
tstat_logical=tstat_abs>=cutoff;
FinalNaturalParameters_logical=FinalNaturalParameters.*tstat_logical;

%KappaQ2=FinalNaturalParameters_logical(2);
KappaP=[FinalNaturalParameters_logical(3),FinalNaturalParameters_logical(4)
;FinalNaturalParameters_logical(5),FinalNaturalParameters_logical(6)];
ThetaP=[FinalNaturalParameters_logical(7);FinalNaturalParameters_logical(8)
];
Sigma1=FinalNaturalParameters_logical(9);
Sigma2=FinalNaturalParameters_logical(10);
Rho12=FinalNaturalParameters_logical(11);

%Set up
Time_to_mat=10; %expressed in years
M=1000; %number of increments from current "t" to Time_to_mat
delta=Time_to_mat/M; %in years
J=10000; %number of simulations
Simulations_ShortRate=NaN(J,M);
Simulations_ShadowRate=NaN(J,M);

%Definition of the elements needed for simulation
%KappaP
%KappaQ
SIGMA=[ Sigma1      ,0                      ;...
        Rho12*Sigma2,Sigma2*sqrt(1-Rho12^2)];

%Initial values and arrays
xt_zero=x_T(:,end); %we set ourself at the time of last observation
currentdate=YieldCurveDateIndex(end,:);

%cycle for all simulations
j=1;
for j=1:2:J %use of antithetic sampling to reduce computational burden
    epselon_norm=randn(2,M);
    Xvectors_simulated=NaN(2,M);
    %single simulation cycle
    m=1;
    xt_minus_one=xt_zero;
    for m=1:M
        xt_one=xt_minus_one+KappaP*(ThetaP-
xt_minus_one)*delta+SIGMA*sqrt(delta)*epselon_norm(:,m);
        Xvectors_simulated(:,m)=xt_one;
        xt_minus_one=xt_one;
        m=m+1;
    end
```

```
%%    Transform increments in terms of days and plot
%     A= (0:1000)*0.01;
%     A=A(2:end); %increments expressed in years
%     B=A*365; %increments expressed in days
%     D=days(B);
%     t1=datetime(TextImported(end,1));
%     t2=t1+D;
%
%     plot(t2,sum(Xvectors_simulated)');
%     hold on
%     yline(rL);
%     hold on
%     title(['Simulations at', TextImported(end,1)]);

%%
    shadow_rate=sum(Xvectors_simulated);
    LowerBound=NaN(1,M);
    LowerBound(:,:)=rL;
    ZLB_shortrate=max(LowerBound,shadow_rate);
    Simulations_ShortRate(j,:)=ZLB_shortrate;
    Simulations_ShadowRate(j,:)=shadow_rate;
%%    antithetic simulation cycle
    m=1;
    xt_minus_one=xt_zero; %
    for m=1:M
        xt_one=xt_minus_one+KappaP*(ThetaP-xt_minus_one)*delta-
SIGMA*sqrt(delta)*epselon_norm(:,m);%
        Xvectors_simulated(:,m)=xt_one;
        xt_minus_one=xt_one;
        m=m+1;
    end

%%    plot
%     plot(t2,sum(Xvectors_simulated)');
%     hold on
%     yline(rL);
%     hold on
%     title(['Simulations at', TextImported(end,1)]);
%%
    shadow_rate=sum(Xvectors_simulated);
    ZLB_shortrate=max(LowerBound,shadow_rate);
    Simulations_ShortRate(j+1,:)=ZLB_shortrate;
    Simulations_ShadowRate(j+1,:)=shadow_rate;

end

%% Calculation LOH
%LOH_threshold=0.0010; %for general LOH estimates (section 4.6.1)
LOH_threshold=-0.0045; %for May 2021 and Sept 2021 estimates (section
4.6.2)
LOHresults=NaN(1,3);
LOH_std=NaN(1,3);

i=1; %indicator "i" for different persistence requirements
for i=1:3
    switch(i)
       case 1
          increments=24; %25 increments correspond to three months (24
additional to the initial time r(t) crosses threshold)
       case 2
          increments=49; %50 increments correspond to half a year (49
additional)
```

```
        case 3
           increments=99; %100 increments correspond to a year (99
additional)
    end
    LOH_sim=NaN(J,1);
    j=1;
    for j=1:J
       ShortRate_logical=Simulations_ShortRate(j,:)>=LOH_threshold
       %find crossing date and check persistence
       %find all crossing dates
       CDC=1; %crossing date counter
       for CDC=1:M
           crossingdates=find(ShortRate_logical,CDC);
           CDC=CDC+1;
       end
       %check duration
       try
          CDC=1;
          for CDC=1:M
              crossingdates_check= crossingdates(1,CDC) + (0:increments);
              if
crossingdates(1,CDC:(CDC+increments))==crossingdates_check;
                  LOH_sim(j,:)=crossingdates(1,CDC);
                  break
              else CDC=CDC+1;
              end
          end
       catch
           LOH_sim(j,:)=M;
       end
    end

%median time
LOH=median(LOH_sim);
LOH=LOH*delta; %in years
LOHresults(1,i)=LOH;
%std dev
LOH_std=std(LOH_sim);
LOH_std=LOH_std*delta;
LOHstd(1,i)=LOH_std;

end

%save
DataFileName='AUGUST 2021_K_ANSM_realtime';
SaveName=AAL_CommonSaveName(DataFileName,ZLB_Imposed,IEKF_Count,SampleMatur
ities,N,DataFrequency,FINAL,-10);
save(SaveName)
```

Regime-switching LB model

```
%% MONTE CARLO SIMULATION and LOH CALCULATION %%

clc
clear
close all

%UPLOAD estimation results at the date of interest and (manually) insert
the simulation date
workspace_name='MAY 2021_K_ANSM_Expost';
load([workspace_name,'.mat']);
SimulationDate={'31-May-2021'}; %insert simulation date (i.e. the
estimation date)

%Selection of parameters statistically significant
tstat_abs=abs(tstat);
cutoff=1.96;
tstat_logical=tstat_abs>=cutoff;
FinalNaturalParameters_logical=FinalNaturalParameters.*tstat_logical;

%KappaQ2=FinalNaturalParameters_logical(2);
KappaP=[FinalNaturalParameters_logical(3),FinalNaturalParameters_logical(4)
;FinalNaturalParameters_logical(5),FinalNaturalParameters_logical(6)];
ThetaP=[FinalNaturalParameters_logical(7);FinalNaturalParameters_logical(8)
];
Sigma1=FinalNaturalParameters_logical(9);
Sigma2=FinalNaturalParameters_logical(10);
Rho12=FinalNaturalParameters_logical(11);
SIGMA=[ Sigma1      ,0                      ;...
        Rho12*Sigma2,Sigma2*sqrt(1-Rho12^2)];

%Set up
Time_to_mat=10; %expressed in years
M=1000; %number of increments from current "t" to Time_to_mat
delta=Time_to_mat/M; %in years
A=(1:1000)*delta; %increments expressed in years for plot
B=A*365; %increments expressed in days for plot
J=10000; %number of simulations
Simulations_ShortRate=NaN(J,M);
Simulations_ShadowRate=NaN(J,M);

%Initial values and arrays
SimulationDate=datenum(SimulationDate);
[row,col]=find(YieldCurveDateIndex==SimulationDate);
xt_zero=x_T(:,row); %we set ourself at the time of last observation
%currentdate=YieldCurveDateIndex(end,:);

%% creation of lower bound vector for simulation
LowerBound=NaN(1,M);

%find how many days between simulation date (current date) and cuts
firstcut=datenum('11-Jun-2014');
if SimulationDate>firstcut
    inc1=0;
else
NumDays1=daysact(SimulationDate,firstcut);
inc1=NumDays1*100/365; %increment up to firstcut in terms of days
LowerBound(1,1:round(inc1))=rL; %set LB to rL (i.e. estimated LB up to
first cut)
end
```

```
secondcut=datenum('10-Sep-2014');
if SimulationDate>secondcut
    inc2=0;
else
NumDays2=daysact(SimulationDate,secondcut);
inc2=NumDays2*100/365;
LowerBound(1,(round(inc1)+1):round(inc2))=-0.001; %estimated LB regime
(whole sample estimate)
end

thirdcut=datenum('09-Dec-2015');
if SimulationDate>thirdcut
    inc3=0;
else
NumDays3=daysact(SimulationDate,thirdcut);
inc3=NumDays3*100/365;
LowerBound(1,(round(inc2)+1):round(inc3))=-0.002025; %estimated LB regime
(whole sample estimate)
end

fourthcut=datenum('16-Mar-2016');
if SimulationDate>fourthcut
    inc4=0;
else
NumDays4=daysact(SimulationDate,fourthcut);
inc4=NumDays4*100/365;
LowerBound(1,(round(inc3)+1):round(inc4))=-0.003019; %estimated LB regime
(whole sample estimate)
end

fifthcut=datenum('18-Sep-2019');
if SimulationDate>fifthcut
    inc5=0;
else
NumDays5=daysact(SimulationDate,fifthcut);
inc5=NumDays5*100/365;
LowerBound(1,(round(inc4)+1):round(inc5))=-0.004; %estimated LB regime
(whole sample estimate)
end

LowerBound(1,(round(inc5)+1):end)=-0.005;
%% cycle for all simulations

j=1;
for j=1:2:J %use of antithetic sampling
    epselon_norm=randn(2,M);
    Xvectors_simulated=NaN(2,M);
    %single simulation cycle
    m=1;
    xt_minus_one=xt_zero;
    for m=1:M
        xt_one=xt_minus_one+KappaP*(ThetaP-
xt_minus_one)*delta+SIGMA*sqrt(delta)*epselon_norm(:,m);
        Xvectors_simulated(:,m)=xt_one;
        xt_minus_one=xt_one;
        m=m+1;
    end

    %% Transform increments in terms of days and plot
%     A= (0:1000)*0.01;
%     A=A(2:end); %increments expressed in years
%     B=A*365; %increments expressed in days
%     D=days(B);
```

```
%     t1=datetime(TextImported(row,1));
%     t2=t1+D;
%
%     plot(t2,sum(Xvectors_simulated)');
%     hold on
%     title(['Simulations at', TextImported(row,1)]);

    %%
    shadow_rate=sum(Xvectors_simulated);
    ZLB_shortrate=max(LowerBound,shadow_rate);
    Simulations_ShortRate(j,:)=ZLB_shortrate;
    Simulations_ShadowRate(j,:)=shadow_rate;
%%    antithetic simulation cycle
    m=1;
    xt_minus_one=xt_zero; %
    for m=1:M
        xt_one=xt_minus_one+KappaP*(ThetaP-xt_minus_one)*delta-
SIGMA*sqrt(delta)*epselon_norm(:,m);%
        Xvectors_simulated(:,m)=xt_one;
        xt_minus_one=xt_one;
        m=m+1;
    end

%%    plot
%     plot(t2,sum(Xvectors_simulated)');
%     hold on
%     title(['Simulations at', TextImported(row,1)]);
%%
    shadow_rate=sum(Xvectors_simulated);
    ZLB_shortrate=max(LowerBound,shadow_rate);
    Simulations_ShortRate(j+1,:)=ZLB_shortrate;
    Simulations_ShadowRate(j+1,:)=shadow_rate;

end

%% Calculation LOH
%LOH_threshold=0.0010; %for general LOH estimates (section 4.6.1)
LOH_threshold=-0.0045; %for May 2021 and Sept 2021 estimates (section
4.6.2)
LOHresults=NaN(1,3);
LOH_std=NaN(1,3);

i=1; %indicator "i" for different persistence requirements
for i=1:3
   switch(i)
      case 1
         increments=24;
      case 2
         increments=49;
      case 3
         increments=99;
   end

   LOH_sim=NaN(J,1);
   j=1;
   for j=1:J
       ShortRate_logical=Simulations_ShortRate(j,:)>=LOH_threshold;
       %find crossing date and check persistence
       %find all crossing dates
       CDC=1; %crossing date counter
       for CDC=1:M
           crossingdates=find(ShortRate_logical,CDC);
           CDC=CDC+1;
```

```
        end
        %check duration
        try
           CDC=1;
           for CDC=1:M
               crossingdates_check= crossingdates(1,CDC) + (0:increments);
               if
crossingdates(1,CDC:(CDC+increments))==crossingdates_check;
                   LOH_sim(j,:)=crossingdates(1,CDC);
                   break
               else CDC=CDC+1;
               end
           end
        catch
            LOH_sim(j,:)=M;
        end
    end

%median time
LOH=median(LOH_sim);
LOH=LOH*delta; %in years
LOHresults(1,i)=LOH;
%std dev
LOH_std=std(LOH_sim);
LOH_std=LOH_std*delta;
LOHstd(1,i)=LOH_std;

end

%save
DataFileName='MAY 2021_K_ANSM_Expost'
SaveName=AAL_CommonSaveName(DataFileName,ZLB_Imposed,IEKF_Count,SampleMatur
ities,N,DataFrequency,FINAL,-10);
save(SaveName)
```

Bibliography

- Arteta, C., et al (2016). *Negative Interest Rate Policies, Sources and Implications* [online]. World Bank Group, Working Paper 7791. Available at https://openknowledge.worldbank.org/bitstream/handle/10986/25036/Negative0inter0ces0and0implications.pdf?sequence=1&isAllowed=y [18/04/2021]

- Bank of Japan (2016). *Introduction of "Quantitative and Qualitative Monetary Easing with a Negative Interest Rate".* [press release]. 29 January 2016. Available at https://www.boj.or.jp/en/announcements/release_2016/k160129a.pdf [14/04/2021]

- Bech, M. and A. Malkhozov (2016). *How Have Central Banks Implemented Negative Policy Rates?* [online]. BIS, Working Paper. Available at https://www.bis.org/publ/qtrpdf/r_qt1603e.pdf [13/04/2021]

- Beyer, A., at al (2017). *The Transmission Channels of Monetary, Macro- and Microprudential Policies and their Interrelations* [online]. ECB, Occasional Paper Series 191. Available at https://www.ecb.europa.eu/pub/pdf/scpops/ecb.op191.en.pdf [18/04/2021]

- Björk, T. (2009). *Arbitrage Theory in Continuous Time*. 3rd ed. Oxford Finance.

- Black, F. (1995). Interest rates as options. *The Journal of Finance*, 50(5), 1371–1376.

- Blanke, J. and S. Krogstrup (2016). *Negative Interest Rates: Absolutely Everything You Need to Know* [online]. World Economic Forum. Available at https://www.weforum.org/agenda/2016/11/negative-interest-rates-absolutely-everything-you-need-to-know/ [02/04/2021]

- Brigo, D. and F. Mercurio (2006). *Interest Rate Models – Theory and Practice. With Smile, Inflation and Credit.* 2nd ed. Springer Finance.

- Christensen, J.H. and G. D. Rudebusch (2016a). Modeling yields at the zero lower bound: Are shadow rates the solution? *Advances in Econometrics* 35, 75–125.

- Christensen, J.H. and G. D. Rudebusch (2016b). Monetary policy expectations at the zero lower bound. *Journal of Money, Credit and Banking* 48(7), 1439–1465.

- Dai, Q. and K. Singleton (2002). Expectation puzzles, time-varying risk premia, and affine models of the term structure. *Journal of Financial Economics* 63, 415–441.

- Draghi, M. (2014). *Introductory statement to the press conference*. Frankfurt am Main, 05/06/2014. Available at https://www.ecb.europa.eu/press/pressconf/2014/html/is140605.en.html#qa [15/04/2021]

- ECB (2010). The ECB's Response to the Financial Crisis. *Monthly Bulletin* [online]. *Issue October 2010*. Available at: https://www.ecb.europa.eu/pub/pdf/other/art1_mb201010en_pp59-74en.pdf [19/05/2021]

- ECB (2011). *The Monetary Policy of the ECB*. 3° ed. Frankfurt am Main: European Central Bank.

- ECB (2014a). *ECB Announces Monetary Policy Measures to Enhance the Functioning of the Monetary Policy Transmission Mechanism*. [press release]. 5 June 2014. Available at https://www.ecb.europa.eu/press/pr/date/2014/html/pr140605_2.en.html [10/04/2021]

-ECB (2014b). *Monetary policy decisions*. [press release]. 5 June 2014. Available at https://www.ecb.europa.eu/press/pr/date/2014/html/pr140605.en.html [15/04/2021]

- ECB (2020a). Update on Economic and Monetary Developments. *Economic Bulletin* [online]. *Issue 3/2020.* Available at: https://www.ecb.europa.eu/pub/economic-bulletin/html/eb202003.en.html [18/04/2021]

- ECB (2020b). The Euro Area Bank Lending Survey – First quarter of 2020. *Bank Lending Survey* [online]. Available at: https://www.ecb.europa.eu/stats/ecb_surveys/bank_lending_survey/html/ecb.blssurvey2020q1~17a1b2b7d2.en.html#toc11 [22/04/2021]

- ECB (2020c). *Monetary policy decisions.* Frankfurt am Main, 23/01/2020. Available at https://www.ecb.europa.eu/press/pr/date/2020/html/ecb.mp200123~ae33d37f6e.en.html [13/12/2021]

- ECB (2021a). The ECB Survey of Professional Forecasters – First quarter of 2021. S*urvey of Professional Forecasters* [online]. Available at: https://www.ecb.europa.eu/stats/ecb_surveys/survey_of_professional_forecasters/html/ecb.spf2021q1~041e9cfa36.en.html#toc6 [10/12/2021]

- ECB (2021b). The ECB Survey of Monetary Analysts, Aggregate Results June 2021. *Survey of Monetary Analysts* [online]. Available at: https://www.ecb.europa.eu/stats/ecb_surveys/sma/shared/pdf/ecb.smar210618_june_2021_results.pdf?beb2c1404992779f94f5adb65bdc6a85 [10/12/2021]

- ECB (2021c). The ECB Survey of Monetary Analysts, Aggregate Results September 2021. *Survey of Monetary Analysts* [online]. Available at: https://www.ecb.europa.eu/stats/ecb_surveys/sma/shared/pdf/ecb.smar210917_september_2021_results.en.pdf?1eb449a689efda0f1181cc56d876e94c [10/12/2021]

- Eurostat (2021). *Euro-indicators news release*. Luxemburg, 17/12/2021 Available at https://ec.europa.eu/eurostat/documents/2995521/0/2-17122021-AP-EN.pdf/ebf0659e-db3c-fc20-9faa-e74964b1827d#:~:text=European%20Union%20annual%20inflation%20was,%25)%20and%20France%20(3.4%25) [22/12/2021]

- Hull, J. and A. White (1990). Pricing Interest Rate Derivative Securities. *Review of Financial Studies*, 3(4), 573-92.

- Hull, J. (2014). *Options, Futures and Other Derivatives.* 9th ed. Pearson.

- IMF (2017). Negative Interest Rate Policies – Initial Experiences and Assessments. *IMF Policy Paper* [online]. Available at https://www.imf.org/en/Publications/Policy-Papers/Issues/2017/08/03/pp080317-negative-interest-rate-policies-initial-experiences-and-assessments [15/04/2021]

- IMF (2019). Sweden: 2019 Article IV Consultation-Press Release; Staff Report; and Statement by the Executive Director for Sweden. *IMF Staff Country Reports 19/88* [online]. Available at https://www.imf.org/en/Publications/CR/Issues/2019/03/26/Sweden-2019-Article-IV-Consultation-Press-Release-Staff-Report-and-Statement-by-the-46709 [12/04/2021]

- Jarrow R. A. (2013). The zero-lower bound on interest rates: Myth or reality?. *Finance Research Letters,* 10(4): 151–156.

- Kim, D. H. and M. Priebsch (2013). Estimation of Multi-Factor Shadow-Rate Term Structure Models.

- Klein, M. (2020). *Implications of Negative Interest Rates for the Net Interest Margin and Lending of Euro Area Banks* [online]. BIS, Working Paper 848. Available at https://www.bis.org/publ/work848.pdf [13/04/2021]

- Kortela, T. (2016). A shadow rate model with time-varying lower bound of interest rates. *Bank of Finland Research Discussion Paper*, (19).

- Krippner, L. (2015). *Zero Lower Bound Term Structure Modeling. A Practitioner's Guide.* 1st ed. Palgrave Macmillan.

- Lemke, W., A. Vladu (2016). Below the zero lower bound: A shadow-rate term structure model for the euro area. *Bundesbank Discussion Paper*, (32).

- Musiela, M. and M. Rutkowski (1998). *Martingale Methods in Financial Modelling*. 2nd ed. Springer.

- Nelson, C. and A. Siegel (1987). Parsimonious modelling of yield curves. *Journal of Business* 60(4), 473–489

- Pericoli, M. and M. Taboga (2015). Understanding policy rates at the zero lower bound: insights from a Bayesian shadow rate model. *Banca d'Italia Working Papers 1023*.

- Sveriges Riksbank (2019). The Riksbank's Experiences of a Negative Repo Rate. *Account of Monetary Policy 2019* [online]. Available at https://www.riksbank.se/globalassets/media/rapporter/rpp/engelska/2020/the-riksbanks-experiences-of-a-negative-repo-rate-article-in-account-of-monetary-policy-2019.pdf [12/04/2021]

- Swiss National Bank (2011). *Swiss National Bank Sets Minimum Exchange Rate at CHF 1.20 per Euro.* [press release]. 6 September 2011. Available at https://www.snb.ch/en/mmr/reference/pre_20110906/source/pre_20110906.en.pdf [16/04/2021]

- Swiss National Bank (2014). *Swiss National Bank Introduces Negative Interest Rates: Minimum Exchange Rate Reaffirmed, and Target Range for Three Month Libor Lowered Into Negative Territory.* [press release]. 18 December 2014. Available at https://www.snb.ch/en/mmr/reference/pre_20141218/source/pre_20141218.en.pdf [16/04/2021]

- Wu, J. C. and F. D. Xia (2016). Measuring the Macroeconomic Impact of Monetary Policy at the Zero Lower Bound. *Journal of Money, Credit and Banking* 48(2-3), 253-291.

- Wu, J. C. and F. D. Xia (2017). Time-Varying Lower Bound of Interest Rates in Europe. *Chicago Booth Research Paper*, (17–06).

- Wu, J. C. and F. D. Xia (2020). Negative interest rate policy and the yield curve. *Journal of Applied Econometrics* 35(6), 653–672.